

ABSTRACT

Title of Dissertation: **THE ROLE OF CHARGE IN SOLVATION AT LIQUID/LIQUID INTERFACES**

Carmen Louise Huffman, Doctor of Philosophy, 2005

Dissertation directed by: Professor Robert A. Walker
Department of Chemistry and Biochemistry

This dissertation describes the development and characterization of new surfactants, dubbed “molecular rulers,” that provide an upper limit to the dipolar width in aqueous/organic systems. Here, dipolar width describes the distance required for the dielectric properties of one phase to converge to those of the adjacent phase. Molecular rulers consist of a hydrophobic, solvatochromic chromophore and a charged headgroup connected via a variable length methylene chain. These surfactants are anchored to the aqueous phase by the ionic headgroup while the solvatochromic probe “floats” into the organic phase. The length of the alkyl chain controls the position of the chromophore within the interfacial region. Resonance-enhanced second harmonic generation (SHG) is used to profile the electronic excitation energy of the chromophore as a function of alkyl chain length. Since the solute’s excitation energy depends on solvent polarity, we can infer interfacial dipolar width.

In previous work anionic molecular rulers were used to characterize the water/cyclohexane interface. Anionic rulers having two carbon alkyl chains sample a polarity between that of bulk water and bulk cyclohexane. Analogous cationic rulers described in this dissertation sample an environment equivalent to that of bulk cyclohexane. These results suggest that interfacial polarity may depend on surface charges having a close proximity to the adsorbed solute.

This idea was tested using cationic rulers adsorbed to the water/vapor surface of an electrolyte solution saturated with 1-octanol (a mimic of the water/alkane interface). As ionic strength increases, cationic ruler SHG behavior approaches that of the anionic species, suggesting that the ions in solution shield the cationic charge from a probe-headgroup interaction that was observed with NMR experiments for bulk aqueous solution samples.

A neutral organic molecule at the electrolyte solution/cyclohexane interface was employed to elucidate the role of charge in interfacial solvation. Observed shifts in SHG spectra from salt-free limits are similar to those of absorbance spectra for the solute in bulk electrolyte solutions. We conclude that, in the absence of direct charge-probe correlation, charges have a similar influence on interfacial solvation of neutral species as they do in bulk solution.

**THE ROLE OF CHARGE IN SOLVATION
AT LIQUID/LIQUID INTERFACES**

by

Carmen Louise Huffman

Dissertation submitted to the Faculty of the Graduate School of the
University of Maryland, College Park in partial fulfillment
of the requirements for the degree of
Doctor of Philosophy
2005

Advisory Committee:

Professor Robert A. Walker, Chair
Professor Millard H. Alexander
Professor Michael A. Coplan
Professor Bryan W. Eichhorn
Professor Janice E. Reutt-Robey

©Copyright by

Carmen Louise Huffman

2005

Dedicated in loving memory to my grandparents,
Walter and Martha Beildeck and Donald and Clare Happes

Acknowledgements

Although mine is the only name on the cover of this text, many deserve credit for their contributions, since without their support this thesis could not have been completed. The most significant contributions to the success of this project have been made by my advisor and collaborator, Dr. Rob Walker. Through many difficult struggles from experimental difficulties and scientific conundrums to career planning and job seeking, he has counseled and encouraged me. His scientific knowledge and experience have guided me to become the chemist I am today. I am grateful for his dedication to my success.

Throughout my graduate career, I often held many stimulating discussions with my peers, both past and present, in the Walker Research Group. From their graduate experiences with the SHG experimental setup and the anionic rulers project, Drs. Xiaoyi Zhang and Bill Steel gave me expert advice in the areas of technique and experimental design. Dr. Okan Esenturk provided thoughtful insight into my many scientific questions.

Current graduate students in the Walker Research Group, Mike Pomfret, Suleyman Can, Wendy Heiserman, Mike Brindza, and Tony Dylla, have provided me with meaningful companionship and intellectual stimulation. I thank all my graduate student colleagues for their support and friendship.

I have had the opportunity to mentor several undergraduate students during my time at the University of Maryland. Not only have they helped me to hone my teaching skills, but many have also made significant contributions to the work described herein. In particular, Radika Rupasinghe synthesized some of the molecular rulers used in this

work. Mandi Stevens and Dan Cole have worked diligently at synthesizing new molecular rulers to probe specific solvation at liquid/liquid interfaces. Also, Milton Liu has made countless surface tension measurements to guide our understanding of the relative surface activities of neutral and charged organic species.

I thank Dr. Yiu-Fai Lam for his guidance with NOE experiments. His expertise in NMR spectroscopy was most valuable in the understanding of bulk solution cationic molecular ruler behavior.

Finally, I thank my family for their love and support. My parents, my sisters, and my in-laws have held my hand through good times and bad, incessantly encouraging me with my best interests in mind.

And most of all, I thank my husband. Without his love, support, consideration, and understanding, I could never have succeeded. Thank you.

Financial support for this work has been provided by the Research Corporation (RI0362), the National Science Foundation (CAREER, CHE0094246) and the HHMI fellowship programs at the University of Maryland, College Park. Clark-MXR, Inc. is also acknowledged for its donation of equipment.

Table of Contents

Acknowledgements	iii
Table of Contents	v
List of Figures	vii
List of Tables	ix
List of Abbreviations	x
Chapter 1. Introduction	1
References.....	12
Chapter 2. Experimental Considerations	19
2.1. Materials	19
2.2. Molecular Ruler Synthesis.....	19
2.3. UV Absorbance Spectroscopy	25
2.4. Nuclear Overhauser Enhancement NMR Spectroscopy	26
2.5. Surface Activity	31
2.6. Resonance-Enhanced Second Harmonic Generation	34
References.....	41
Chapter 3. Interfacial Polarity Surrounding Cationic Molecular Rulers at the Water/Cyclohexane Interface	43
3.1. Introduction.....	43
3.2. Cationic Molecular Ruler Characterization	46
<i>Solvent Sensitivity</i>	46
<i>Intramolecular Charge-Dipole Interactions</i>	51
<i>Surface Activity</i>	55
<i>Interfacial Polarity Sampled by Cationic Molecular Rulers</i>	56
3.3. Conclusions.....	59
References.....	60
Chapter 4. Cationic Molecular Rulers with Simple Salts at Liquid/Liquid and Model Liquid/Liquid Interfaces	63
4.1. Introduction.....	63
4.2. Results and Discussion	65
<i>Cationic vs. Anionic Rulers Adsorbed to the Water/Cyclohexane Interface</i>	65
<i>Polarity vs. Surface Charge at Model Liquid/Liquid Interfaces</i>	70

4.3. Conclusion	76
References	77
Chapter 5. Interfacial Solvation of a Neutral Solute as a Function of Ionic Strength and Salt Identity	80
5.1. Introduction	80
5.2. Motivation and Background	81
5.3. Results and Discussion	85
<i>Surface Solvation of PNP with Electrolyte Solutions</i>	<i>85</i>
<i>Distribution of PNP and PNP^- at the Aqueous/Cyclohexane Interface</i>	<i>90</i>
5.4. Conclusions	94
References	95
Chapter 6. Conclusions and Future Directions	98
6.1. Conclusions	98
<i>Cationic Molecular Ruler Development and Characterization</i>	<i>98</i>
<i>Cationic Rulers and Simple Salts at Liquid/Liquid and Model Liquid/Liquid Interfaces</i>	<i>99</i>
<i>Interfacial Solvation of PNP as a Function of Ionic Strength and Salt Identity</i>	<i>100</i>
6.2. Future Directions	101
Appendix A. Characterization of Cationic Molecular Rulers	104
Appendix B. Error Analysis of SHG Data	144
Bibliography	149

List of Figures

Figure 1.1. Positive solvatochromism.....	4
Figure 1.2. Chemical structures of molecules used to characterize solvent polarity.....	5
Figure 1.3. A schematic representation of how different length molecular ruler surfactants vary the position of a hydrophobic probe (white ellipses) across an aqueous/organic liquid/liquid interface while the ionic headgroup (gray circles) anchors the ruler to the aqueous phase.	8
Figure 2.1. Reaction scheme depicting the two-step synthesis of anionic rulers via a neutral alcohol precursor.....	20
Figure 2.2. Reaction scheme depicting the two-step synthesis of cationic rulers via a neutral dimethylamine precursor.	20
Figure 2.3. Bulk aqueous solution spectra of PNP under acidic, neutral, and basic conditions.....	26
Figure 2.4. Energy level diagram for a two-spin system.	27
Figure 2.5. Transitions giving rise to NOE enhancement in a homonuclear two-spin system.	29
Figure 2.6. Schematic representation of how enhancement in NOE spectra can vary depending on the relaxation rate of a nucleus.....	31
Figure 2.7. Schematic representation of the Wilhelmy plate experimental setup used to determine the surface tension of surfactant containing liquid/liquid interfaces.	32
Figure 2.8. Resonance of ω_{eg} and 2ω	35
Figure 2.9. Block diagram of SHG experiment.....	39
Figure 3.1. Molecular structure of cationic molecular rulers and their neutral, dimethylamine precursors.	48
Figure 3.2. Solvatochromic behavior of neutral dimethylamine precursors.....	49
Figure 3.3. Comparisons of absorbance maxima for C ₂ dimethylamine and the C ₂ cationic ruler in various solvents.	50
Figure 3.4. NOE spectra of cationic rulers.	53
Figure 3.5. Intramolecular charge-dipole interaction for cationic molecular ruler surfactants.	53
Figure 3.6. Surface pressure isotherms of C ₂ and C ₆ anionic (top panel) and cationic (bottom panel) molecular rulers.....	56
Figure 3.7. SHG spectrum of the C ₂ cationic ruler adsorbed to the aqueous/cyclohexane interface (bottom).....	58
Figure 4.1. SH behavior of anionic and cationic molecular rulers at the water/cyclohexane interface.....	67

Figure 4.2. Schematic representation of the formation of a self-assembled monolayer of 1-octanol at the water/vapor surface.	71
Figure 4.3. SHG spectra of C ₄ cationic ruler adsorbed to the water/cyclohexane interface and the water/vapor interface where the water has been saturated with 1-octanol. . .	72
Figure 4.4. Interfacial solvation of the C ₄ cationic ruler adsorbed to the 1-octanol saturated water/vapor interface as a function of NaI concentration.....	73
Figure 4.5. Schematic representation of the interfacial environment in the absence (top panel) and presence (bottom panel) of excess bulk solution charge (in the form of additional Γ^-).	75
Figure 5.1. Molecular structure of <i>p</i> -nitrophenol (PNP).....	85
Figure 5.2. SHG spectra of PNP at the aqueous/cyclohexane interface where the electrolyte solutions are (a) 1 M NaF, 1 M NaCl, and 1 M NaBr, (b) 10 mM NaF, 50 mM NaF, and 1 M NaF, and (c) 10 mM NaCl, 1 M NaCl, and 3 M NaCl.....	86
Figure 5.3. Wavelength maxima for electronic absorbance spectra of PNP in bulk electrolyte solutions.	88
Figure 5.4. Equilibrium equations governing the distribution of PNP and PNP ⁻ in bulk solution (a) and at the water/cyclohexane interface (b).	91
Figure 5.5. Surface pressure isotherms for PNP and PNP ⁻	92
Figure B.1. SHG spectra of <i>p</i> -nitrophenol collected on two different days.	146
Figure B.2. Composite spectrum of <i>p</i> -nitrophenol at the water/cyclohexane interface using the individual spectra collected on 09/14/2004 and 09/20/2004.....	148

List of Tables

Table 3.1. UV data for cationic rulers, neutral dimethylamine precursors, C ₂ anionic ruler and its neutral alcohol precursor in several solvents.....	51
Table 5.1. Comparisons of wavelength maxima for bulk and interface electrolyte solution spectra of PNP.....	87
Table B.1. Data used to calculate the normalized intensity of points A and B from Figure B.1.....	147

List of Abbreviations

A	interfacial area
a	activity
c	bulk solution concentration
d	doublet
DEPNA	<i>N,N</i> -diethyl- <i>p</i> -nitroanisole
e	excited state
EI	electron ionization
E _T (30)	4-(2,4,6-triphenylpyridinium)-2,6-diphenylphenoxide
EtOAc	ethyl acetate
$f(\varepsilon)$	Onsager polarity function
FAB	fast atom bombardment
g	ground state or the acceleration of gravity
HRMS	high-resolution mass spectrometry
$I(\omega)$	intensity of the incident visible light
$I(2\omega)$	intensity of the detected second harmonic signal
k	virtual intermediate state
$K_{\text{eq}}(\text{bulk})$	equilibrium constant in bulk solution
$K_{\text{ads}}(i)$	equilibrium constant for the adsorption of i
$K_{\text{eq}}(\text{surface})$	equilibrium constant for surface distribution
l	perimeter of the platinum plate
LRMS	low-resolution mass spectrometry
m	multiplet
m	mass from force on the platinum plate
NaPNP	sodium <i>p</i> -nitrophenoxide
NLO	nonlinear optical

NMR	nuclear magnetic resonance
NOE	nuclear Overhauser enhancement
OPA	optical parametric amplifier
pFNB	<i>p</i> -fluoronitrobenzene
pNAs	<i>p</i> -nitroanisole
PNP	<i>p</i> -nitrophenol
PNP ⁻	<i>p</i> -nitrophenoxide
q	quintet
R	gas constant
r_{ij}	distance between two points <i>i</i> and <i>j</i>
s	singlet
SH	second harmonic
SHG	second harmonic generation
t	triplet
T	temperature
T _i	relaxation time of nucleus <i>i</i>
THF	tetrahydrofuran
$\chi^{(2)}$	second-order susceptibility tensor
$\chi^{(2)}_{NR}$	nonresonant contribution to $\chi^{(2)}$
$\chi^{(2)}_R$	resonant contribution to $\chi^{(2)}$
X _{<i>i</i>} ^{ads}	mole fraction of adsorbed surfactant <i>i</i>
X _{<i>i</i>}	mole fraction of <i>i</i> in bulk solution
ϵ	solvent static dielectric constant
γ_0	surface tension of the neat interface
γ	surface tension of the interface containing surfactants
Γ	spectral line width
Γ	surface excess

λ_{\max}	absorbance wavelength maximum
λ_{SH}	second harmonic wavelength maximum
μ_e	dipole moment of the electronically excited state
μ_g	dipole moment of the electronic ground state
μ_{ij}	transition matrix element between states i and j
π	interfacial pressure
π^*	Kamlet-Taft solvent parameter
ω_{ij}	frequency corresponding to the transition between states i and j

Chapter 1. Introduction

Liquid/liquid interfaces are important in many systems that we often take for granted. The milk in our morning cereal is a suspension of many colloidal particles, and the liquid/liquid boundary surrounding such particles governs their stability. The oil spill that we hear about in the news and the oil and vinegar dressing used on our salad are actually aqueous/organic interfaces. The membranes that surround the cells in our bodies have hydrophobic and hydrophilic phases adjacent to one another that control the transport of species across the cell membrane.

Not only do liquid/liquid interfaces abound in nature, but they also play a prominent role in many processes, phenomena, and techniques. In phase transfer catalysis, the catalyst carries reactants and products across a liquid/liquid boundary when a mutual solvent for products and reactants does not exist.¹⁻³ Solvent extractions exploit the preferential solubility of compounds to separate them from a mixture. Modern methods use supercritical carbon dioxide to remove the caffeine (and other components) from coffee beans.⁴⁻⁶ Since caffeine is often resold for use in soft drinks and pharmaceuticals, the caffeine is separated from this organic mixture through aqueous/organic extractions. Many biochemical processes involve the transport of compounds across cell membranes, which are made up of a lipid bilayer containing a hydrophilic/hydrophobic phase boundary. Often, liquid/liquid interfaces, such as the water/1-octanol interface, are used as a model for such systems.⁷⁻⁹

Despite the prevalence and importance of liquid/liquid interfaces in science and our everyday lives, relatively little research has been done to investigate their properties. Studies of air/liquid and solid/liquid interfaces have been well established. A variety of

reflection experiments that make use of neutron,^{10,11} X-ray,^{12,13} and photon^{14,15} sources can be carried out at the air/liquid surface. Solid/liquid interfaces also lend themselves to such experiments¹⁶⁻¹⁸ provided the solid medium is transparent to these sources. While these systems have been extensively explored, many questions about the structure and dynamics of liquid/liquid interfaces remain unanswered since their buried nature makes studying these systems quite a challenge.

Although the presence of two condensed phases makes the experimental acquisition of surface specific information challenging, molecular dynamics simulations have been widely used to model this boundary.¹⁹⁻²⁴ These studies examine molecular structure at liquid/liquid interfaces such as the organization of ionic surfactants,²⁵ charge distribution within mixed monolayer systems,¹⁹ interfacial width,²¹ interfacial polarity,^{22,24} and ion transport across water/organic interfaces.^{20,23} Though these studies have initiated interesting discussions about interfacial properties, many predictions from theoretical studies have gone untested.

Despite the challenges involved with studying buried interfaces, several experimental methods have been employed to explore interfacial structure. From a variety of scattering experiments (quasi-elastic laser scattering,²⁶ neutron reflection,²⁷⁻²⁹ and X-ray reflection³⁰⁻³³) has come information about the frequency and amplitude of capillary waves²⁶ and the extent of interfacial roughness.²⁸ Total internal reflection fluorescence experiments³⁴⁻³⁸ have been informative, but due to the penetration depth of the incident light, findings are convoluted by signals arising from bulk solution.

One technique that has been used successfully to acquire surface-specific details about buried interfaces is nonlinear optical (NLO) spectroscopy.³⁹⁻⁴¹ The intrinsic

anisotropy of the interface dictates that only surface-specific signals reach the detector. In this study NLO spectroscopy, specifically resonance-enhanced second harmonic generation (SHG), is used to acquire *effective* excitation spectra of solutes adsorbed to liquid/liquid interfaces. A detailed description of the origins of the surface-specific and molecularly-specific second harmonic (SH) response from liquid/liquid interfaces is provided in Chapter 2.

In this work, SHG spectra of solvent-sensitive surfactants adsorbed to water/alkane interfaces are collected and used to determine interfacial polarity. Solvent polarity has been shown to play a key role in determining the chemical and physical behavior of bulk liquids, e.g. isomerization rates of a cyanine dye;⁴² the rate of singlet to triplet intersystem crossing in aromatic carbenes;⁴³ and the dynamics of the twisted intramolecular charge-transfer that occurs in polar solvents.⁴⁴ Determining interfacial polarity will provide a means to understanding molecular properties, equilibrium, and reaction dynamics at liquid/liquid interfaces.

Polarity is a vague term most often used to describe the dipolar properties of bulk liquids. Many studies have attempted to quantify solvent polarity by using empirical quantities such as the Dimroth-Reichardt E_T parameter,^{45,46} the Grunwald-Winstein equation,⁴⁷⁻⁵⁰ Kamlet-Taft solvent parameters (π^*),⁵¹ and Z-values.⁵² These parameters take advantage of the solvatochromic behavior of various solutes. Solvatochromism describes the solvent-dependent shift of the electronic transition energy of a solute. If the dipole moment of the solute in the electronically excited state, μ_e , is greater than the dipole moment of the solute in the ground state, μ_g , as is shown in Figure 1.1, a bathochromic (red) shift in the electronic transition energy of the solute will occur with

increasing solvent polarity. This is denoted as positive solvatochromism and is due to the preferential solvation of the excited state relative to the ground state. Conversely, if $\mu_g > \mu_e$, the electronic transition energy will exhibit negative solvatochromism, a hypsochromic (blue) shift with increasing solvent polarity.

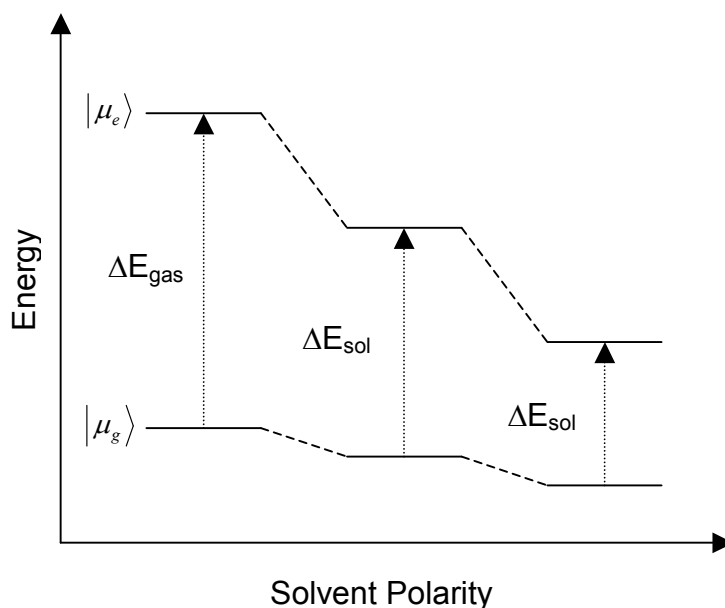


Figure 1.1. Positive solvatochromism. For a molecule whose dipole moment is larger in the excited state than in the ground state, the electronic absorbance or emission spectrum will red shift monotonically as a function of solvent polarity as described by the Onsager polarity function. ΔE_i represents the electronic excitation energy for the solute in the gas phase ($i=\text{gas}$) or in solution ($i=\text{sol}$).

The relative excitation energies of solutes in polar and nonpolar solvents have given rise to more than 30 polarity “scales.”^{53,54} Two well-known empirical scales, the π^* scale and the $E_T(30)$ scale, have been widely characterized and used to evaluate solvent polarity. Both scales compare the electronic excitation energy of a solute in a given solvent to the same solute’s excitation energy in polar and nonpolar solvents. The main difference between the two scales lies in the solute identity. The $E_T(30)$ scale is based on the hypsochromic shift of a betaine dye, 4-(2,4,6-triphenylpyridinium)-2,6-diphenylphenoxide ($E_T(30)$),^{45,46} while the π^* scale is based on the bathochromic shift of

a variety of solutes,⁵¹ e.g. *N,N*-diethyl-*p*-nitroaniline (DEPNA) and *p*-nitroanisole (pNAs). Figure 1.2 shows the structures of these compounds.

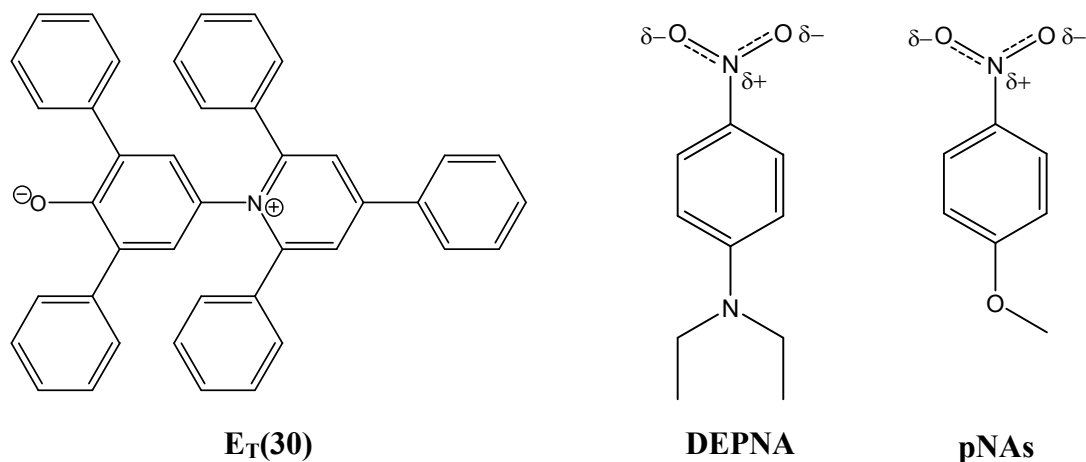


Figure 1.2. Chemical structures of molecules used to characterize solvent polarity.

The basis of solvent-dependent shifts in electronic spectra of solutes limits the flexibility of polarity measurements due to the necessary presence of a solute. Reaction field models, on the other hand, rely on a solvent's dielectric properties alone and are independent of solute identity. Perhaps most widely acknowledged is the Onsager polarity function,⁵⁵ $f(\epsilon)$, which is based on the solvent's static dielectric constant, ϵ :

$$f(\epsilon) = \frac{2(\epsilon - 1)}{2\epsilon + 1} \quad (1.1)$$

This model is based on solvation forces acting on a point dipole in a spherical cavity, rather than empirical quantities, and $f(\epsilon)$ ranges from ~ 0.4 for nonpolar solvents such as alkanes ($\epsilon = 2$) to ~ 1 for very polar solvents such as water and acetonitrile. For solutes that are sensitive to long-range, nonspecific solvation forces, solute excitation energy decreases monotonically with $f(\epsilon)$.^{56,57} Although our choice of polarity scale is somewhat

arbitrary, the Onsager scale is attractive because it enables us to relate excitation energies measured at interfaces to a local dielectric environment.

Clearly, in a system containing immiscible liquids, there is a difference in the polarities of the two solvents. Previous reports indicated that polarity at the interface between two liquids could be described by averaged contributions from the two adjacent phases.^{54,58} This conclusion was based on solvatochromic data from several different probes adsorbed to a number of different interfaces. SHG was used to acquire these results, thus ensuring that data originated only from those solutes in the anisotropic, interfacial region. More recent reports suggest that the “average polarity” model breaks down with polar organic phases, but these conclusions are based on results from fluorescence anisotropy experiments, a technique that is not intrinsically surface-specific.³⁴ Molecular dynamics simulations demonstrated how the average polarity model could arise *if* an interface were molecularly sharp but thermally roughened.⁵⁹ However, these simulations *also* suggested that results should prove very sensitive to solute orientation *and* solute location relative to the interfacial Gibbs dividing surface.

Using SHG techniques,⁵⁸ our group has probed the polarity sampled at an aqueous/cyclohexane interface by chromophores that shared very similar electronic structures but differed subtly in their functionality.⁶⁰ The hydrophilic *p*-nitrophenol sampled an interfacial polarity that was almost water-like, whereas the local dielectric environment surrounding adsorbed 2,6-dimethyl-*p*-nitrophenol was dominated by the nonpolar, alkane phase. These results correlated with bulk solution partitioning experiments and implied that solvation was changing dramatically on very short length scales across this weakly associating, liquid/liquid interface.

One question that this dissertation attempts to answer is how polarity at an aqueous/organic interface converges from that of bulk water to that of the bulk organic liquid. We define the distance required for solvent polarity to converge from an aqueous to a bulk organic limit as the interfacial “dipolar width.” To probe interfacial width, we exploit the solvatochromic properties of solutes. The effective excitation spectrum of a solute adsorbed to a liquid/liquid interface is collected using SHG, and by comparing the excitation energy of an adsorbed chromophore with bulk solution limits, we can infer how solvent polarity varies across aqueous/organic boundaries.

In order to use SHG to determine interfacial width, a solvent sensitive probe is required. Since we are specifically investigating the interfacial region, the probe must also be surface active. Perhaps the most critical necessity is the ability to control the position of the probe within the interfacial region in order to quantify the distance required for polarity to converge to the bulk solvent limit. An ionic headgroup tethered to a hydrophobic, solvatochromic chromophore by a variable length alkyl chain spacer will fulfill these requirements. We dub these newly designed surfactants “molecular rulers.” Figure 1.3 shows a schematic representation of molecular rulers adsorbed to a liquid/liquid interface. As alkyl chain length increases, the hydrophobic chromophore is allowed to “float” closer to the organic phase while the ionic headgroup anchors the molecular ruler to the aqueous phase.

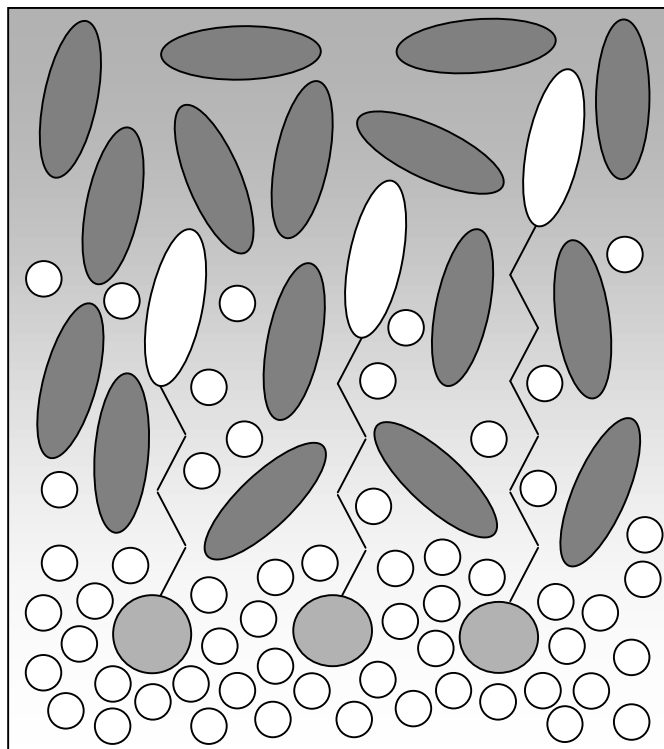


Figure 1.3. A schematic representation of how different length molecular rulers vary the position of a hydrophobic probe (white ellipses) across an aqueous/organic liquid/liquid interface while the ionic headgroup (gray circles) anchors the ruler to the aqueous phase. White circles represent water molecules, and dark ellipses represent organic solvent molecules. While packing densities may not be to scale, the z-direction accurately reflects the dipolar width of the water/cyclohexane interface sampled by anionic molecular rulers.

Chapter 3 focuses on the development and characterization of a new class of molecular rulers that contain a cationic headgroup. Results from SHG studies indicate that the dipolar width of a water/cyclohexane interface, when probed by both anionic and cationic molecular rulers, is ≤ 10 Å. However, short cationic molecular rulers adsorbed to the water/cyclohexane interface sample a less polar environment than that sampled by short anionic rulers adsorbed to the same interface. Several explanations are presented to rationalize this surprising result. Since the only difference between the aforementioned water/cyclohexane experiments is the charge of the surfactant headgroup, we surmise that charge may play an important role in interfacial polarity.

The question of how charges behave at an interface, be it air/water, solid/liquid, or liquid/liquid, is not a new one. In particular, how charges are distributed at a surface has been a major area of focus for several decades.^{15,61-67} At any surface of an electrolyte solution, there exists an unequal distribution of charges at the boundary between the two phases described as an electrical double layer.^{61,68-71} This double layer describes an accumulation of ions close to the surface resulting in a net surface charge. This area of excess charge is referred to as the compact double layer, or the Stern layer.⁶² To maintain charge neutrality, a more diffuse Gouy layer of opposite charge lies adjacent to this layer such that the potential falls off exponentially with distance according to the Debye-Hückel model.⁶² Beyond the Gouy layer, ions in bulk solution are uniformly distributed, and electroneutrality is preserved. The electrical double layer formation is particularly well defined when a surfactant is responsible for localizing charge at a surface. For example, a system containing a monolayer film of *N,N,N*-trimethyloctadecyl ammonium cations occupying $85 \text{ \AA}^2/\text{molecule}$ on an aqueous sodium chloride subphase creates an electrostatic potential across the diffuse layer of 177 mV .⁷²

Other studies have explored the distribution of ions at liquid surfaces. Surface tension measurements have been carried out to determine whether ions are adsorbed or depleted from the surface. Typically, ionic surfactants adsorb to a liquid surface to reduce the surface free energy leading to a *decrease* in the surface tension of the solution relative to that of the neat liquid. However, early surface tension measurements of aqueous, simple salt solutions at air/water^{64,73} and aqueous/organic⁷⁴ interfaces showed a prominent *increase* in surface tension relative to that of the neat water interface. This observation was interpreted as negative surface activity and a depletion of simple salt

ions at the air/water and aqueous/organic interfaces.^{63,74-77} Simple thermodynamic considerations suggest that this view of ion depletion at the surface is reasonable, given the unfavorable enthalpy change required to desolvate surface ions.

In contrast to this traditional picture of simple ion surface depletion, recent molecular dynamics simulations suggest that some simple ions will, in fact, migrate to a liquid surface, and the degree to which an ion will partition to the surface depends on the ion's polarizability.⁶⁵ *Ab initio* quantum calculations, Car-Parrinello molecular dynamics simulations and molecular dynamics simulations based on polarizable force fields were used to examine aqueous slabs doped with sodium fluoride, chloride, bromide, and iodide at effective concentrations of ~1 M. Density profiles of the ions and water oxygen atoms indicate that highly polarizable iodide and bromide ions exhibit positive excess surface concentrations. The authors suggest that such surface accumulation is possible because the nonzero net dipole of water molecules asymmetrically solvating the surface ions polarizes the ions leading to a stabilization that balances the energy penalty of incomplete solvation. Because chloride ions are not as polarizable as bromide and iodide ions, their surface concentration is predicted to be slightly less than bulk concentration. Very small, nonpolarizable, strongly hydrated fluoride ions are depleted from the surface region.⁶⁵ Very recent results from X-ray photoelectron spectroscopy support these predictions.⁷⁸

The studies described above focus on ion distribution at the air/water interface. Few studies have explored the effects of charge on liquid/liquid interfacial environments. Given that simple ions in aqueous solutions influence interfacial properties such as surface tension, one may wonder how these altered properties change the local environment experienced by molecular solutes adsorbed to liquid/liquid interfaces.

Both Chapters 4 and 5 describe how charges from simple salts in an electrolyte solution affect the solvation of a solute adsorbed to a liquid/liquid interface. In Chapter 4, the ionic surfactants are molecular rulers. Salts are added to the aqueous phase to determine whether increasing the ionic strength of the solution affects the solvation of the charged surfactants. SHG results reveal that as aqueous sodium iodide concentration increases, cationic molecular rulers tend toward anionic molecular ruler behavior with a spectral red shift. We conclude that the apparent nonpolar interfacial region sampled by short cationic molecular rulers at the water/cyclohexane interface is actually the result of an intramolecular charge-dipole interaction between the cationic headgroup and the electron-rich aromatic ring of the surfactant. This interaction leads to a reduction in the change in dipole moment resulting from electronic excitation, and a spectral blue shift relative to spectra collected for anionic molecular rulers that display no signs of intramolecular interaction.

To determine whether charge can influence solvation around a probe even if the charge and the probe are not chemically connected, we extend SHG experiments to a neutral molecule, *p*-nitrophenol (PNP), adsorbed to the water/cyclohexane interface. In Chapter 5 we show that the addition of electrolytes to the aqueous phase does not change surface spectra relative to absorbance spectra collected for PNP in bulk electrolyte solutions. We conclude that, while charges in the aqueous phase can contribute to changes in the solvation of surface molecules, these changes are similar to those found in bulk solution. By extension, we conclude that, in the absence of a direct correlation between the charged species and a probe molecule, charges have a similar influence on interfacial solvation of neutral organic species such as PNP as they do in bulk solution.

Previous results are a direct consequence of close correlation between the charged headgroup and the aromatic probe.

While the experiments contributing to this work are completed, there remain many unanswered questions about solvation at water/organic interfaces and the influence of charge. Chapter 6 is dedicated to the conclusions found from these studies and the future directions of this project.

Note that several of these chapters have been previously published or submitted for publication as independent articles. Therefore, there exists some redundancy throughout this text in discussing the motivation for this work and the analysis of results. For the sake of clarity within each chapter, these duplications were not omitted.

References

- (1) Starks, C. M. *J. Am. Chem. Soc.* **1971**, *93*, 195.
- (2) Starks, C. M.; Owens, R. M. *J. Am. Chem. Soc.* **1973**, *95*, 3613.
- (3) Volkov, A. G. *Interfacial Catalysis*, 2003.
- (4) Katz, S. N.; Spence, J. E.; O'Brien, M. J.; Skiff, R. H.; Vogel, G. J.; Prasad, R. Decaffeination of Coffee Green Beans with Supercritical Carbon Dioxide; General Foods Corp.: U.S., 1990; pp 11.
- (5) Saldana, M. D. A.; Mazzafera, P.; Mohamed, R. S. *Ciencia e Tecnologia de Alimentos* **1997**, *17*, 371.
- (6) Zekovic, Z. P.; Lepojevic, Z. D.; Milosevic, S. G.; Tolic, A. S. *Acta Periodica Technologica* **2001**, *32*, 163.

- (7) Safran, S. A. *Statistical Thermodynamics of Surfaces, Interfaces, and Membranes*; Addison-Wesley Publishing Co.: Reading, MA, 1994; Vol. 90.
- (8) Chipot, C.; Wilson, M. A.; Pohorille, A. *J. Phys. Chem. B* **1997**, *101*, 782.
- (9) *Liquid Interfaces in Chemical, Biological, and Pharmaceutical Applications*; Volkov, A. G., Ed.; Marcel Dekker, Inc.: New York, 2001; Vol. 95, pp 853.
- (10) Lu, J. R.; Su, T. J.; Li, Z. X.; Thomas, R. K.; Staples, E. J.; Tucker, I.; Penfold, J. *J. Phys. Chem. B* **1997**, *101*, 10332.
- (11) Purcell, I. P.; Thomas, R. K.; Penfold, J.; Howe, A. M. *Colloids Surf., A* **1995**, *94*, 125.
- (12) Schlossman, M. L.; Schwartz, D. K.; Kawamoto, E. H.; Kellogg, G. J.; Pershan, P. S.; Kim, M. W.; Chung, T. C. *J. Phys. Chem.* **1991**, *95*, 6628.
- (13) Lee, E. M.; Simister, E. A.; Thomas, R. K. *Mol. Cryst. Liq. Cryst.* **1990**, *179*, 151.
- (14) Ma, G.; Liu, D.; Allen, H. C. *Langmuir* **2004**, *20*, 11620.
- (15) Raymond, E. A.; Richmond, G. L. *J. Phys. Chem. B* **2004**, *108*, 5051.
- (16) Becraft, K. A.; Moore, F. G.; Richmond, G. L. *Phys. Chem. Chem. Phys.* **2004**, *6*, 1880.
- (17) Fragneto-Cusani, G. *J. Phys.: Condens. Matter* **2001**, *13*, 4973.
- (18) Majewski, J.; Kuhl, T. L.; Wong, J. Y.; Smith, G. S. *Rev. Molec. Biotech.* **2000**, *74*, 207.
- (19) Dominguez, H. *J. Phys. Chem. B* **2002**, *106*, 5915.

- (20) Dang, L. X. *J. Phys. Chem. B* **2001**, *105*, 804.
- (21) Senapati, S.; Berkowitz, M. L. *Phys. Rev. Lett.* **2001**, *87*, 176101.
- (22) Michael, D.; Benjamin, I. *J. Chem. Phys.* **2001**, *114*, 2817.
- (23) Dang, L. X. *J. Phys. Chem. B* **1999**, *103*, 8195.
- (24) Michael, D.; Benjamin, I. *J. Chem. Phys.* **1997**, *107*, 5684.
- (25) Dominguez, H.; Berkowitz, M. L. *J. Phys. Chem. B* **2000**, *104*, 5302.
- (26) Tsuyumoto, I.; Noguchi, N.; Kitamori, T.; Sawada, T. *J. Phys. Chem. B* **1998**, *102*, 2684.
- (27) Strutwolf, J.; Barker, A. L.; Gonsalves, M.; Caruana, D. J.; Unwin, P. R.; Williams, D. E.; Webster, J. R. P. *J. Electroanal. Chem.* **2000**, *483*, 163.
- (28) Zorbakhsh, A.; Bowers, J.; Webster, J. R. P. *Meas. Sci. Technol.* **1999**, *10*, 738.
- (29) Cosgrove, T.; Phipps, J. S.; Richardson, R. M. *Colloids Surf.* **1992**, *62*, 199.
- (30) Mitrinovic, D. M.; Williams, S. M.; Schlossman, M. L. *Phys. Rev. E: Stat. Phys., Plasmas, Fluids, Relat. Interdiscip. Top.* **2001**, *6302*, art. no. 021601.
- (31) Mitrinovic, D. M.; Tikhonov, A. M.; Li, M.; Huang, Z. Q.; Schlossman, M. L. *Phys. Rev. Lett.* **2000**, *85*, 582.
- (32) Schlossman, M. L.; Li, M.; Mitrinovic, D. M.; Tikhonov, A. M. *High Perform. Polym.* **2000**, *12*, 551.

- (33) Mitrinovic, D. M.; Zhang, Z. J.; Williams, S. M.; Huang, Z. Q.; Schlossman, M. L. *J. Phys. Chem. B* **1999**, *103*, 1779.
- (34) Ishizaka, S.; Kim, H. B.; Kitamura, N. *Anal. Chem.* **2001**, *73*, 2421.
- (35) Ishizaka, S.; Habuchi, S.; Kim, H. B.; Kitamura, N. *Anal. Chem.* **1999**, *71*, 3382.
- (36) Nakatani, K.; Ishizaka, S.; Kitamura, N. *Anal. Sci.* **1996**, *12*, 701.
- (37) Kovaleski, J. M.; Wirth, M. J. *J. Phys. Chem.* **1995**, *99*, 4091.
- (38) Sassaman, J. L.; Wirth, M. J. *Colloids Surf., A* **1994**, *93*, 49.
- (39) Zhuang, X.; Miranda, P. B.; Kim, D.; Shen, Y. R. *Phys. Rev. B: Condens. Matter* **1999**, *59*, 12632.
- (40) Antoine, R.; Bianchi, F.; Brevet, P. F.; Girault, H. H. *J. Chem. Soc., Faraday Trans.* **1997**, *93*, 3833.
- (41) Shen, Y. R. *Nature* **1989**, *337*, 519.
- (42) Hicks, J. M.; Vandersall, M. T.; Sitzmann, E. V.; Eisenthal, K. B. *Chem. Phys. Lett.* **1987**, *135*, 413.
- (43) Langan, J. G.; Sitzmann, E. V.; Eisenthal, K. B. *Chem. Phys. Lett.* **1984**, *110*, 521.
- (44) Fonseca, T.; Kim, H. J.; Hynes, J. T. *J. Photochem. Photobiol., A* **1994**, *82*, 67.
- (45) Dimroth, K.; Reichardt, C.; Siepmann, T.; Bohlmann, F. *Ann.* **1963**, *661*, 1.

- (46) Reichardt, C. *Solvents and Solvent Effects in Organic Chemistry*, 2nd ed., 1988.
- (47) Fainberg, A. H.; Winstein, S. *J. Am. Chem. Soc.* **1956**, *78*, 2770.
- (48) Grunwald, E.; Winstein, S. *J. Am. Chem. Soc.* **1948**, *70*, 846.
- (49) Bentley, T. W.; Llewellyn, G. *Prog. Phys. Org. Chem.* **1990**, *17*, 121.
- (50) Bentley, T. W.; Schleyer, P. v. R. *Adv. Phys. Org. Chem.* **1977**, *14*, 1.
- (51) Kamlet, M. J.; Abboud, J. L. M.; Taft, R. W. *Prog. Phys. Org. Chem.* **1981**, *13*, 485.
- (52) Kosower, E. M. *J. Am. Chem. Soc.* **1958**, *80*, 3253.
- (53) Katritzky, A. R.; Fara, D. C.; Yang, H.; Taemm, K.; Tamm, T.; Karelson, M. *Chem. Rev.* **2004**, *104*, 175.
- (54) Wang, H.; Borguet, E.; Eisenthal, K. B. *J. Phys. Chem. B* **1998**, *102*, 4927.
- (55) Onsager, L. *J. Am. Chem. Soc.* **1936**, *58*, 1486.
- (56) Suppan, P.; Ghoneim, N. *Solvatochromism*; The Royal Society of Chemistry: Cambridge, UK, 1997.
- (57) Wong, M. W.; Frisch, M. J.; Wiberg, K. B. *J. Am. Chem. Soc.* **1991**, *113*, 4776.
- (58) Wang, H.; Borguet, E.; Eisenthal, K. B. *J. Phys. Chem. A* **1997**, *101*, 713.
- (59) Michael, D.; Benjamin, I. *J. Phys. Chem. B* **1998**, *102*, 5145.
- (60) Steel, W. H.; Walker, R. A. *J. Am. Chem. Soc.* **2003**, *125*, 1132.

- (61) Gouy. *J. Phys. IV* **1910**, 9, 457.
- (62) Stern, O. *Z. Elektrochem.* **1924**, 30, 508.
- (63) Randles, J. E. B. *Phys. Chem. Liq.* **1977**, 7, 107.
- (64) Weissenborn, P. K.; Pugh, R. J. *J. Colloid Interface Sci.* **1996**, 184, 550.
- (65) Jungwirth, P.; Tobias, D. J. *J. Phys. Chem. B* **2002**, 106, 6361.
- (66) Petersen, P. B.; Saykally, R. J. *Chem. Phys. Lett.* **2004**, 397, 51.
- (67) Liu, D.; Ma, G.; Levering, L. M.; Allen, H. C. *J. Phys. Chem. B* **2004**, 108, 2252.
- (68) Rosen, M. J. *Surfactants and Interfacial Phenomena*, 3rd ed.; John Wiley & Sons, Inc.: Hoboken, NJ, 2004.
- (69) Gouy, G. *Ann. Phys.* **1917**, 7, 129.
- (70) Debye, P.; Hückel, E. *Phys. Z.* **1923**, 24, 185.
- (71) Debye, P. *Phys. Z.* **1924**, 25, 97.
- (72) Davies, J. T. *Proc. R. Soc. London* **1951**, A208, 224.
- (73) Onsager, L.; Samaras, N. N. T. *J. Chem. Phys.* **1934**, 2, 528.
- (74) Aveyard, R.; Saleem, S. M. *J. Chem. Soc., Faraday Trans. 1* **1976**, 72, 1609.
- (75) Adam, N. K. *The Physics and Chemistry of Surfaces*; Oxford University Press: London, 1941.

(76) Bikerman, J. J. *Surface Chemistry: Theory and Applications*; Academic Press: New York, 1958.

(77) Chatteraj, D. K.; Birdi, K. S. *Adsorption and the Gibbs Surface Excess*; Plenum: New York, 1984.

(78) Ghosal, S.; Hemminger, J. C.; Bluhm, H.; Mun, B. S.; Hebenstreit, E. L. D.; Ketteler, G.; Ogletree, D. F.; Requejo, F. G.; Salmeron, M. *Science* **2005**, *307*, 563.

Chapter 2. Experimental Considerations

2.1. Materials

Solvents were purchased from either Fisher Scientific or J. T. Baker with the exception of 1-octanol, which was purchased from Aldrich. *p*-Fluoronitrobenzene (pFNB), *p*-nitrophenol (PNP) and sodium *p*-nitrophenoxide (NaPNP) were purchased from Aldrich. Methyl iodide was purchased from Acros, and *n*-alkanolamines were purchased from TCI America. Potassium hydroxide and all simple salts were purchased from either Fisher Scientific or J.T. Baker. All compounds and solvents were used without further purification. Salt purity was confirmed by infrared absorbance spectroscopy and surface tension measurements. Salts were stored in open containers in an oven set to ~100 °C and cooled to room temperature in closed containers immediately before use to keep them dry.

All glassware was immersed in an acid bath containing a 50:50 mixture of nitric and sulfuric acids for at least one hour and rinsed copiously with distilled, deionized water prior to use. All aqueous solutions were made using distilled, deionized water and, unless specified otherwise, are at $\text{pH} = 5.7 \pm 0.2$ due to the presence of dissolved CO_2 .

2.2. Molecular Ruler Synthesis

Much of the work presented in this dissertation involves the use of variable length ionic surfactants – dubbed “molecular rulers” – that consist of a hydrophobic, solvatochromic surfactant and an ionic headgroup connected by a variable length alkyl chain spacer. The synthesis of anionic rulers is shown in Figure 2.1 and has been described elsewhere.¹

The cationic rulers synthesized for this study consist of a solvatochromic probe and a cationic headgroup connected by a methylene chain. Throughout this work, these molecules and their neutral precursors will be referred to as C_n rulers and C_n dimethylamines, respectively, where n represents the number of methylenes in the alkyl chain. Cationic rulers were synthesized in a two-step process by first creating a dimethylamine-substituted neutral precursor **2** and then quaternizing the amine with methyl iodide to create a quaternary trimethylammonium salt with an iodide counterion **3** as shown in Figure 2.2. These processes are described in greater detail in Procedures I and II, below.

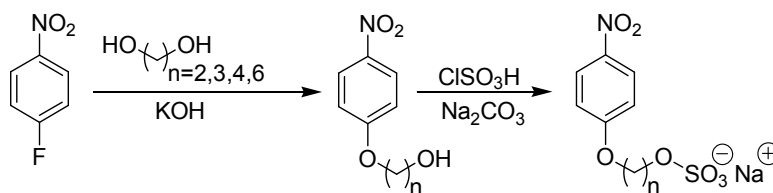


Figure 2.1. Reaction scheme depicting the two-step synthesis of anionic rulers via a neutral alcohol precursor.

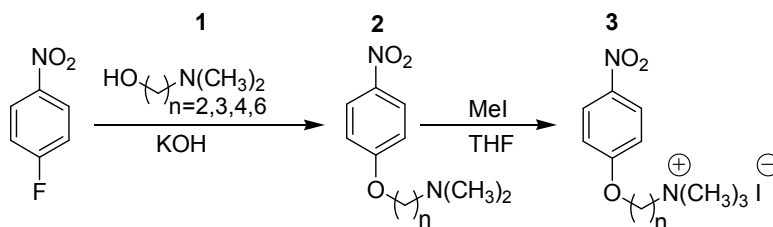


Figure 2.2. Reaction scheme depicting the two-step synthesis of cationic rulers via a neutral dimethylamine precursor.

Mass spectrometry and nuclear magnetic resonance (NMR) were used to identify the products from each reaction. Low-resolution mass spectrometry (LRMS) of the neutral species was performed using a JEOL JMS-SX102A in either fast atom

bombardment (FAB) or electron ionization (EI) mode. In some cases, high-resolution mass spectrometry (HRMS) was performed with the same instrument. Mass spectra of the ionic species were collected on a Finnigan LCQ mass spectrometer using an electrospray ionization technique. Both anionic and cationic detection modes were used for the ionic species. The mass spectra of the cationic rulers show clustering similar to that observed for anionic rulers.¹ The mass spectra from the cationic detection mode show clusters of $n + 1$ cations and n anions, while analogous spectra were observed in negative ion mode with clusters of $n + 1$ anions and n cations. Gas phase clusters are thought to result from the formation of small, highly charged droplets that have a solute concentration ~ 100 times greater than the bulk concentration,² although the formation mechanism is still not well understood.³ The NMR spectra were collected using a 400 MHz Bruker DRX-400 spectrometer. Spectral descriptions are given for each compound below where chemical shift is given in parts per million, coupling constants are given in hertz, and multiplicity is indicated as follows: s (singlet), d (doublet), t (triplet), q (quintet), or m (multiplet). Due to excessive noise and weak signals, not all of the surfactant ¹³C NMR peaks are clearly discernible. ¹H NMR, ¹³C NMR, and mass spectra for all synthesized compounds can be found in Appendix A.

Procedure I: One aliquot of pFNB was added dropwise to a stirring solution of 10 aliquots of **1** and 1.3 aliquots of KOH under a nitrogen atmosphere.⁴ After 3 h of stirring, the reaction was quenched with distilled, deionized water, and the product was extracted into diethyl ether. The product was washed two times with a saturated NaCl solution and dried by rotary evaporation. For each neutral compound except

C₂ dimethylamine, the product was purified by column chromatography using silica gel and the solvent system for which the R_f value is given below.

Procedure II: The pure oil from Procedure I was dissolved in ~50 mL of tetrahydrofuran (THF). While stirring the solution, two aliquots of methyl iodide were added dropwise, and the mixture was allowed to stir for ~3 h. The white-yellow precipitate was filtered and, for the C₄ and C₆ rulers, further purified by an extraction from deionized water and chloroform. The ionic product was removed from the aqueous phase by rotary evaporation. Rulers were then dried under vacuum.

N,N-Dimethyl-2-(*p*-nitrophenoxy)ethylamine (C₂ Dimethylamine): Following Procedure I, this compound was prepared by adding 3.88 g (47.6 mmol) of **1** to 0.347 g (6.19 mmol) of KOH. The KOH was allowed to dissolve for approximately 1 h. Then, 0.672 g (4.76 mmol) of pFNB was added dropwise to the stirring solution over 10 min. Upon completion, the reaction mixture was treated as described above giving a yellow oil (65%): R_f = 0.20 (2:3, hexanes/EtOAc); ¹H NMR (CDCl₃) 2.274 (s, ~7H), 2.695 (t, J = 5.6, 2H), 4.081 (t, J = 5.6, 2H), 6.903 (d, J = 7.2, 2H), 8.101 (d, J = 7.2, 2H); ¹³C NMR (CDCl₃) 45.9, 58.0, 66.7, 114.7, 126.1, 141.8, 163.9; LRMS (FAB) 211.2 (MH⁺, 100), 58.0 (63), 72 (43).

N,N-Dimethyl-3-(*p*-nitrophenoxy)propylamine (C₃ Dimethylamine): Following Procedure I, this compound was prepared by adding 4.61 g (44.6 mmol) of **1** to 0.326 g (5.80 mmol) of KOH. The KOH was allowed to dissolve for ~1 h. Then, 0.630 g (4.46 mmol) of pFNB was added dropwise to the stirring solution over 10 min. Upon completion, the reaction mixture was treated as described above giving a yellow oil: R_f = 0.33 (1:1, CHCl₃/MeOH); ¹H NMR (CDCl₃) 1.956 (q, J = 6.8, 2H), 2.221 (s, ~7H),

2.424 (t, $J = 7.2$, 2H), 4.079 (t, $J = 6.4$, 2H), 6.914 (d, $J = 9.2$, 2H), 8.144 (d, $J = 9.2$, 2H); ^{13}C NMR (CDCl_3) 27.3, 45.5, 56.1, 67.1, 114.6, 126.1, 141.6, 164.3; LRMS (EI) 58.0 (100), 224 (M^+ , 18); HRMS (EI) calcd for $\text{C}_{11}\text{H}_{16}\text{N}_2\text{O}_3$ 224.1161(M^+), observed 224.1153 (13.2).

N,N-Dimethyl-4-(*p*-nitrophenoxy)butylamine (C_4 Dimethylamine): Following Procedure I, this compound was prepared by adding 4.92 g (42.0 mmol) of **1** to 0.307 g (5.46 mmol) of KOH. The KOH was allowed to dissolve for approximately 1 h. Then, 0.593 g (4.20 mmol) of pFNB was added dropwise to the stirring solution over 10 min. Upon completion, the reaction mixture was treated as described above giving a yellow oil (80%): $R_f = 0.85$ (7:1:0.12, $\text{CHCl}_3/\text{MeOH}/\text{NH}_4\text{OH}$); ^1H NMR (CDCl_3) 1.632 (m, 2H), 1.827 (m, 2H), 2.218 (s, ~7H), 2.316 (t, $J = 7.6$, 2H), 4.043 (t, $J = 6.4$, 2H), 6.906 (d, $J = 8.8$, 2H), 8.156 (d, $J = 8.8$, 2H); ^{13}C NMR (CDCl_3) 24.2, 27.0, 45.6, 59.3, 68.8, 114.6, 126.1, 141.5, 164.3; LRMS (FAB) 239.3 (MH^+ , 100), 58.1 (64); HRMS (FAB) calcd for $\text{C}_{12}\text{H}_{18}\text{N}_2\text{O}_3$ 239.1396 (MH^+), observed 239.1397 (13.2).

N,N-Dimethyl-2-(*p*-nitrophenoxy)hexylamine (C_6 Dimethylamine): Following Procedure I, this compound was prepared by adding 5.453 g (37.5 mmol) of **1** to 0.274 g (4.88 mmol) of KOH. The KOH was allowed to dissolve for approximately 1 h. Then, 0.530 g (3.75 mmol) of pFNB was added dropwise to the stirring solution over 10 min. Upon completion, the reaction mixture was treated as described above giving a yellow oil (48%): $R_f = 0.85$ (5:2:0.12, $\text{CHCl}_3/\text{MeOH}/\text{NH}_4\text{OH}$); ^1H NMR (CDCl_3) 1.34-1.47 (m, ~6H), 1.783 (m, 2H), 2.182 (s, ~7H), 2.228 (t, $J = 6.8$, 2H), 3.999 (t, $J = 6.0$, 2H), 6.886 (d, $J = 7.6$, 2H), 8.136 (d, $J = 7.6$, 2H); ^{13}C NMR (CDCl_3) 26.0, 27.3, 27.7, 45.5, 59.8,

68.9, 114.5, 126.0, 141.4, 164.4; LRMS (FAB) 267 (MH⁺, 100), 58 (85); (EI) 58 (100) 266 (M⁺, 3).

N,N-Trimethyl-2-(*p*-nitrophenoxy)ethylammonium Iodide (C₂ Ruler): Following Procedure II, this compound was prepared by adding ~50 mL of THF to 0.443 g (2.12 mmol) of **2**. While stirring, 0.601 g (4.24 mmol) of MeI was added dropwise to the solution over 10 min. Upon completion, the reaction mixture was treated as described above giving a bright yellow powder (~95%): ¹H NMR (D₂O) 3.131 (s, ~10H), 3.76 (m, 2H), 4.51 (m, 2H), 7.012 (d, *J* = 9.6, 2H), 8.127 (d, *J* = 9.2, 2H); ¹³C NMR (D₂O) -22.6, 53.9, 62.3, 114.8, 126.1, ~164, ~142.

N,N-Trimethyl-3-(*p*-nitrophenoxy)propylammonium Iodide (C₃ Ruler): Following Procedure II, this compound was prepared by adding ~50 mL of THF to the yield of **2** from above. While stirring, 1.268 g (8.93 mmol) of MeI was added dropwise to the solution over 10 min. Upon completion, the reaction mixture was treated as described above giving a pale yellow powder (58% from the two-step process): ¹H NMR (D₂O) 2.212 (m, 2H), 3.037 (s, ~10H), 3.445 (m, 2H), 4.138 (t, *J* = 5.6, 2H), 6.956 (d, *J* = 9.2, 2H), 8.095 (d, *J* = 8.8, 2H); ¹³C NMR (D₂O) -22.6, 22.4, 52.9, 65.2, 114.7, 126.1, 163.6.

N,N-Trimethyl-4-(*p*-nitrophenoxy)butylammonium Iodide (C₄ Ruler): Following Procedure II, this compound was prepared by adding ~50 mL of THF to 0.692 g (2.91 mmol) of **2**. While stirring, 0.955 g (6.72 mmol) of MeI was added dropwise to the solution over 10 min. Upon completion, the reaction mixture was treated as described above giving a pale yellow powder (75%): ¹H NMR (D₂O) 1.75-1.92 (m, 4H), 2.999 (s, ~10H), 3.29 (m, 2H), 4.108 (t, *J* = 6.0, 2H), 6.981 (d, *J* = 9.2, 2H), 8.121 (d, *J* = 9.6, 2H); ¹³C NMR (D₂O) -22.6, 19.3, 25.0, 30.1, 52.8, 67.9, 114.7, 126.1, 163.9.

N,N-Trimethyl-6-(*p*-nitrophenoxy)hexylammonium Iodide (C₆ Ruler): Following Procedure II, this compound was prepared by adding ~50 mL of THF to 0.258 g (0.97 mmol) of **2**. While stirring, 0.275 g (1.94 mmol) of MeI was added dropwise to the solution over 10 min. Upon completion, the reaction mixture was treated as described above giving a pale yellow powder (81%): ¹H NMR (D₂O) 1.28-1.43 (m, 4H), 1.704 (m, 4H), 2.962 (s, 9H), 3.184 (m, 2H), 4.053 (t, *J* = 6.0, 2H), 6.959 (d, *J* = 8.0, 2H), 8.104 (d, *J* = 8.4, 2H); ¹³C NMR (D₂O) -22.6, 22.1, 24.6, 25.0, 27.8, 52.7, 66.5, 68.9, 114.7, 126.1, 140.9, 164.1.

2.3. UV Absorbance Spectroscopy

Electronic absorption spectra were obtained for neutral dimethylamine and cationic ruler species in various protic and aprotic solvents to determine their solvent-dependent absorbance maxima. These data were acquired using either a double-beam Hitachi U-3010 or a single-beam Hewlett-Packard 8452 A diode array spectrophotometer with 2 nm resolution. In all cases, spectra were acquired in various solvents with concentrations of 1 mM or less to keep the absorbance <1.0. An unexpected disparity in wavelength maxima for neutral amine and cationic ruler species was observed. Results from nuclear Overhauser enhancement NMR experiments indicate that this inconsistency can be attributed to intramolecular charge-dipole interactions between the aromatic probe and the cationic headgroup (see below).

UV spectra were collected using the Hitachi U-3010 (resolution was 0.5 nm) for PNP aqueous solutions containing simple salts at varying salt concentrations. Solutions were prepared using distilled, deionized water, and PNP concentrations were 0.1 mM or less to keep the absorbance <1.0. Since the pK_a of PNP is 7.15,⁵ an equilibrium

distribution of PNP and the conjugate base, *p*-nitrophenoxide (PNP^-) exists in bulk solution at neutral pH. UV spectra of salt-free neutral, acidic, and basic PNP solutions are shown in Figure 2.3. Acidic and basic solutions give rise to PNP and PNP^- spectra, respectively. Both bands fit Gaussian distributions and are separated from one another by ~ 80 nm. For bulk solution salt-dependence studies of PNP, the solute was kept in its neutral state by ensuring that all solutions were at a pH of ~ 3 .

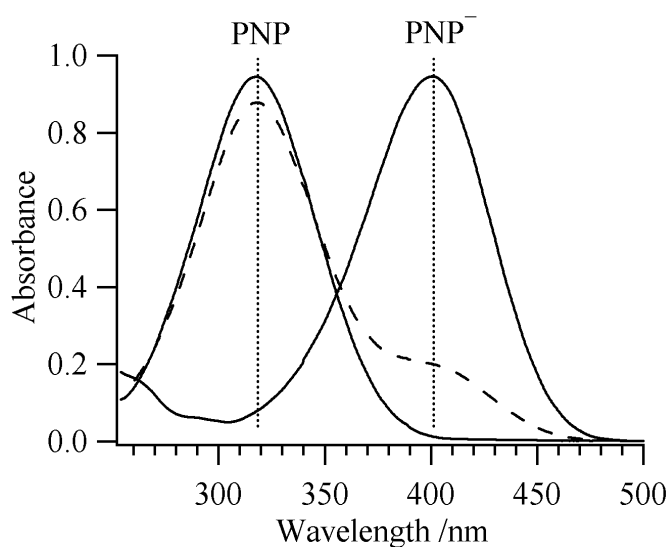


Figure 2.3. Bulk aqueous solution spectra of PNP under acidic, neutral, and basic conditions. At neutral pH (dashed line), the spectrum contains contributions from both PNP and PNP^- . Under acidic or basic conditions (solid lines), the solution contains entirely PNP ($\lambda_{\text{max}} = 318$ nm) or PNP^- ($\lambda_{\text{max}} = 400$ nm), respectively.

2.4. Nuclear Overhauser Enhancement NMR Spectroscopy

The presence of through-space intramolecular interactions in cationic molecular rulers was confirmed by nuclear Overhauser enhancement (NOE) NMR spectroscopy. A NOE experiment probes the proximity of protons on different parts of the same molecule,⁶ and assumes that the spins are close enough together to experience dipole-

dipole interactions but do not experience spin-spin coupling (the coupling that gives rise to the multiplicity in traditional NMR experiments). Additionally, we assume that the solute molecule is rigid and tumbles isotropically in solution. The nuclear spins in the NOE experiment are referred to as I and S where I is the spin whose resonance is measured and S is the spin whose resonance is saturated, irradiated so that the observable net magnetization disappears. Each spin can exist in a low energy state, α , or a high energy state, β , according to the energy level diagram shown in Figure 2.4.

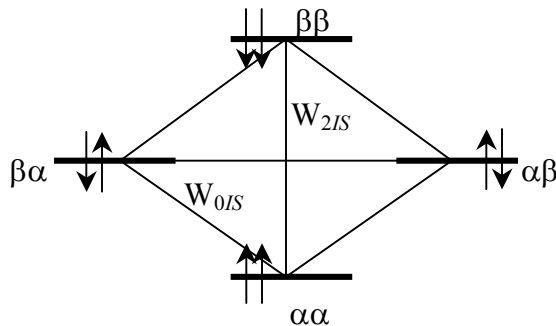


Figure 2.4. Energy level diagram for a two-spin system. Spin states are written with the state of I first and that of S second.

Provided that the two spins are close enough in space to experience dipole-dipole (through-space) coupling, there are two cross-relaxation pathways that give rise to NOE enhancement. The simultaneous transition of both spins from the α state to the β state is referred to as the W_2 transition and has a transition probability equal to W_{2IS} . The transition associated with the flip of both spins from opposite states is called the W_0 transition and has a transition probability of W_{0IS} . Our discussion of NOE enhancement focuses on the W_{2IS} relaxation mechanism since that is the relevant relaxation mechanism

for small molecules such as molecular rulers. NOE enhancement $f_I\{S\}$ is defined as the fractional change in the intensity of resonance I upon saturation of spin S and is given as

$$f_I\{S\} = \frac{(I - I^0)}{I^0} \quad (2.1)$$

where I^0 is the equilibrium intensity of spin I and I is the intensity of resonance I measured during the NOE experiment.

For the two-spin system at thermal equilibrium, level $\alpha\alpha$ lies lowest in energy and is the most populated state. The highest energy state is the $\beta\beta$ state, and it is the least populated. The degenerate $\alpha\beta$ and $\beta\alpha$ states are of an intermediate energy and are equally populated. The intensity of a resonance peak is proportional to the sum of the population differences of each state corresponding to the transitions of the particular spin ($\alpha\alpha \leftrightarrow \beta\alpha$ and $\alpha\beta \leftrightarrow \beta\beta$ for I or $\alpha\alpha \leftrightarrow \alpha\beta$ and $\beta\alpha \leftrightarrow \beta\beta$ for S). Since the differences in population for each of the four single quantum transitions ($\alpha\alpha \leftrightarrow \beta\alpha \leftrightarrow \beta\beta \leftrightarrow \alpha\beta$) are equal, it follows that I^0 equals S^0 , the equilibrium intensity of spin S . Figure 2.5a shows the relative population distributions for a system at equilibrium.

As resonance S is saturated, as in an NOE experiment, the populations of levels $\alpha\alpha$ and $\alpha\beta$ become equal. The same is true for the population of states $\beta\alpha$ and $\beta\beta$. This causes the population of states $\alpha\beta$ and $\beta\beta$ to increase and the population of states $\alpha\alpha$ and $\beta\alpha$ to decrease relative to their equilibrium populations as shown in Figure 2.5b. A relaxation through the W_2 mechanism will act to restore the populations of $\alpha\alpha$ and $\beta\beta$ to their equilibrium populations. Decreasing the population of state $\beta\beta$ and increasing the population of $\alpha\alpha$ results in an increase in the population difference

corresponding to the transitions $\alpha\alpha \leftrightarrow \beta\alpha$ and $\alpha\beta \leftrightarrow \beta\beta$, as shown in Figure 2.5c.

Increasing the population difference in these states results in an enhancement in the intensity of resonance I .

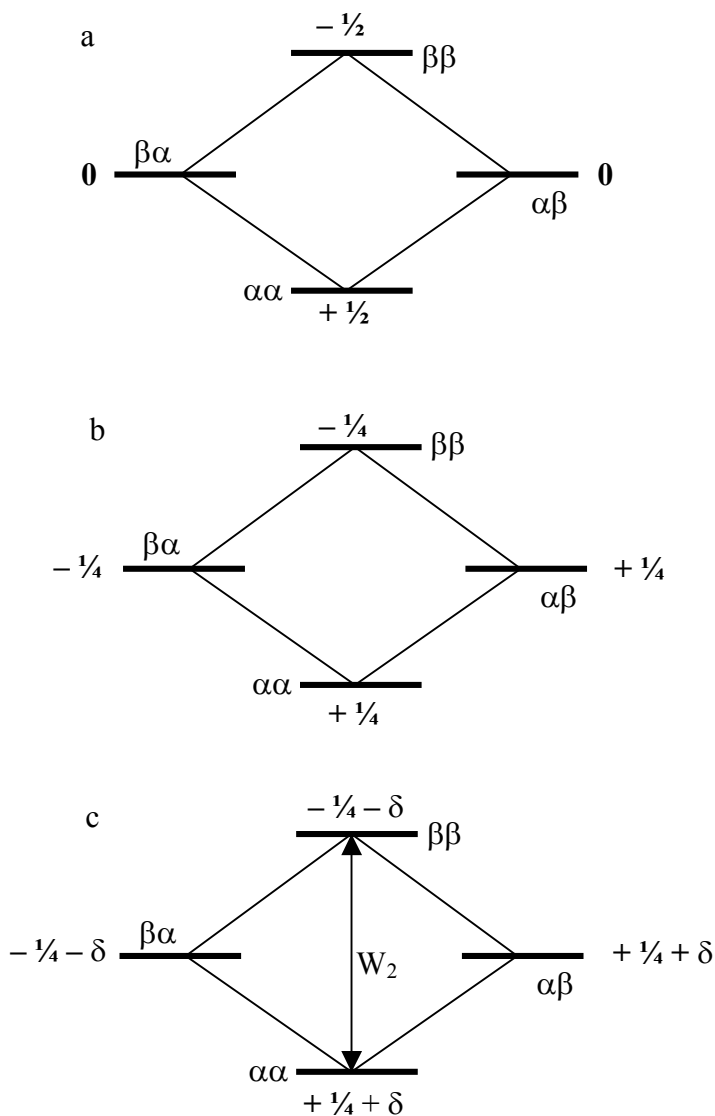


Figure 2.5. Transitions giving rise to NOE enhancement in a homonuclear two-spin system. System a shows the relative populations of each state when the system is at equilibrium. Immediately after spin S is saturated, the populations shift to reflect those shown in system b. As the system relaxes through the W_2 cross-relaxation mechanism, the populations shift by δ giving rise to an enhancement in the intensity of resonance I .

For the surfactants in question, a selective excitation NOE experiment using Gaussian mixing pulses⁷⁻⁹ can examine headgroup-chromophore association in the cationic rulers. A 400 MHz Bruker AM400 was used to irradiate the cationic rulers dissolved in D₂O at the chemical shift corresponding to the methyl groups of the quaternary trimethylammonium headgroup with a mixing time of 1 s. Neutral precursors dissolved in CDCl₃ were also inspected by irradiating at the chemical shift corresponding to the methyl groups of the dimethylamine using the same mixing time as for the rulers. All solutions were saturated. Percent enhancement is determined by peak integration. Values are reported relative to the irradiated peak, which is assigned a value of (-) 100%. Because the irradiated protons appear as isolated singlets in most ruler NMR spectra, the issue of incomplete saturation can be avoided.⁶ (The alkyl region of the NMR spectrum for the C₆ ruler is too crowded for clean excitation of the methyl singlet). Thus, percent enhancement results are reported with no correction for partial saturation. Also, paramagnetic species such as O₂ were not removed from the sample, and enhancement may be reduced due to the rapid spin-lattice relaxation that these species provide.⁶

We note that differences in NOE enhancement do not have to arise solely from proximity effects.¹⁰ Enhancement is also inversely proportional to the relaxation rate (T_i) of the detected nucleus (i) and this rate is not necessarily identical for all spins. For example, if two magnetically inequivalent protons are such that a nucleus close to the irradiated spin has a faster relaxation rate than a nucleus that is further from the irradiated spin, enhancement could be the same for each resonance despite their different proximities to the saturated spin (Figure 2.6a). Another possibility is that two spins having different relaxation rates can show different enhancement although they are the

same distance from the irradiated spin (Figure 2.6b). In the NOE spectra of the cationic molecular rulers, we observe the enhancement of equivalent protons in each ruler spectrum. Given that each ruler is magnetically similar (analogous proton spins in each ruler have similar relaxation rates), we assume that differences in enhancement from spectrum to spectrum are due solely to proximity effects rather than a combination of distance and varying spin relaxation rates.



Figure 2.6. Schematic representation of how enhancement in NOE spectra can vary depending on the relaxation rate of a nucleus. (a) If the relaxation times of the nuclei are such that $T_2 > T_1$ and $r_2 > r_1$, it is possible for the peaks corresponding to nuclei 1 and 2 to show the same enhancement even though their proximities to the saturated nucleus are different. (b) If two nuclei are the same distance from the saturated spin, but the relaxation times are different ($T_1 \neq T_2$), the enhancement in the peaks corresponding to nuclei 1 and 2 will be different.

2.5. Surface Activity

The surface activity of surfactants can be determined by measuring the surface tension of surfactant-containing aqueous/organic interfaces using the Wilhelmy plate method.¹¹ A platinum plate attached to a balance is submerged into the aqueous phase below the aqueous/organic interface. As the plate is drawn up through the interfacial region, the aqueous phase will wet the plate, exerting a tension (γ) on the plate that can be calculated from the mass (m) displayed on the balance:

$$\gamma = \frac{mg}{l} \quad (2.2)$$

where g is the acceleration of gravity and l is the perimeter of the plate (2x the length of the plate). Figure 2.7 illustrates the experimental setup used for determining the interfacial tension of the neat water/cyclohexane interface.

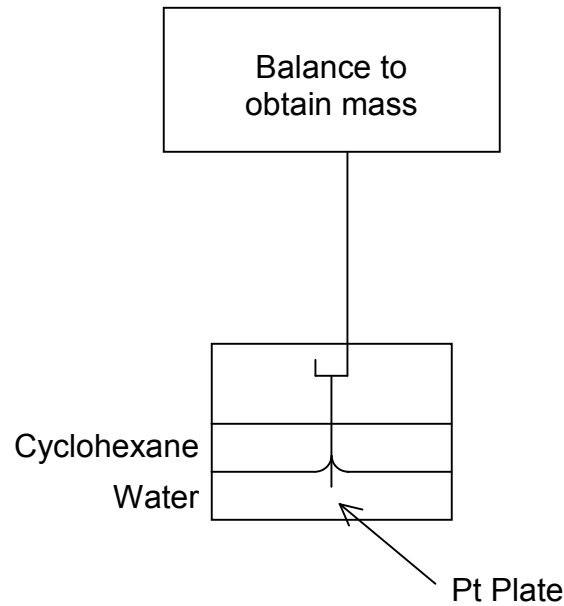


Figure 2.7. Schematic representation of the Wilhelmy plate experimental setup used to determine the surface tension of surfactant containing liquid/liquid interfaces. A more detailed explanation and derivation of equations can be found in Ref. 11.

As surfactants adsorb to the interfacial region, interfacial free energy decreases. The aqueous phase has a lesser tendency to wet the plate resulting in a decrease in the surface tension relative to that of the neat interface (γ_0). Excess surface concentration, the number of molecules in a given surface area (Γ/A), can be determined by plotting the interfacial pressure (π) as a function of the bulk solution activity (a) according to the Gibbs equation:¹¹

$$A\pi = A(\gamma_0 - \gamma) = \Gamma RT \ln(a) \quad (2.3)$$

where R is the gas constant, and T is the temperature. Since measurements are taken at millimolar concentrations or less, the activity can be approximated by the bulk solution concentration, c . The slope of steepest ascent in a plot of π versus $\ln(c)$ will yield the limiting terminal surface concentration, Γ/A for a given surfactant.

$$\frac{\partial \pi}{\partial \ln(c)} = \frac{\Gamma}{A} RT \quad (2.4)$$

Surface tension measurements were performed for cationic molecular rulers, PNP, and NaPNP at the water/cyclohexane interface. Aqueous solutions were allowed to equilibrate for at least one hour with an adjoining cyclohexane phase. The solubilities of PNP and NaPNP dictate that the concentrations ranged from 0 to 20 mM for PNP solutions and 0 to 500 mM for NaPNP solutions. To measure the surface activity of “pure” PNP (without contributions from PNP^-), acidic solutions were prepared by adding HCl to lower the pH to 2-3. The total ion concentration for PNP and NaPNP solutions comes from hydronium and chloride ions and the Na^+ counterion, respectively. In acidic PNP solutions the concentrations of H_3O^+ and Cl^- are small compared to the total PNP concentration (~10%). Assuming total dissociation, in NaPNP solutions the Na^+ concentration is equal to the PNP^- concentration, but sodium ions are small and positively charged and therefore have a tightly bound hydration shell. Compared to the aromatic PNP^- , Na^+ ions are less likely to adsorb to the surface and should have a negligible effect on PNP^- adsorption. Also, surface tension measurements of PNP at the water/cyclohexane interface in the presence of 1 M sodium salts show little deviation (~7%) in interfacial pressure compared to measurements in the absence of the sodium salts.

2.6. Resonance-Enhanced Second Harmonic Generation

To observe the polarity surrounding a solute adsorbed to a liquid/liquid interface, we use resonance-enhanced second harmonic generation (SHG). SHG is a nonlinear optical spectroscopic method that allows for the measurement of the electronic excitation energy of a surfactant adsorbed to an interface.^{12,13} This technique is both surface-specific and molecularly-specific, making it a very powerful method for probing buried interfaces.¹⁴⁻¹⁶ Experimentally, light with frequency ω is focused onto an interface, and a signal with frequency 2ω is detected. The intensity of the detected signal is proportional to the square of the second-order susceptibility tensor, $\chi^{(2)}$:

$$I(2\omega) \propto |\chi^{(2)}|^2 I(\omega)^2 \quad (2.5)$$

where $I(2\omega)$ and $I(\omega)$ are the intensities of the detected (2ω) and incident light (ω), respectively. Within the dipole approximation, $\chi^{(2)}$ is zero in isotropic environments meaning that any detected second harmonic (SH) signal necessarily arises from the anisotropic boundary between the aqueous and organic phases. The $\chi^{(2)}$ tensor is composed of both nonresonant and resonant contributions:¹⁷

$$\chi^{(2)} = \chi_{NR}^{(2)} + \chi_R^{(2)} \quad (2.6)$$

The resonant contribution is typically quite large relative to the nonresonant contribution. $\chi_R^{(2)}$ is related to the microscopic hyperpolarizability through the following relationship:

$$\chi_R^{(2)} = \sum_{k,e} \frac{\langle \mu_{gk} \mu_{ke} \mu_{eg} \rangle}{(\omega_{gk} - \omega - i\Gamma)(\omega_{eg} - 2\omega + i\Gamma)} \quad (2.7)$$

where μ_{ij} represents the transition matrix element between states i and j (g is the ground state, e is the first excited state, and k is some virtual intermediate state), ω_{ij} is the energy of the transition from state i to j , and Γ is the spectral line width.¹⁷ According to this relation, when 2ω is resonant with ω_{eg} , as depicted in Figure 2.8, $\chi^{(2)}$ becomes large yielding a strong resonant enhancement in the intensity of the detected signal, $I(2\omega)$, according to Eq. 2.5. Measuring $I(2\omega)/I(\omega)^2$ as a function of 2ω and fitting the data with Eqs. 2.5-2.7 yields an *effective* excitation spectrum of a surfactant adsorbed to an interface. The uncertainty associated with the reported intensities of the second harmonic signals is discussed in detail in Appendix B.

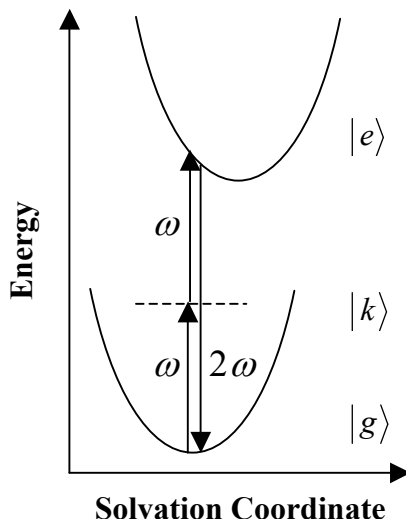


Figure 2.8. Resonance of ω_{eg} and 2ω . Intensity of the second harmonic signal is enhanced when the frequency of the incident light corresponds to the difference in energy between the ground state g and some virtual state k that lies halfway between the energies of the ground and excited states.

The fit to the above equations gives four parameters that describe the spectrum: the excitation energy of the surfactant adsorbed to the interface, the spectral line width, the line strength of the excitation band, and the nonresonant contribution to $\chi^{(2)}$. When analyzing spectral data, all four parameters are considered since each one provides useful information about the system. The wavelength of the excitation is used primarily to characterize interfacial polarity by comparing it to bulk solution limits. The width of each spectrum stems from both underlying vibronic transitions and inhomogeneous broadening. The FWHM of a spectrum tells us about the heterogeneity of the solute's surroundings. The more microenvironments sampled by a solute, the broader the spectrum will be. No trends associated with line width were observed in the collection of the data presented in this work.

The line strength of a spectrum is dependent on the cross-section of the dipole moment transition matrix. The better the overlap between the ground and excited states, the greater the intensity of the SH signal. Another explanation for an increase in the line strength would be an increase in the excess surface concentration. However, since the same chromophore is used throughout, and surface concentration (which is controlled by bulk solution concentration) is kept relatively constant, the line strength for each spectrum is of the same order of magnitude, and no systematic trends were observed.

Finally, the nonresonant contribution to $\chi^{(2)}$ can provide qualitative information about the symmetry within the interfacial region. Since $\chi^{(2)}$ is related to the hyperpolarizability, a less polarizable interface will have a weaker nonresonant SH signal. $\chi_{NR}^{(2)}$ for each spectrum is relatively small and varies from day to day. When spectra are averaged together, nonresonant contributions to $\chi^{(2)}$ are typically canceled out.

SHG spectra in this work were acquired under either $P_{\omega}P_{2\omega}$ or $P_{\omega}A_{2\omega}$ polarization conditions, where P polarized light describes light that is polarized in the plane defined by the direction of propagation and the surface normal, and A indicates no discrimination of polarization. However, different polarizations did not lead to qualitatively different SHG spectra.

Varying the incident and detected polarizations enables us to determine the average chromophore orientation using methods described previously.¹⁸ The chromophores used in these studies have three nonzero $\chi^{(2)}$ elements that can be determined by measuring the polarization-dependent SH intensity at the chromophore's electronic excitation wavelength. In principle, these elements can be used to calculate solute orientation in the laboratory frame of reference. However, the calculated orientation is only an ensemble average and does not quantify the distribution of molecular orientations. Only by measuring the phase of the SH signal relative to a known reference can absolute molecular orientations be determined. Such experiments are common at air/liquid and air/solid interfaces but are prohibitively difficult at buried interfaces due to the dispersive nature of both phases.¹⁹ We note that the calculated molecular orientations are slightly larger than the SH "magic angle" of 39° described by Simpson and Rowlen.²⁰ This difference suggests that, whatever contribution surface roughness may make to the measurement of SH intensity, the solutes preferentially adopt an "in-plane" arrangement when adsorbed to the liquid/liquid interfaces studied in this work.

The intensities of P and S (perpendicular to the plane of incidence) polarized SH signals can be related to the three nonzero components of $\chi^{(2)}$. By measuring the intensity

of the S polarized SH signal with an incident beam polarization set at 45° from the plane defined by the surface normal and the field of propagation, we can determine $\chi^{(2)}_{XXZ}$, one of the three nonzero components of $\chi^{(2)}$. The other two nonzero components $\chi^{(2)}$ are determined by measuring the intensity of the P polarized SH signal as a function of the polarization of the incident light. Since $\chi^{(2)}$ is related to the molecular hyperpolarizability, through fitting routines developed in our lab,²¹ we can determine the molecular orientation of solutes adsorbed to liquid/liquid and liquid/vapor interfaces.

The SHG apparatus is built around a Ti:sapphire regeneratively amplified, femtosecond laser (Clark-MXR CPA 2001) that produces 130 fs pulses with energies of 700 μ J at a wavelength of 775 nm and a repetition rate of 1 kHz. The output of the Ti:sapphire laser pumps a commercial optical parametric amplifier (OPA, Clark-MXR). The visible output of the OPA is tunable from 700 nm down to 550 nm, with a bandwidth of 0.5-2.5 nm. The polarization of the incident beam is controlled using a Glan-Taylor polarizer and a half-wave plate. A series of filters blocks the fundamental 775 nm light and any SH light generated from the preceding optical components. SH photons are detected at the angle of reflection using photon-counting electronics. Typical signal levels average 0.01-0.1 photon per shot. A second polarizer selects the polarization of the SH signal, and a short pass filter and monochromator serve to separate the SH signal from background radiation. A schematic diagram of the experimental setup is illustrated in Figure 2.9.

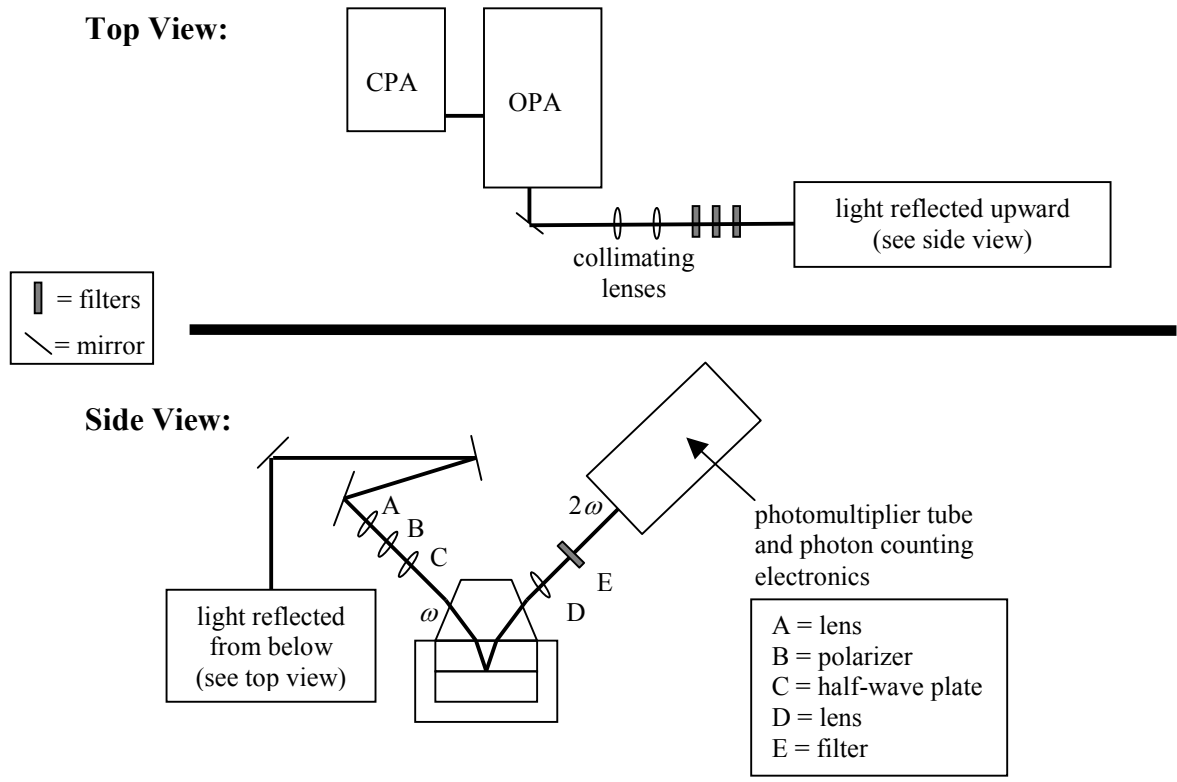


Figure 2.9. Block diagram of SHG experiment. 775 nm light from a chirped pulsed amplifier (CPA) is directed into an optical parametric amplifier (OPA) that allows the wavelength of the incident beam to be tuned from 550 to 700 nm. Light with frequency ω is focused onto the interface and the intensity of the coherently scatter second harmonic signal is recorded from photon counting electronics.

Because the visible OPA cannot be synchronously tuned, acquisition of a complete SHG spectrum requires several hours. A typical procedure entails allowing the sample to equilibrate and manually tuning the incident visible light to each desired wavelength. System alignment is reoptimized at every wavelength to account for the wavelength-dependent changes in the angle of the reflected SH signal. At each wavelength, SH data are collected for four 10-s intervals and normalized for incident power. Although tedious, this procedure ensures that spectra are reproducible. A single wavelength might be sampled three separate times several hours apart (beginning, middle, and end of an acquisition sequence). If the normalized SH signal from each of

these three samplings does not fall within experimental uncertainty (typically ~15%), data acquisition is halted and the spectrum is discarded. In addition, data at the same wavelength were often acquired using several different incident powers and then normalized to confirm quadratic dependence of the SH signal intensity on the incident field intensity predicted by Eq. 2.5. To within limits of experimental accuracy (~15%), the predicted quadratic behavior was always observed.

Interfacial systems probed by cationic surfactants typically had surface coverages of less than 20% of a full monolayer. These fractional coverages lead to surface excess concentrations of $\sim 1 \times 10^{13}$ molecules/cm². Spectra of anionic surfactants were acquired from monolayers having similar fractional coverage, although absolute surface concentrations were $\sim 5 \times 10^{13}$ molecules/cm² due to the reduced surface activity of the anionic species. Studies involving PNP at liquid/liquid interfaces had surface coverage of about 80% of a full monolayer corresponding to a surface excess concentration of 1×10^{14} molecules/cm².

Liquid/liquid interfaces were generated by first adding aqueous solutions to a cylindrical kel-F cell having a reservoir 4 cm in diameter. Then, an application of a thin layer (~1-3 mm) of organic solvent atop the aqueous solution creates the aqueous/organic interface. A trapezoidal fused silica prism (50 x 50 x 30 mm, JDSU Casix) is secured atop the reservoir, preventing evaporation of the solvent. Prior to use the prism is cleaned in a 50:50 mixture of sulfuric and nitric acids. Prisms cleaned in this way have been shown to be hydrophilic, as demonstrated by complete wetting of the surface. All SHG spectra were acquired at room temperature, 22 ± 1.5 °C. Experiments carried out at the liquid/vapor interfaces of octanol-containing aqueous solutions took advantage of the

1-octanol monolayer that forms spontaneously at the liquid/vapor interface. At room temperature, 1-octanol is soluble in water up to concentrations of ~ 2.8 mM (mole fraction $\sim 5 \times 10^{-5}$).²² 1-Octanol in saturated aqueous solutions spontaneously self assembles to form monolayers that are reasonably compressed (4.8×10^{14} molecules/cm² or $21 \text{ \AA}^2 \text{ molecule}^{-1}$), and surface vibrational spectra show that these monolayers possess a high degree of conformational order.²³

References

- (1) Steel, W. H.; Damkaci, F.; Nolan, R.; Walker, R. A. *J. Am. Chem. Soc.* **2002**, *124*, 4824.
- (2) Siuzdak, G.; Bothner, B. *Angew. Chem., Int. Ed. Engl.* **1995**, *34*, 2053.
- (3) Hao, C.; March, R. E. *J. Mass Spectrom.* **2001**, *36*, 509.
- (4) Rarick, M. J.; Brewster, R. Q.; Dains, F. B. *J. Am. Chem. Soc.* **1933**, *55*, 1289.
- (5) *CRC Handbook of Chemistry and Physics*; 77th ed.; Lide, D. R., Ed.; CRC Press: Boca Raton, Florida, 1996.
- (6) Neuhaus, D.; Williamson, M. P. *The Nuclear Overhauser Effect in Structural and Conformational Analysis*, 2nd ed., 2000.
- (7) Kessler, H.; Oschkinat, H.; Griesinger, C.; Bermel, W. *J. Magn. Reson., Ser.* **1986**, *70*, 106.
- (8) Stonehouse, J.; Adell, P.; Keeler, J.; Shaka, A. J. *J. Am. Chem. Soc.* **1994**, *116*, 6037.

- (9) Stott, K.; Stonehouse, J.; Keeler, J.; Hwang, T.-L.; Shaka, A. J. *J. Am. Chem. Soc.* **1995**, *117*, 4199.
- (10) Noggle, J. H.; Schirner, R. E. *The Nuclear Overhauser Effect: Chemical Applications*, 1971.
- (11) Adamson, A. W. *Physical Chemistry of Surfaces*; John Wiley & Sons: New York, 1990.
- (12) Eienthal, K. B. *J. Phys. Chem.* **1996**, *100*, 12997.
- (13) Richmond, G. L. *Annu. Rev. Phys. Chem.* **2001**, *52*, 357.
- (14) Wang, H.; Borguet, E.; Eienthal, K. B. *J. Phys. Chem. A* **1997**, *101*, 713.
- (15) Zhang, X.; Esenturk, O.; Walker, R. A. *J. Am. Chem. Soc.* **2001**, *123*, 10768.
- (16) Zhang, X.; Walker, R. A. *Langmuir* **2001**, *17*, 4486.
- (17) Shen, Y. R. *Nature* **1989**, *337*, 519.
- (18) Zhang, X.; Steel, W. H.; Walker, R. A. *J. Phys. Chem. B* **2003**, *107*, 3829.
- (19) Stolle, R.; Marowsky, G.; Schwarzberg, E.; Berkovic, G. *Applied Physics B: Lasers and Optics* **1996**, *B63*, 491.
- (20) Simpson, G. J.; Rowlen, K. L. *Chem. Phys. Lett.* **2000**, *317*, 276.
- (21) Zhang, X. Investigations of Surface Mediated Solvation at Solid/Liquid Interfaces by SHG Spectroscopy, University of Maryland, 2003.
- (22) Schefflan, L.; Jacobs, M. B. *The Handbook of Solvents*, 1953.
- (23) Esenturk, O.; Mago, D.; Walker, R. A. *In preparation* **2005**.

Chapter 3. Interfacial Polarity Surrounding Cationic Molecular Rulers at the Water/Cyclohexane Interface

3.1. Introduction

Liquid/liquid interfaces play prominent roles in phenomena ranging from solvent extraction to emulsification to phase transfer catalysis.¹⁻³ These boundaries also frequently serve as models for biological processes occurring at membrane surfaces.^{3,4} However, despite the importance of these interfaces in chemistry, physics, and biology, they have not received the same level of scrutiny as more accessible vapor/liquid and solid/liquid systems. Molecular dynamics simulations provide some insight into structure and dynamics at these boundaries, but many predictions from these studies have gone untested due to a lack of experimental information.⁵⁻⁸ Of particular interest is the distance required for an aqueous solvation environment to converge to an organic limit. The width of a liquid/liquid interface will control the concentrations, conformations, and reactivities of adsorbed solutes.

In this work, we describe the characterization of a new family of cationic surfactants designed to characterize interfacial widths of different aqueous/organic boundaries. These surfactants, dubbed “molecular rulers,” consist of solvent-sensitive, hydrophobic chromophores attached to quaternary ammonium headgroups by means of variable length alkyl spacers. Varying the length of the spacer changes the separation between the headgroup and the chromophore. For most aqueous/organic systems, dielectric considerations require that the headgroup remain solvated in the aqueous phase. The hydrophobic chromophore, however, prefers to be solvated by the organic solvent.

Lengthening the alkyl spacer enables the chromophore to extend further into the organic phase (Figure 1.3). The surfactants described below integrate an aromatic, solvatochromic chromophore into the molecular ruler architecture. The chromophore is based on *p*-nitroanisole (pNAs), a solute whose excitation wavelength varies monotonically by ~25 nm as solvent polarity varies between that of alkanes and that of polar solvents such as water, dimethyl sulfoxide, and *N,N*-dimethylformamide. Thus, these surfactants can serve as sensitive indicators of how the local dielectric environment around a solute changes across different liquid/liquid interfaces.

Surface-specific, nonlinear optical methods can probe the electronic structure of surfactant chromophores as a function of surfactant chain length.⁹⁻¹² By observing how the solvent-sensitive chromophore response varies with headgroup-chromophore separation, one can infer a dipolar width of different liquid/liquid interfaces. Here, dipolar width refers to the distance required for solvent polarity to converge from an aqueous to an organic limit.¹³ This point raises an important distinction between spectroscopic and scattering studies of liquid/liquid interfacial properties. Neutron and X-ray scattering experiments probe structure and can provide important information about molecular conformation and solvent densities across a liquid/liquid boundary.¹⁴⁻¹⁶ Scattering experiments report on structure directly but *cannot* identify solute-solvent interactions responsible for interfacial solvation and solution phase surface chemistry. In contrast, spectroscopic experiments are explicitly sensitive to intermolecular interactions and identify both long- and short-range interactions between a solute and its environment. In other words, the nonlinear optical experiments described in this work and elsewhere

report on the solvation environment surrounding chromophores adsorbed to interfaces.¹⁷⁻¹⁹ From these data, interfacial solvent structure is inferred.

Previous reports indicated that the polarity of different liquid/liquid interfaces could be described by averaged contributions from the two adjacent phases.^{20,21} This conclusion was based on solvatochromic data from several different probes adsorbed to a number of different interfaces. Resonance enhanced second harmonic generation (SHG) was used to acquire these results, thus ensuring that data originated only from those solutes in the anisotropic, interfacial region. More recent reports suggest that the “average polarity” model breaks down with polar organic phases, but these conclusions are based on results from fluorescence anisotropy experiments, a technique that is not intrinsically surface-specific.²² Molecular dynamics simulations demonstrated how the average polarity model could arise *if* an interface were molecularly sharp but thermally roughened.²³ However, these simulations *also* suggested that results should prove very sensitive to solute orientation *and* solute location relative to the interfacial Gibbs dividing surface.

Using SHG techniques²¹ our group has probed the polarity sampled at an aqueous/cyclohexane interface by chromophores that shared very similar electronic structures but differed subtly in their functionality.²⁴ The hydrophilic *p*-nitrophenol sampled an interfacial polarity that was almost water-like, whereas the local dielectric environment surrounding adsorbed 2,6-dimethyl-*p*-nitrophenol was dominated by the nonpolar, alkane phase. These results correlated with bulk solution partitioning experiments and implied that solvation was changing dramatically on very short length scales across this weakly associating, liquid/liquid interface.

To identify these length scales quantitatively, one would like to vary chromophore position relative to the interface in a systematic manner. Molecular ruler surfactants are designed with this goal in mind. The cationic surfactants described in this work complement an existing family of anionic surfactants already developed in our laboratory.²⁵ Both cationic and anionic rulers rely upon the solvatochromic behavior of a pNAs analogue to probe local polarity. However, the cationic surfactants described below have headgroups that are much less hydrophilic than their anionic counterparts. The former consist of quaternized trimethyl ammonium ions, whereas the anionic surfactants have simple sulfate groups. This difference in headgroup identity could, in principle, affect surfactant “float depth,” the equilibrium distribution of surfactant headgroups adsorbed to the liquid/liquid interface. Consequently, molecular rulers having identical probes and alkyl spacers could sample different interfacial environments simply by virtue of differences in surfactant headgroup solvation.

In the process of characterizing the solvatochromic behavior of the cationic surfactants and their neutral precursors, we discovered that the short-chain surfactants self-associate through intramolecular charge-dipole interactions in bulk solution. These interactions were observed with nuclear Overhauser enhancement magnetic resonance experiments. Second harmonic spectra are presented, and results show that cationic surfactants can, in fact, probe solvent polarity across liquid/liquid interfaces.

3.2. Cationic Molecular Ruler Characterization

Solvent Sensitivity

Solvatochromism refers to solvent-dependent shifts in a solute’s electronic excitation or emission spectrum. Thus, solvatochromic solutes are useful tools for

assessing the polarity of a local environment.²⁶ Solvent sensitivity results from differential solvation of a solute's ground and excited states. A solute having a larger dipole in the excited state relative to the ground state will show a red shift in its excitation energy that becomes more pronounced as solvent polarity increases (Figure 1.1). This model forms the basis of empirical solvent polarity scales such as the π^* scale.²⁷

In this work, we choose to characterize solvent polarity according to $f(\epsilon)$, the Onsager polarity function²⁸ (Eq. 1.1). For solutes that are sensitive to long-range, nonspecific solvation forces, solute excitation energy decreases monotonically with $f(\epsilon)$.^{26,29} The Onsager scale is attractive because it enables us to relate excitation energies measured at interfaces to a local dielectric environment. By comparing the excitation energy of an adsorbed chromophore with bulk solution limits, we can infer how solvent polarity changes across different aqueous/organic boundaries.

Of the many solvatochromic probes available, pNAs stands out as an ideal chromophore for probing local polarity at liquid/liquid interfaces. It is a relatively small chromophore that can sample finer variation in local polarity than more traditional probes containing multiple fused aromatic rings. Also, the excitation maximum of pNAs shifts more than 20 nm as solvent polarity increases from that of cyclohexane to that of water.²⁷ This relatively large spectral window enables resonance enhanced SHG measurements to unambiguously identify the local environment surrounding the probe adsorbed to the interface. Finally, pNAs can be readily integrated into the molecular ruler architecture. Figure 3.1 depicts the molecular structure of cationic molecular rulers and their neutral, dimethylamine analogues.

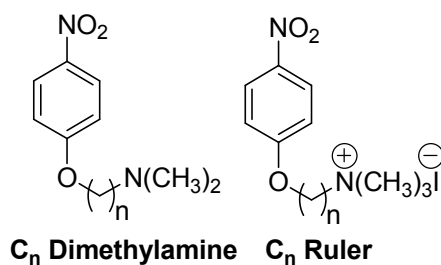


Figure 3.1. Molecular structure of cationic molecular rulers and their neutral, dimethylamine precursors. The subscript n refers to the number of carbons in the alkyl chain separating the chromophore from the headgroup.

Excitation wavelengths of pNAs-based molecular rulers can be measured as a function of $f(\epsilon)$ simply by acquiring solute absorbance spectra in different solvents. Electronic absorption spectra were obtained for neutral and cationic ruler species in various protic and aprotic solvents to determine their solvent-dependent absorbance maxima. Due to the positive charge on the headgroup of cationic molecular rulers, these species could not be dissolved in solvents less polar than 1-octanol. The behavior of the neutral compounds as a function of $f(\epsilon)$ and a representative spectrum can be seen in Figure 3.2.

Previous studies of anionic ruler solvatochromism demonstrated that neither alkyl chain length nor headgroup identity (charged sulfate vs. neutral alcohol) altered the electronic structure of the pNAs-based chromophore.²⁵ One might expect the same to be true for the analogous cationic species. However, in solvents that are capable of solubilizing both neutral and ionic surfactants, the absorbance maxima for the C₂ cationic ruler have an average blue shift of 8 nm from those of the neutral, dimethylamine species, as shown in Figure 3.3. As the spacer length increases, this spectral difference between charged and uncharged species decreases. With spacer lengths of $n = 6$, the

solvatochromic behavior of the cationic species and the neutral precursor are indistinguishable. Wavelength maxima for neutral and cationic species in various solvents are summarized in Table 3.1. Values for the C₂ anionic ruler and its neutral precursor, C₂ alcohol, are included for comparison. Wavelength maxima for the short chain anionic ruler and the neutral alcohol analogue are equivalent for each solvent.

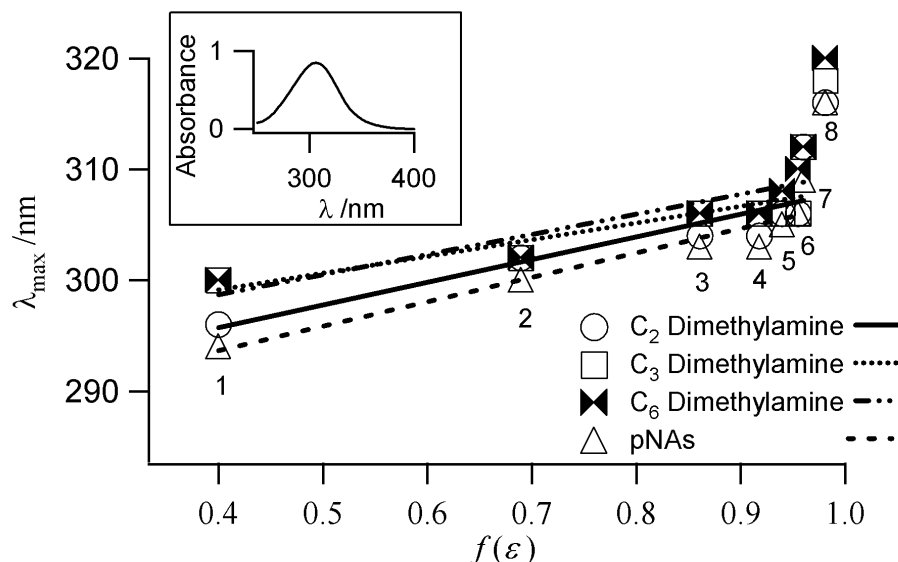


Figure 3.2. Solvatochromic behavior of neutral dimethylamine precursors. These species exhibit absorbance maxima that directly correlate with solvent polarity. Deviations in linearity are a result of specific solvent-solute interactions that occur with solvents that have hydrogen-bonding capabilities. Spectra were acquired in (1) cyclohexane, (2) diethyl ether, (3) 1-octanol, (4) 1-butanol, (5) ethanol, (6) methanol, (7) acetonitrile, and (8) water. The inset shows a typical UV spectrum recorded for C₂ dimethylamine in methanol. Spectral resolution is ± 2 nm.

A blue shift in the excitation spectrum of pNAs usually implies a less polar medium. However, the observed shift described above is for two similar chromophores in the *same* solvent. An alternative explanation for the observed behavior is that the chromophore in the cationic ruler undergoes a smaller change in dipole than the neutral species upon excitation. Such an effect could occur if the cationic headgroup interacted

with the delocalized electron density on the aromatic ring in solution. This intramolecular association would place the headgroup of the cationic ruler spatially near the aromatic ring resulting in an electron withdrawing effect on the chromophore. This interaction would reduce the magnitude of the dipole change arising from excitation and thereby increase the ruler's electronic excitation energy relative to that of the neutral species. A reduction in excited state solvation energy could lead to the observed spectroscopic blue shift.

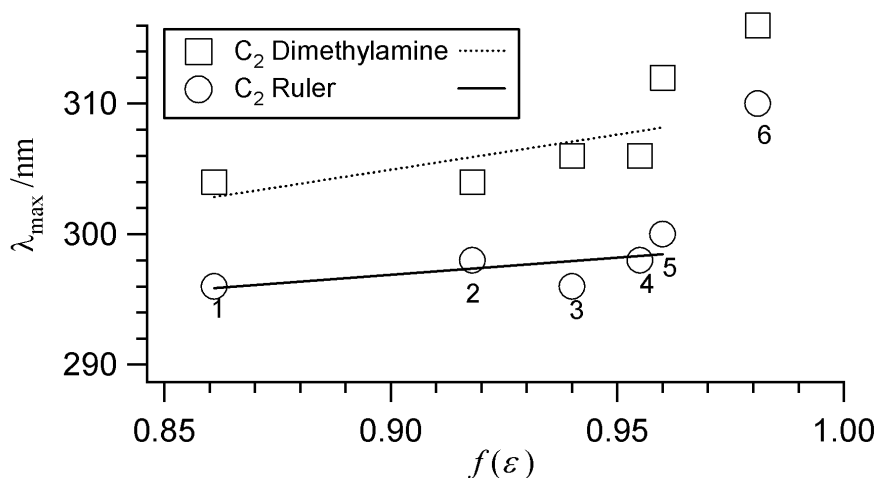


Figure 3.3. Comparisons of absorbance maxima for C₂ dimethylamine and the C₂ cationic ruler in various solvents. Although the electronic behavior of these two compounds was expected to be similar, the absorbance maxima of the C₂ ruler are significantly blue-shifted from those of the C₂ dimethylamine. Spectra were acquired in (1) 1-octanol, (2) 1-butanol, (3) ethanol, (4) methanol, (5) acetonitrile, and (6) water. Spectral resolution is ± 2 nm.

Table 3.1. UV data for cationic rulers, neutral dimethylamine precursors, C₂ anionic ruler and its neutral alcohol precursor in several solvents.

Solvent ^a	$f(\epsilon)$	C ₂ Dimethyl-amine ^b	C ₃ Dimethyl-amine ^c	C ₄ Dimethyl-amine	C ₆ Dimethyl-amine	C ₂ Alcohol
Chex	0.40	296	300	300	300	293
Et ₂ O	0.69	302	302	302	302	302
OctOH	0.86	304	306/308	306/308	306	304
ButOH	0.92	304	306/308	306/308	306/308	306
EtOH	0.94	306	308	308	308	306
MeOH	0.96	306	308	308	310	307
ACN	0.96	312	312/314	312/314	312/314	310
Water	0.98	316	316/318	316/318	318/320	317
		C₂ Cat. Ruler	C₄ Cat. Ruler	C₄ Cat. Ruler	C₆ Cat. Ruler	C₂ An. Ruler
OctOH	0.86	296	304	304	306	306
ButOH	0.92	298	304/306	304/306	308	306
EtOH	0.94	296	302/304	302/304	306	306
MeOH	0.96	298	304/306	304/306	306	306
ACN	0.96	300	308/312	308/312	314	310
Water	0.98	310	318	318	320	316

^a Solvent abbreviations are as follows: Chex=cyclohexane, Et₂O=diethyl ether, OctOH=1-octanol, ButOH=1-butanol, EtOH=ethanol, MeOH=methanol, and ACN=acetonitrile. ^b Wavelength maxima are given in nm. Instrument resolution is 2 nm. ^c When two values are shown, two data sets were recorded.

Intramolecular Charge-Dipole Interactions

An explanation of the observed blue shift in cationic ruler absorbance spectra was tested using nuclear Overhauser enhancement (NOE) nuclear magnetic resonance (NMR) spectroscopy. This technique allows us to probe the “through-space” proximity of inequivalent protons in a molecule. By irradiating a sample at a frequency corresponding

to the chemical shift of a proton in the molecule, an enhancement in the peak intensity corresponding to a nearby proton will be evident in the acquired NMR spectrum.

In the NOE spectra of the cationic rulers shown in Figure 3.4, we compare relative enhancement of features within the same spectrum. This analysis assumes that the interactions between the methyl protons in the headgroup and the protons of the adjacent methylene group are the same in each ruler. Observed enhancement in the aromatic region of the spectrum is scaled accordingly. In the NOE spectrum of the C₂ ruler (Figures 3.4a and 3.4c), the observed enhancement for the methylene protons adjacent to the methyl protons in the headgroup (indicated by *) is 2.76% while the protons meta to the nitro group are enhanced by 0.29%. In the C₃ ruler spectrum (Figure 3.4d), the signal from the methylene protons next to the headgroup is enhanced 2.68%, less than a 0.1% difference when compared to the data for the equivalent protons in the C₂ ruler. In contrast, the NOE enhancement for the protons on the aromatic ring “meta” to the nitro group is only 0.05%, a 5-fold decrease from the C₂ ruler enhancement. Although these enhancements seem small, enhancements smaller than 0.1% can be significant.³⁰ We observe no hint of aromatic proton enhancement for rulers of length longer than $n = 3$ (Figure 3.4e) or in the neutral dimethylamine species.

Since the enhancement of the aromatic signal decreases with increasing chain length, we surmise that the relative distance between the methyl groups on the cationic headgroup and the electron-dense aromatic ring is shorter for short-chain rulers than for rulers having a greater number of methylene spacers (Figure 3.5). That we observe no enhancement in the NOE spectra of neutral species regardless of chain length suggests that the enhancement of the aromatic proton signals in the ruler species is inextricably

correlated with the charge on the cationic headgroup. NOE NMR spectra for neutral dimethylamine species can be found in Appendix A.

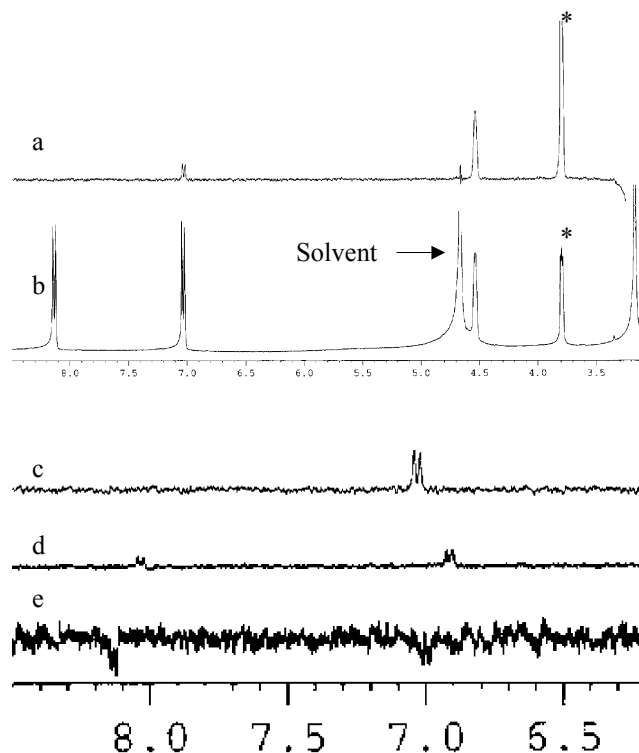


Figure 3.4. NOE spectra of cationic rulers. X-axes are in ppm. The top two spectra show a comparison between an NOE spectrum of C_2 ruler (a) and the corresponding 1H NMR spectrum (b). The signal at ~ 3.8 ppm (indicated by *) arises from the protons on the methylene adjacent to the headgroup and is used to scale the enhancements seen in the aromatic region as described in the text. The bottom three spectra display an expansion of the aromatic region of the NOE spectra for C_2 (c), C_3 (d), and C_4 (e) rulers. A marked decrease in enhancement in signals from protons meta to the nitro group (~ 7 ppm) is evident as the number of alkyl spacers increases. Spectrum e is largely magnified to show that the enhancement there is negligible. Relative enhancement is given with $\pm 0.05\%$ uncertainty.

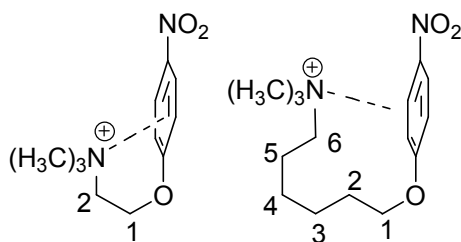


Figure 3.5. Intramolecular charge-dipole interaction for cationic molecular ruler surfactants. The cationic charge on the headgroup interacts with the aromatic ring of the chromophore in cationic molecular ruler surfactants containing two or three carbons in the alkyl chain. One possible configuration for a molecular ruler containing six carbons in the alkyl chain is shown. Note that in this configuration, the methyl protons are not as close to the aromatic ring as they are in the configuration shown for a cationic molecular ruler containing two carbons in the alkyl chain.

There does exist a disparity between the solvatochromic data and the NOE results. UV absorbance experiments imply that headgroup-ring interactions persist in rulers having four methylene spacers, while NOE spectra show that headgroup-ring interactions diminish significantly from the C₂ ruler to the C₃ ruler. According to NOE experiments, such interactions are nonexistent in the C₄ ruler. The differences between the two types of measurements can be readily explained in terms of the forces responsible for each observable. The enhancement of a signal in an NOE experiment is proportional to $\langle 1/r_{ij}^6 \rangle$ where r_{ij} is the distance between the two nuclear spins of interest,³¹ in this case the methyl and aromatic protons. The charge-dipole effects witnessed in the UV spectra correspond to an interaction energy that is proportional to $\langle 1/r_{ij}^2 \rangle$ for a formal charge i interacting with a fixed dipole j .³² Given the long-range nature of charge-dipole forces, we would expect to observe evidence of headgroup-ring interactions in UV absorbance spectra even after NOE enhancement has subsided.

Intramolecular association between the headgroup and the hydrophobic probe could, in principle, inhibit the ability of these cationic surfactants to function as molecular rulers. However, partitioning experiments show pNAs to be 20 times more soluble in cyclohexane than in water,³³ whereas quaternized ammonium species are solubilized by an aqueous solvent exclusively. Given these results, an aqueous/organic interface should promote solvation of the pNAs-based chromophore by the organic phase while the cationic headgroup remains solvated by the aqueous phase thereby inhibiting the intramolecular interactions observed in bulk solution.

Surface Activity

The surface activity and excess surface concentrations of cationic rulers can be determined by measuring adsorption isotherms at different aqueous/organic interfaces as described in Chapter 2. Figure 3.6 shows surface pressure isotherms for the C₂ and C₆ rulers, anionic (top panel) and cationic (bottom panel), acquired from an aqueous/cyclohexane interface using the Wilhelmy plate method.³⁴ The terminal surface concentrations for all of the cationic rulers were between 3 and $8 \pm 1 \times 10^{13}$ molecules/cm². These values agree with surface excess concentrations of other trimethylammonium salts adsorbed to both air/water and other liquid/liquid interfaces.³⁵⁻³⁷ The cationic rulers exhibit terminal surface concentrations that are approximately half that of analogous anionic surfactant rulers.²⁵

This phenomenon can be readily explained by headgroup size considerations. While the surfactants do not pack closely due to charge-charge repulsion, fewer cationic headgroups can adsorb to the interface since the quaternary trimethylammonium headgroup of the cationic rulers is considerably larger than the small sulfate group of the anionic rulers. Also, due to their charge and relative sizes, water molecules do not form as tight a solvation shell around the cationic headgroup as they do around the anionic headgroup. Weaker hydration of the cation leads to a reduction in the shielding of the Coulombic repulsive forces between headgroups resulting in a less dense cationic ruler monolayer. Furthermore, due to the relative hydrophobicity of the cationic headgroup, the terminal surface pressure for cationic rulers is about three times that of the analogous anionic molecular rulers. This additional hydrophobicity allows for an increase in surface activity at lower bulk solution concentrations.

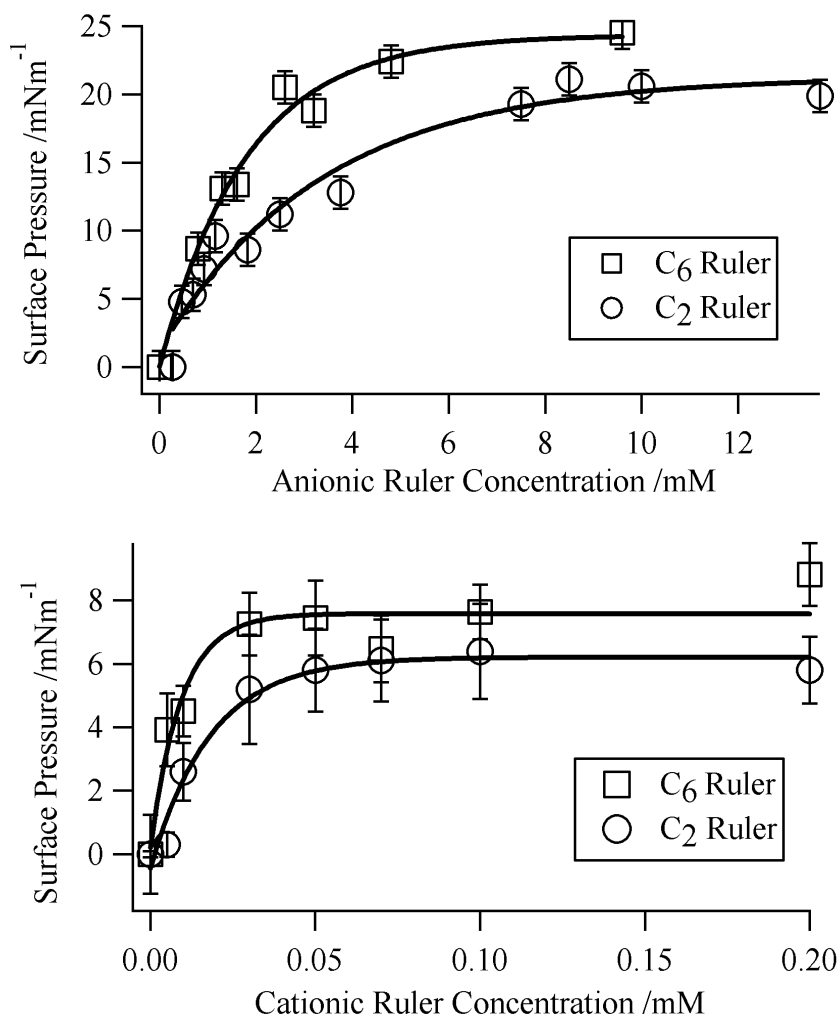


Figure 3.6. Surface pressure isotherms of C₂ and C₆ anionic (top panel) and cationic (bottom panel) molecular rulers. The solid lines represent fits to the Gibbs equation (Eq. 2.3). Terminal surface concentrations are 1.49 and 1.89×10^{14} molecules/cm² for the C₂ and C₆ anionic molecular rulers, respectively. Terminal surface concentrations were calculated to be 4 and 6×10^{13} molecules/cm² for the C₂ and C₆ cationic molecular rulers, respectively.

Interfacial Polarity Sampled by Cationic Molecular Rulers

To test whether this new family of cationic surfactants will function as molecular rulers, we acquired a resonance-enhanced SHG spectrum of the C₂ ruler adsorbed to an aqueous/cyclohexane interface. SHG is a nonlinear optical spectroscopic method that allows for the measurement of an effective excitation spectrum at an interface.^{11,38} This

technique is both surface-specific and molecularly-specific, making it a very powerful means of probing buried interfaces.^{18,21,39}

Figure 3.7 shows a SHG spectrum of the C₂ cationic ruler adsorbed to an aqueous/cyclohexane interface. Also shown are spectra from a C₂ anionic ruler and pNAs adsorbed to aqueous/cyclohexane interfaces. Spectra result from monolayer coverage of less than 0.1 to minimize probe-probe interactions. The spacer in a C₂ ruler separates the headgroup from the probe by >3-4 Å. The only difference between the anionic and cationic surfactants is headgroup identity: the cationic surfactant headgroup is a quaternary trimethylammonium ion, whereas the anionic surfactant headgroup consists of a simple sulfate group.

Both surfactant spectra are shifted to shorter wavelengths relative to the neutral pNAs chromophore. Fitting all three spectra with Eqs. 2.5-2.7 yields excitation maxima of 308 nm for pNAs, 301 nm for the C₂ anionic ruler, and 294 nm for the C₂ cationic ruler. The blue shifts in the surfactant spectra imply that the surfactant chromophores experience a less polar environment at the aqueous/cyclohexane interface than the neutral pNAs probe. This observation supports the idea that the surfactant architecture extends the solvatochromic chromophore into the nonpolar cyclohexane phase while the headgroup remains anchored in the aqueous phase.

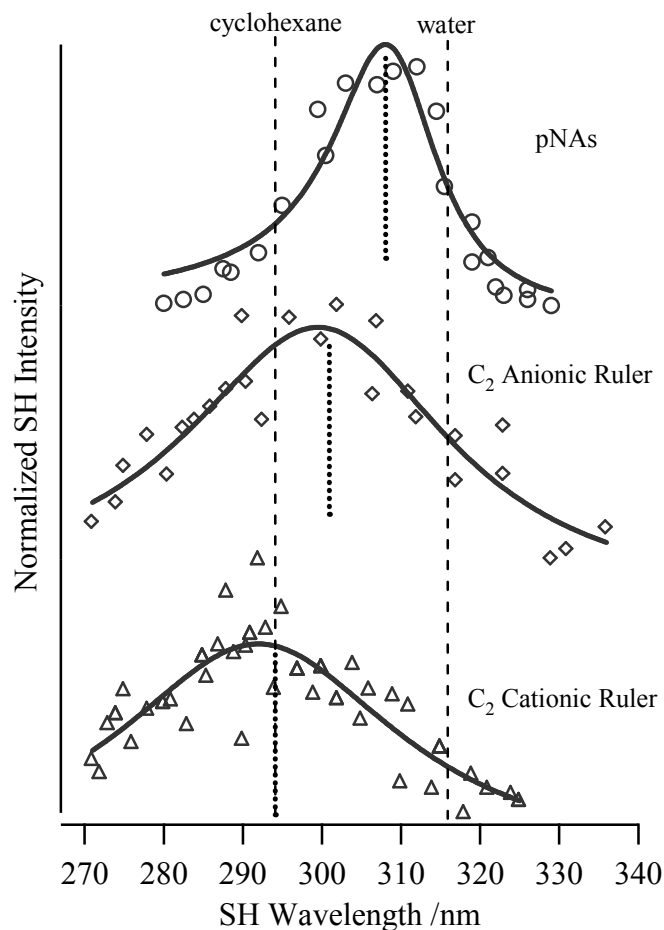


Figure 3.7. SHG spectrum of the C₂ cationic ruler adsorbed to the aqueous/cyclohexane interface (bottom). Shown for comparison are SHG spectra of the C₂ anionic ruler (middle) and the bare pNAs chromophore (top) also adsorbed to the aqueous/cyclohexane interface. Solid lines represent fits of the data to Eqs. 2.5-2.7. Dotted lines show wavelength maxima of adsorbed chromophores resulting from Eq. 2.7. Note that SH maxima do not necessarily coincide with spectral intensity maxima due to the nonresonant term in Eq. 2.6. Dashed vertical lines corresponding to excitation maxima in bulk water (316 nm) and bulk cyclohexane (294 nm) are shown for reference.

While we can offer no immediate explanation for the magnitude of the spectral shift observed in the C₂ cationic ruler spectrum (λ_{\max} lies at the bulk cyclohexane limit), the fact that the C₂ cationic ruler spectral maximum shifts to shorter wavelengths than the C₂ anionic ruler spectrum suggests that the chromophore on the cationic surfactant experiences an environment that is less polar than that sampled by the anionic surfactant chromophore. This situation could arise if the C₂ cationic headgroup were less strongly

solvated by the aqueous phase thus enabling the chromophore to extend further into the cyclohexane phase. In contrast, a strongly solvated anionic headgroup would “pull” the chromophore closer to the polar aqueous phase.

Alternatively, if the headgroups of adsorbed surfactants were still weakly interacting with the aromatic chromophore (as is the case in bulk aqueous solution), we might expect to see a more pronounced blue shift in the probe excitation spectrum. However, partitioning experiments show that the headgroup always remains solvated in the aqueous phase, and the SHG measurement clearly indicates that the probe samples an environment at the nonpolar limit. Consequently, any headgroup-probe interaction would have to occur across multiple solvent diameters and across a sharp interfacial dividing surface.

3.3. Conclusions

A simple synthesis has been devised to generate a new family of surfactants consisting of a hydrophobic solvatochromic probe tethered to a cationic headgroup by alkane chains of variable length. UV absorbance spectra coupled with NOE NMR spectroscopy have shown that surfactants having short spacers appear to self-associate in bulk solution. These interactions diminish and eventually disappear with longer chain cationic surfactants. Furthermore, intramolecular associations are observed only in charged surfactants, not neutral precursors, indicating that charge-dipole forces are responsible for the phenomenon. These cationic surfactants also form charged monolayers at liquid/liquid interfaces. The combination of solvatochromism and surface activity makes these surfactants ideal probes of solvent polarity across liquid/liquid interfaces. The SHG spectrum of a C₂ cationic ruler adsorbed to an aqueous/cyclohexane

interface shows that the ruler chromophore samples a much less polar environment than a bare pNAs chromophore. Differences between the C₂ cationic and C₂ anionic ruler SHG spectra suggest that headgroup identity may also influence local polarity about the ruler chromophore.

References

- (1) *Liquid Interfaces in Chemical, Biological, and Pharmaceutical Applications*; Volkov, A. G., Ed.; Marcel Dekker, Inc.: New York, 2001; Vol. 95, pp 853.
- (2) Volkov, A. G.; Deamer, D. W.; Tanelian, D. L.; Markin, V. S. *Liquid Interfaces in Chemistry and Biology*; John Wiley & Sons, Inc.: New York, 1998.
- (3) Safran, S. A. *Statistical Thermodynamics of Surfaces, Interfaces, and Membranes*; Addison-Wesley Publishing Co.: Reading, MA, 1994; Vol. 90.
- (4) Chipot, C.; Wilson, M. A.; Pohorille, A. *J. Phys. Chem. B* **1997**, *101*, 782.
- (5) Dominguez, H. *J. Phys. Chem. B* **2002**, *106*, 5915.
- (6) Dang, L. X. *J. Phys. Chem. B* **2001**, *105*, 804.
- (7) Senapati, S.; Berkowitz, M. L. *Phys. Rev. Lett.* **2001**, *87*, 176101.
- (8) Michael, D.; Benjamin, I. *J. Chem. Phys.* **1997**, *107*, 5684.
- (9) Zhuang, X.; Miranda, P. B.; Kim, D.; Shen, Y. R. *Phys. Rev. B: Condens. Matter* **1999**, *59*, 12632.
- (10) Antoine, R.; Bianchi, F.; Brevet, P. F.; Girault, H. H. *J. Chem. Soc., Faraday Trans.* **1997**, *93*, 3833.
- (11) Eissenthal, K. B. *J. Phys. Chem.* **1996**, *100*, 12997.

- (12) Higgins, D. A.; Abrams, M. B.; Byerly, S. K.; Corn, R. M. *Langmuir* **1992**, *8*, 1994.
- (13) Benjamin, I. *J. Phys. Chem. A* **1998**, *102*, 9500.
- (14) Li, Z. X.; Bain, C. D.; Thomas, R. K.; Duffy, D. C.; Penfold, J. *J. Phys. Chem. B* **1998**, *102*, 9473.
- (15) Li, M.; Tikhonov, A. M.; Schlossman, M. L. *Europhys. Lett.* **2002**, *58*, 80.
- (16) Gang, O.; Wu, X. Z.; Ocko, B. M.; Sirota, E. B.; Deutsch, M. *Phys. Rev. E: Stat. Phys., Plasmas, Fluids, Relat. Interdiscip. Top.* **1998**, *58*, 6086.
- (17) Scatena, L. F.; Brown, M. G.; Richmond, G. L. *Science* **2001**, *292*, 908.
- (18) Zhang, X.; Walker, R. A. *Langmuir* **2001**, *17*, 4486.
- (19) Bell, G. R.; Li, Z. X.; Bain, C. D.; Fischer, P.; Duffy, D. C. *J. Phys. Chem. B* **1998**, *102*, 9461.
- (20) Wang, H.; Borguet, E.; Eisenthal, K. B. *J. Phys. Chem. B* **1998**, *102*, 4927.
- (21) Wang, H.; Borguet, E.; Eisenthal, K. B. *J. Phys. Chem. A* **1997**, *101*, 713.
- (22) Ishizaka, S.; Kim, H. B.; Kitamura, N. *Anal. Chem.* **2001**, *73*, 2421.
- (23) Michael, D.; Benjamin, I. *J. Phys. Chem. B* **1998**, *102*, 5145.
- (24) Steel, W. H.; Walker, R. A. *J. Am. Chem. Soc.* **2003**, *125*, 1132.
- (25) Steel, W. H.; Damkaci, F.; Nolan, R.; Walker, R. A. *J. Am. Chem. Soc.* **2002**, *124*, 4824.
- (26) Suppan, P.; Ghoneim, N. *Solvatochromism*; The Royal Society of Chemistry: Cambridge, UK, 1997.

- (27) Laurence, C.; Nicolet, P.; Dalati, M. T.; Abboud, J.-L. M.; Notario, R. *J. Phys. Chem.* **1994**, *98*, 5807.
- (28) Onsager, L. *J. Am. Chem. Soc.* **1936**, *58*, 1486.
- (29) Wong, M. W.; Frisch, M. J.; Wiberg, K. B. *J. Am. Chem. Soc.* **1991**, *113*, 4776.
- (30) Stonehouse, J.; Adell, P.; Keeler, J.; Shaka, A. J. *J. Am. Chem. Soc.* **1994**, *116*, 6037.
- (31) Noggle, J. H.; Schirner, R. E. *The Nuclear Overhauser Effect: Chemical Applications*, 1971.
- (32) Israelachvili, J. N. *Intermolecular and Surface Forces*, 2nd ed.; Academic Press: London, 1992.
- (33) Steel, W. H.; Lau, Y. Y.; Beildeck, C. L.; Walker, R. A. *J. Phys. Chem. B* **2004**, *108*, 13370.
- (34) Adamson, A. W. *Physical Chemistry of Surfaces*; John Wiley & Sons: New York, 1990.
- (35) Rosen, M. J. *Surfactants and Interfacial Phenomena*, 1978.
- (36) Davies, J. T. *Trans. Faraday Soc.* **1952**, *48*, 1052.
- (37) Davies, J. T. *Proc. R. Soc. London* **1951**, *A208*, 224.
- (38) Richmond, G. L. *Annu. Rev. Phys. Chem.* **2001**, *52*, 357.
- (39) Zhang, X.; Esenturk, O.; Walker, R. A. *J. Am. Chem. Soc.* **2001**, *123*, 10768.

Chapter 4. Cationic Molecular Rulers with Simple Salts at Liquid/Liquid and Model Liquid/Liquid Interfaces

4.1. Introduction

In the most general sense, solvation describes the interaction of a solute with its surroundings. These interactions can be strong (e.g. Coulomb) or weak (e.g. dispersion) and may extend over large distances (energy $\propto 1/r^2$) or short distances (energy $\propto 1/r^6$).¹ Solvation forces will influence a solute's eigenstate structure as well as its equilibrium conformation, dynamic behavior and, ultimately, its reactivity. While numerous studies have examined static and dynamic aspects of solvation in bulk solution,²⁻⁵ solvation at surfaces has received less attention. In part, this situation has arisen because experiments probing interfacial properties are typically more difficult to execute than measurements of bulk solution phenomena. Furthermore, surface properties do not always scale in a way that can be predicted by bulk solution or mean field behavior.^{6,7} Solvents having very similar bulk solvating properties can create markedly different environments at surfaces simply by virtue of the fact that they have different shapes.

Of particular relevance to the experiments discussed below is how a solute in one phase is influenced by charges in an adjacent phase. Electrolytes having different surface activities will create an electrical double layer at an interface. These double layers are particularly well defined if one charged species is a surfactant, and double layers play prominent roles in controlling micelle formation and morphology, colloid stability and adsorption at membrane surfaces.⁸ Important properties used to characterize double layers include the surface potential and the spatial extent of the anisotropic charge distribution.⁹

Both properties can be described in terms of classical electrostatics, and in the limit of low concentration, surface potential decays exponentially with distance in the electrolyte containing phase as described by Debye-Hückel theory.⁸

Less clear is how a double layer in one phase will affect solute structure and solvation in an adjacent, immiscible phase. Understanding how electric fields generated by double layers at a water surface propagate into a low dielectric medium has important consequences in chemistry and biology. For example, double layers set up at the outer or inner walls of cell membranes will directly influence the local environment within the lipid bilayer and control concentration gradients and orientations of membrane components such as cholesterol.¹⁰ Molecular dynamics simulations and continuum models have predicted how double layer electric fields in one phase persist across liquid surfaces,¹¹⁻¹⁷ but simulations must overcome difficult technical issues associated with accurately modeling interaction potentials between charged species in anisotropic environments. In order to assist simulations and better refine our understanding of solvation at electrolyte solution surfaces, more extensive experimental data are needed.

Studies described below examine the effect that bulk solution charge has on interfacial solvation. Specifically, experiments begin to identify how charged species in one phase alter the local environment surrounding a solute in an adjacent, immiscible phase. Surface specific, second harmonic generation (SHG) is used to measure the solvatochromic response of hydrophobic chromophores anchored to an aqueous phase by formally charged anionic and cationic headgroups, molecular rulers. Ionic strength is varied by changing the simple salt concentration of the underlying, aqueous subphase. In addition, we explore the use of neutral, self-assembled monolayers as mimics for

liquid/liquid interfaces. Given recent experiments that show the interface between bulk 1-octanol and water to be dominated by an exceedingly nonpolar region,¹⁸ we wanted to determine whether or not monolayers formed at liquid/vapor interfaces of aqueous solutions saturated with linear alcohols would approximate the environments observed at water/alkane boundaries. While these monomolecular films adsorbed to the liquid/vapor interface do not reproduce quantitatively the properties of boundaries between bulk liquids, they can serve as qualitative models of weakly associating liquid/liquid interfaces and help identify how bulk solution charge effects extend into low dielectric media.

4.2. Results and Discussion

Cationic vs. Anionic Rulers Adsorbed to the Water/Cyclohexane Interface

The initial report describing cationic molecular rulers noted behavior that contrasted with that shown by related anionic surfactants.¹⁹ At the same interface (water/cyclohexane), anionic and cationic rulers having similar fractional monolayer surface coverages appear to sample very different dielectric environments. The excitation wavelength of the C₂ anionic ruler exhibits a distinct maximum at 301 nm in its resonant SHG spectrum. This value lies between the bulk aqueous and organic limits of 316 and 294 nm, respectively. In contrast, the spectrum of the C₂ cationic ruler shows an excitation maximum at 294 nm, a wavelength that is slightly lower than the bulk alkane limit of 296 nm. (Bulk organic limits were determined by bulk solution absorbance spectra of a neutral analogue containing an alcohol headgroup and a dimethylamine headgroup for the anionic and cationic rulers, respectively.) This effect appears general as evidenced by the spectra acquired from C₄ cationic and C₄ anionic rulers adsorbed to the water/cyclohexane interface (Figure 4.1, upper panel). Again, the cationic ruler's

excitation wavelength is blue-shifted slightly from the bulk cyclohexane limit while the anionic ruler's excitation wavelength is still longer than the bulk solution limit. The lower panel in Figure 4.1 summarizes the water/cyclohexane interfacial behavior of cationic and anionic surfactants having 2, 4 and 6 carbon spacers.

From the data, one readily sees that the behavior of cationic and anionic species converges for longer length surfactants. For both species of surfactants (cationic and anionic) the polarization dependent SHG signal was measured in order to calculate the average chromophore orientation. Data shows that chromophores in cationic and anionic surfactants have equivalent orientations of $44 \pm 3^\circ$ relative to the interfacial normal. Chromophore orientation exhibits no systematic dependence on alkyl spacer length. Despite uncertainties regarding the width of the distribution about this average orientation, similarities between the cationic and anionic results are reassuring because they imply that chromophores from both surfactants are solvated in a similar manner, regardless of headgroup identity. There appears to be no charge-dependent effect forcing the chromophore of the cationic surfactant to adopt an orientation that is more perpendicular or more parallel to the interface, relative to the anionic species.

The disparity between cationic and anionic solvatochromic behavior for the shorter surfactants is especially significant. These results imply that the same probe, *p*-nitroanisole (pNAs), integrated into the same surfactant architecture (C₂ or C₄) adsorbed to the same interface (water/cyclohexane) with the same relative surface coverage (~20% full monolayer) samples markedly different polarities depending on the headgroup identity. One possible source of the disparity might be the difference in the

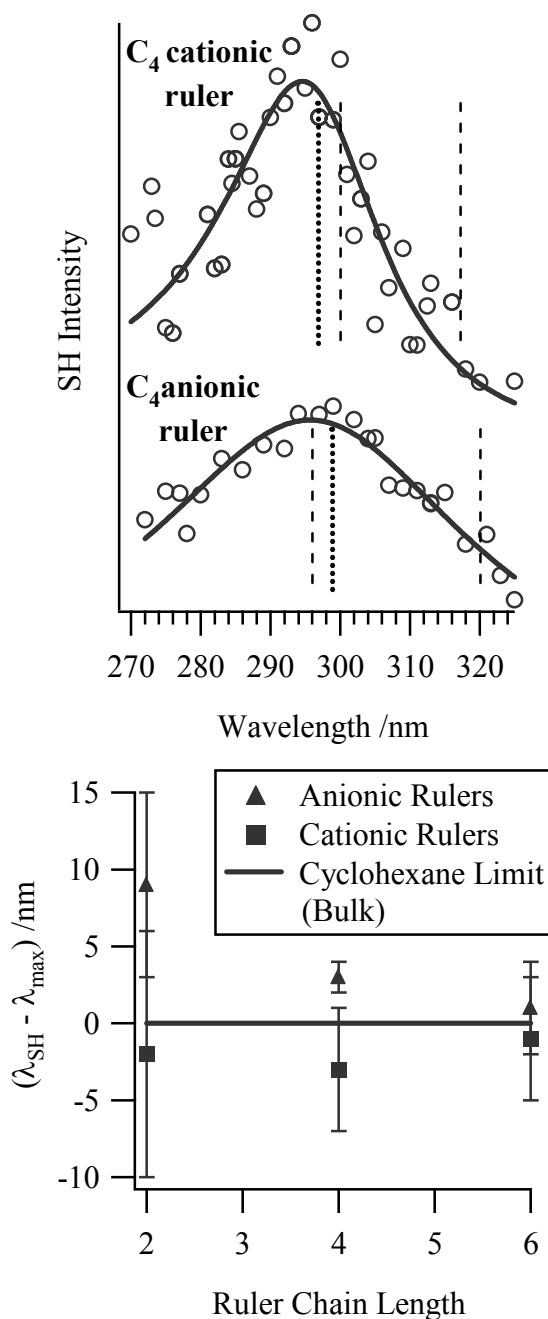


Figure 4.1. SH behavior of anionic and cationic molecular rulers at the water/cyclohexane interface. The top panel shows SHG data for the C₄ cationic and the C₄ anionic rulers at the water/cyclohexane interface. Solid lines represent fits of the data to Eqs. 2.5-2.7. Dotted lines show excitation maxima of adsorbed chromophores resulting from Eq. 2.7. Note that SH maxima do not necessarily coincide with spectral intensity maxima due to the nonresonant term in Eq. 2.6. Dashed vertical lines corresponding to excitation maxima in bulk water (shorter wavelength) and bulk cyclohexane (longer wavelength) are shown for reference. The bottom panel summarizes the solvatochromic behavior of different length cationic and anionic molecular rulers at the water/cyclohexane interface where $(\lambda_{SH} - \lambda_{max})$ represents the difference between the SHG wavelength maximum and the bulk cyclohexane limit.

probe distributions across the interface, an effect we refer to as “float depth.” While neither headgroup is soluble in the organic phase, the cationic, trimethyl ammonium headgroup is considerably more hydrophobic than the anionic sulfate headgroup. *If* the interface were molecularly sharp and *if* the headgroups were solvated differently (with the ammonium headgroup being located closer to the interfacial Gibbs dividing surface than the sulfate group), then we would expect the pNAs probe attached to the cationic surfactant to sample a less polar environment than the probe attached to the anionic headgroup.

This explanation cannot be ruled out as a contributing cause of the headgroup-dependent behavior, although it fails to account for the small but persistent blue shift in cationic SHG spectra relative to the bulk alkane limit. A more likely source of the observed differences is the charge of the headgroup. For cationic surfactants, bulk solution nuclear Overhauser enhancement (NOE) nuclear magnetic resonance experiments clearly show that the cationic headgroup interacts with the electronic structure of the aromatic chromophore as evidenced by through-space coupling between methyl protons on the headgroup and the aromatic protons *meta* to the nitro group (Figure 3.4).¹⁹ This interaction is strongest for the shortest surfactants (Figure 3.5). Surfactants having alkyl chain lengths of four methylene groups or more show no evidence of chromophore-headgroup association. The charge-dipole interaction between the headgroup and the aromatic chromophore reduces the change in dipole experienced by the solute in solution, leading to less pronounced (or blue-shifted) solvatochromic behavior relative to the behavior of neutral species (Figure 3.3). Anionic surfactants show no such intramolecular interaction (Table 3.1). Adding excess salt (NaI) to a solution of

cationic surfactants reduces the intramolecular interactions, and the surfactant's solvatochromic behavior begins to resemble that of analogous anionic species. For example, aqueous solutions of the C₂ anionic ruler and a neutral C₂ cationic ruler analogue containing a dimethylamine headgroup, rather than the quarternized ammonium, both exhibit bulk solution excitation wavelengths of 316 nm in water. The excitation wavelength of C₂ cationic ruler in water is 310 nm, but this value shifts to 316 nm in aqueous solutions saturated with NaI.

A final cause for the unexpected behavior of cationic surfactants adsorbed to the water/cyclohexane interface could be aggregation. If adsorbed surfactants were interacting with each other, then the observed solvatochromic responses would reflect probe-probe interactions or, perhaps, interactions between the probe of one surfactant and the cationic headgroup of an adjacent surfactant. However, even at very low surfactant concentrations adsorption isotherms show no characteristic signature of surfactant aggregation (Figure 3.6). In addition, surfactant concentrations are several orders of magnitude below the critical micelle concentration of quarternized ammonium surfactants having longer hydrophobic tails.⁸ Finally, five-fold changes in surface coverage (full monolayer to < 20% of full monolayer coverage) lead to no observed changes in the SHG response of adsorbed chromophores. Thus we believe that differences in interfacial solvation sampled by cationic and anionic surfactants having similar lengths arise from having different charges located at well-defined distances relative to the solvatochromic probe.

Polarity vs. Surface Charge at Model Liquid/Liquid Interfaces

The headgroup dependent water/cyclohexane results lend themselves to two possible interpretations. Either the cationic headgroup influences the environment surrounding the chromophore leading to a lower apparent interfacial polarity or the headgroup alters the electronic structure of the chromophore making it less sensitive to the local dielectric environment. In order to investigate further the effect of bulk solution ionic strength on solvation in an adjacent phase, we sought to mimic the weakly associating water/alkane interface with a system that proved logistically easier to assemble during day-to-day operation.

Aqueous solutions saturated with 1-octanol appear to capture most of the important features of the water/alkane systems studied previously. SHG studies of the boundary created between bulk water and bulk 1-octanol show that the interface is dominated by a very nonpolar region having a local dielectric environment similar to that of bulk alkanes.^{18,20} Furthermore, this region appears to extend for the length of a single, all-trans octanol molecule suggesting that the surface octanol species hydrogen bond to the underlying sub-phase and create a dense Langmuir film at the water/1-octanol interface. Surface tension data coupled with surface-specific vibrational spectra have been used to characterize the liquid/vapor interface created by aqueous solutions saturated with 1-octanol.²¹ Not surprisingly, the solvated organic species spontaneously self-assemble at the liquid/vapor interface forming a tightly packed monolayer (21 Å²/molecule) in which the 1-octanol species are very well ordered (Figure 4.2).

Figure 4.3 shows the resonance enhanced SHG spectra of the C₄ cationic ruler adsorbed to both the water/cyclohexane interface and the liquid/vapor interface formed

by an aqueous solution saturated by 1-octanol. The spectrum from the liquid/vapor interface is slightly broader than that from the liquid/liquid interface (45 nm vs. 27 nm FWHM) suggesting a more heterogeneous environment, but the actual excitation wavelengths of the same surfactant in these two different systems are equivalent. In addition, the C₄ cationic ruler chromophore is deflected $44 \pm 3^\circ$ off of surface normal in both systems.

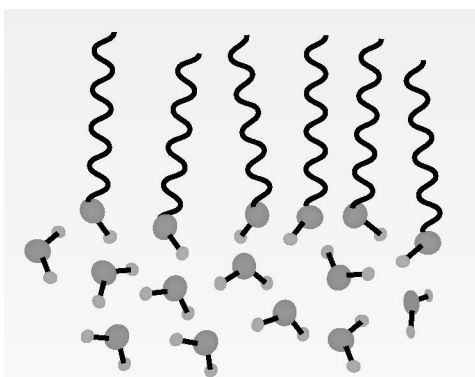


Figure 4.2. Schematic representation of the formation of a self-assembled monolayer of 1-octanol at the water/vapor surface. Details about surface coverage and orientation are discussed in the text and in Ref. 21.

Water/1-octanol interfacial mimics were used to investigate the effects of bulk solution ionic strength on interfacial solvation. Solutions of C₄ cationic rulers (60 μ M) were prepared in aqueous solvents saturated with 1-octanol. The ionic strength was controlled by dissolving NaI into the aqueous solution. The SHG spectrum of the adsorbed C₄ cationic ruler was then acquired and fit according to Eqs. 2.5-2.7. Representative spectra and a summary of SH wavelength maxima for systems having varied NaI concentrations appear in Figure 4.4. Though subtle, changes in the interfacial environment (as sampled by the surfactant chromophores) clearly depend on the electrolyte concentration of the aqueous subphase. As the NaI concentration increases,

chromophore excitation shifts to longer wavelengths and approaches the C_4 anionic ruler limit. Given the solvatochromic properties of the probe, this behavior could signify increasing polarity within the 1-octanol film. Alternatively, a red shift in excitation wavelength could represent a weakening of probe-headgroup interactions that allow the electronic structure of pNAs to become more sensitive to solvent polarity.

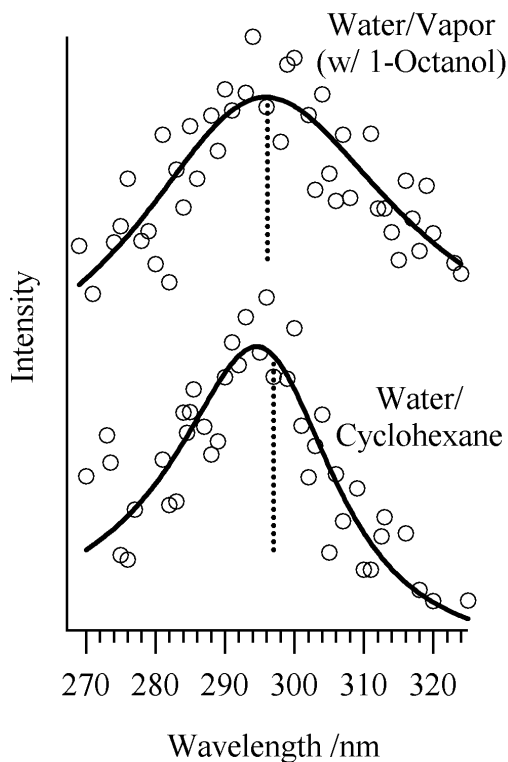


Figure 4.3. SHG spectra of C_4 cationic ruler adsorbed to the water/cyclohexane interface and the water/vapor interface where the water has been saturated with 1-octanol. Solid lines represent fits of the data to Eqs. 2.5-2.7. Dotted lines show excitation maxima of adsorbed chromophores resulting from Eq. 2.7. Note that SH maxima do not necessarily coincide with spectral intensity maxima due to the nonresonant term in Eq. 2.6.

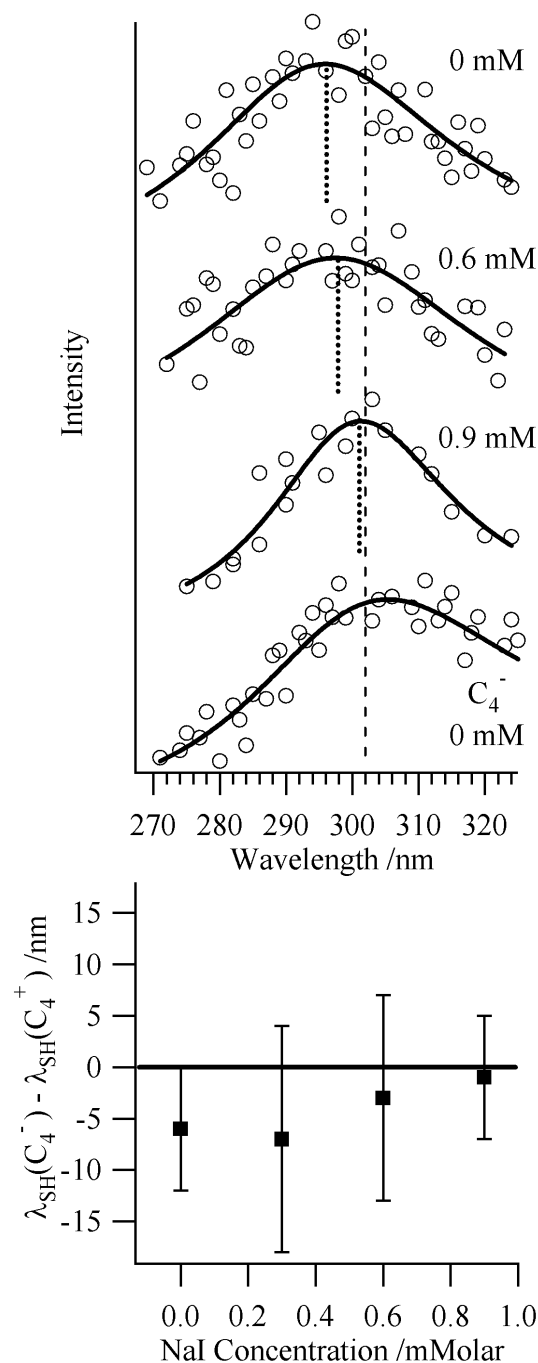


Figure 4.4. Interfacial solvation of the C₄ cationic ruler adsorbed to the 1-octanol saturated water/vapor interface as a function of NaI concentration. The top panel displays spectra for the C₄ cationic ruler with 0 mM, 0.6 mM, and 0.9 mM NaI concentrations in the aqueous subphase. Solid lines represent fits of the data to Eqs. 2.5-2.7. Dotted lines show SHG maxima of adsorbed chromophores resulting from Eq. 2.7. The dashed line corresponds to the SHG maximum of the C₄ anionic ruler adsorbed to the same interface with no additional salt present. The bottom panel summarizes the results of fitting the spectra to Eqs. 2.5-2.7 where $\lambda_{SH}(C_4^-) - \lambda_{SH}(C_4^+)$ is the difference in SHG wavelength maxima for the cationic and anionic species as a function of salt concentration.

Deconvoluting these two effects – interfacial polarity vs. intramolecular alterations of chromophore electronic structure – is not trivial, and both are likely to contribute to the observed variations in chromophore behavior that accompany changes in the aqueous solution ionic strength. Nevertheless, we believe that the intramolecular interactions bear more responsibility for the observed behavior than changes in the local dielectric properties of the film. Based on thermodynamic,²² spectroscopic^{6,18,20,21} and neutron and X-ray scattering data,²³⁻²⁵ we assume that the interior of the monolayer films are alkane-like in nature, meaning that external fields (from the electric double layer in the aqueous phase) are unable to induce a large polarization within the organic film.²⁶ Consequently, the intrinsic dielectric character of the film is unlikely to change significantly. However, chromophore-headgroup interactions can be attenuated if the cationic headgroup charge is screened effectively.

Several considerations suggest that increasing aqueous NaI concentration should inhibit the headgroup's ability to interact with the attached chromophore. First, large, monovalent anions such as Br^- and I^- bind more effectively than smaller anions (e.g. Cl^-) to quarternized ammonium surfactants in solution. This effect shows up most dramatically in a lowering of the surfactant critical micelle concentration as ionic strength increases.²⁷⁻²⁹ Stronger cation-anion association at the interface would necessarily reduce the strength of cation-chromophore interaction (Figure 4.5). Again, bulk solution absorption data support this model, as do preliminary SHG results using NaCl rather than NaI as the aqueous electrolyte. The effect of increasing chloride concentration on the chromophore's solvatochromic behavior is much less pronounced than for equivalent concentrations of NaI.

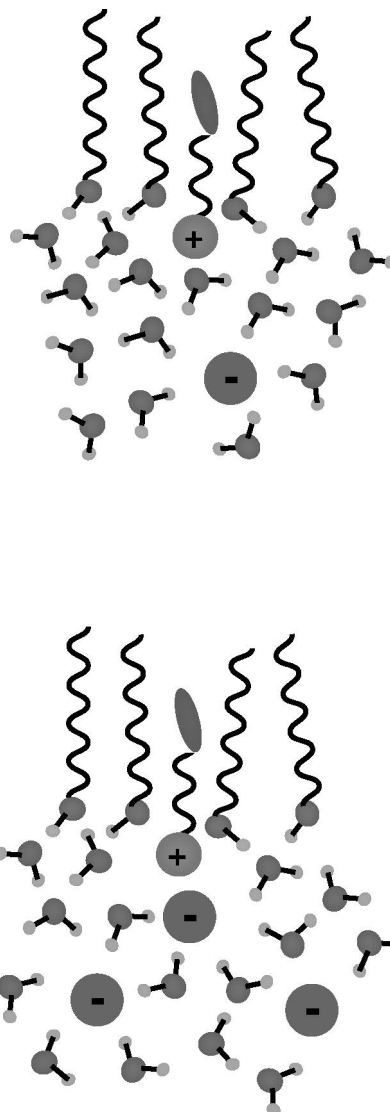


Figure 4.5. Schematic representation of the interfacial environment in the absence (top panel) and presence (bottom panel) of excess bulk solution charge (in the form of additional I^-). As the iodide concentration in aqueous solution increases (by addition of NaI), the cationic headgroups can be more effectively screened from the chromophore solvated in the adjacent phase. The dimensions of the interfacial region are not to scale. Debye-Hückel theory predicts a double layer screening distance of ~ 40 nm in the absence of excess salt and ~ 10 nm at salt concentrations of ~ 1 mM. (See Ref. 8, Chapter 11 for more details.)

Another source of headgroup screening may arise from the surface activity of the iodide anion itself. Recent molecular dynamics simulations predict that smaller anions such as F^- and Cl^- are depleted at the liquid/vapor surface, but larger ions such as Br^- and I^- preferentially partition to the interface.³⁰ Such surface activity of the I^- would

again help “neutralize” the ammonium headgroup from the perspective of the aromatic chromophore in the adjacent, nonpolar medium. Comparisons between the simulations and results presented above cannot be quantitative given the large disparity in electrolyte concentrations – simulations modeled effective 1 M salt solutions while salt solution concentrations used in experiments were sub-millimolar. We also note that there exists a degree of ambiguity associated with this picture in light of recent experiments examining the vibrational structure of different aqueous/electrolyte interfaces,³¹⁻³³ but any difference in anion surface activities will necessarily influence the structure of the electrical double layer and solvation in an adjacent phase.

4.3. Conclusion

Results presented in this work have begun to identify how charges can “reach” across interfaces to influence solvation in an adjacent phase. Two effects must be considered: the effect of charge on the properties of the adjacent medium and the effect of charge on the electronic structure of the solvated chromophore. Results show that oppositely charged headgroups in close proximity to a hydrophobic probe lead to qualitatively different pictures of interfacial solvation based on the probe’s bulk solution solvatochromic behavior. The effect of headgroup charge on interfacial solvation falls off with increasing headgroup-chromophore separation. Neutral, self-assembled monolayers can serve as useful models of weakly associating, liquid/liquid interfaces. These systems readily lend themselves to studying the effects of surface charge on interfacial solvation. By changing the ionic strength of the aqueous phase, we believe that the headgroup dependent differences in interfacial solvation result from direct headgroup-chromophore interactions between the positively charged alkyl ammonium headgroup and the aromatic

chromophore. Screening the headgroup with an excess of Γ^- ions allows cationic surfactant behavior to converge to anionic surfactant limits. Clearly, considerable work remains to be done, but the data presented above provide an enticing picture of how charges influence solvation across liquid/liquid interfaces.

References

- (1) Winde, H. *Z. Phys. Chem. (Munich)* **1996**, *193*, 217.
- (2) Bardeen, C. J.; Rosenthal, S. J.; Shank, C. V. *J. Phys. Chem. A* **1999**, *103*, 10506.
- (3) Fleming, G. R.; Cho, M. *Annu. Rev. Phys. Chem.* **1996**, *47*, 109.
- (4) Horng, M. L.; Gardecki, J. A.; Papazyan, A.; Maroncelli, M. *J. Phys. Chem.* **1995**, *99*, 17311.
- (5) Laurence, C.; Nicolet, P.; Dalati, M. T.; Abboud, J.-L. M.; Notario, R. *J. Phys. Chem.* **1994**, *98*, 5807.
- (6) Zhang, X.; Walker, R. A. *Langmuir* **2001**, *17*, 4486.
- (7) Zhang, X.; Steel, W. H.; Walker, R. A. *J. Phys. Chem. B* **2003**, *107*, 3829.
- (8) *Principles of Colloid and Surface Chemistry*; 3rd ed.; Hiemenz, P. C.; Rajagopalan, R., Eds.; Marcel Dekker: New York, 1997, pp 688.
- (9) Makov, G.; Nitzan, A. *J. Phys. Chem.* **1994**, *98*, 3459.
- (10) Safran, S. A. *Statistical Thermodynamics of Surfaces, Interfaces, and Membranes*; Addison-Wesley Publishing Co.: Reading, MA, 1994; Vol. 90.
- (11) Dang, L. X.; Chang, T.-M. *J. Phys. Chem. B* **2002**, *106*, 235.

- (12) Dominguez, H. *J. Phys. Chem. B* **2002**, *106*, 5915.
- (13) Michael, D.; Benjamin, I. *J. Phys. Chem.* **1995**, *99*, 16810.
- (14) Pratt, L. R. *J. Phys. Chem.* **1992**, *96*, 25.
- (15) Wilson, M. A.; Pohorille, A.; Pratt, L. R. *J. Phys. Chem.* **1987**, *91*, 4873.
- (16) Benjamin, I. *J. Phys. Chem. A* **1998**, *102*, 9500.
- (17) Pratt, L. R.; Tawa, G. J.; Hummer, G.; Garcia, A. E.; Corcelli, S. A. *Int. J. Quantum Chem.* **1997**, *64*, 121.
- (18) Steel, W. H.; Walker, R. A. *Nature* **2003**, *424*, 296.
- (19) Beildeck, C. L.; Steel, W. H.; Walker, R. A. *Langmuir* **2003**, *19*, 4933.
- (20) Cramb, D. T.; Wallace, S. C. *J. Phys. Chem. B* **1997**, *101*, 2741.
- (21) Esenturk, O.; Mago, D.; Walker, R. A. *In preparation* **2005**.
- (22) Gaines, G. L., Jr. *Insoluble Monolayers at Liquid-Gas Interfaces*; Interscience Publishers: New York, 1966.
- (23) Als-Nielsen, J.; Jacquemain, D.; Kjaer, K.; Leveiller, F.; Lahav, M.; Leiserowitz, L. *Phys. Rep.* **1994**, *246*, 251.
- (24) Penfold, J.; Richardson, R. M.; Zorbakhsh, A.; Webster, J. R. P.; Bucknall, D. G.; Rennie, A. R.; Jones, R. A. L.; Cosgrove, T.; Thomas, R. K.; Higgins, J. S.; Fletcher, P. D. I.; Dickinson, E.; Roser, S. J.; McLure, I. A.; Hillman, A. R.; Richards, R. W.; Staples, E. J.; Burgess, A. N.; Simister, E. A.; White, J. W. *J. Chem. Soc., Faraday Trans.* **1997**, *93*, 3899.
- (25) Schalke, M.; Losche, M. *Adv. Colloid Interface Sci.* **2000**, *88*, 243.

- (26) Böttcher, C. J. F. *Theory of Electric Polarization*; Elsevier: New York, 1973; Vol. 1: Dielectrics in Static Fields.
- (27) Magid, L. J.; Han, Z.; Warr, G. G.; Cassidy, M. A.; Butler, P. D.; Hamilton, W. A. *J. Phys. Chem. B* **1997**, *101*, 7919.
- (28) Velegol, S. B.; Fleming, B. D.; Biggs, S.; Wanless, E. J.; Tilton, R. D. *Langmuir* **2000**, *16*, 2548.
- (29) Haverd, V. E.; Warr, G. G. *Langmuir* **2000**, *16*, 157.
- (30) Jungwirth, P.; Tobias, D. J. *J. Phys. Chem. B* **2002**, *106*, 6361.
- (31) Weber, R.; Winter, B.; Schmidt, P. M.; Widdra, W.; Hertel, I. V.; Dittmar, M.; Faubel, M. *J. Phys. Chem. B* **2004**, *108*, 4729.
- (32) Liu, D.; Ma, G.; Levering, L. M.; Allen, H. C. *J. Phys. Chem. B* **2004**, *108*, 2252.
- (33) Raymond, E. A.; Richmond, G. L. *J. Phys. Chem. B* **2004**, *108*, 5051.

Chapter 5. Interfacial Solvation of a Neutral Solute as a Function of Ionic Strength and Salt Identity

5.1. Introduction

The surface activity of simple salt ions in electrolyte solutions has been debated for decades¹⁻⁴ and continues to be an area of active interest.⁵⁻⁹ Typically, ionic surfactants adsorb to a liquid surface to reduce the surface free energy leading to a decrease in the surface tension of the solution relative to that of the neat liquid. However, early surface tension measurements of aqueous electrolyte solutions at the air/water interface showed a prominent *increase* in surface tension relative to that of neat water.^{4,10} This observation was interpreted as a negative surface activity and a depletion of simple salt ions at the air/water interface.^{3,11-13} Simple thermodynamic considerations suggest that this view of ion depletion at the surface is reasonable given the unfavorable enthalpy change required to desolvate surface ions.

In contrast to this traditional picture of simple ion surface depletion, recent molecular dynamics simulations suggest that some simple ions will, in fact, migrate to a liquid surface, and the degree to which an ion will partition to the surface depends on the ion's polarizability.⁵ *Ab initio* quantum calculations, Car-Parrinello molecular dynamics simulations and molecular dynamics simulations based on polarizable force fields were used to examine aqueous slabs doped with sodium fluoride, chloride, bromide, and iodide at effective concentrations of ~ 1 M. Density profiles of the ions and water oxygen atoms indicate that highly polarizable iodide and bromide ions exhibit positive excess surface concentrations. Results show that such surface accumulation is possible because the

nonzero net dipole of water molecules asymmetrically solvating the surface ions polarizes the ions leading to a stabilization that balances the energy penalty of incomplete solvation. Because chloride ions are not as polarizable as bromide and iodide ions, their surface concentration is predicted to be slightly less than bulk concentration. Very small, nonpolarizable, strongly hydrated fluoride ions are depleted from the surface region.⁵ Very recent results from X-ray photoelectron spectroscopy measurements support these predictions.⁹

The studies described above focus on ion activity at the air/water interface. Few studies have explored the effects of charge on liquid/liquid interfacial environments, although measurements have shown that the surface tension of a water/organic interface increases with the addition of alkali halide salts by almost the same amount as the air/water surface tension.¹⁴ Given that simple ions in aqueous solutions influence interfacial properties, one may wonder how these altered properties change the local environment experienced by molecular solutes adsorbed to liquid/liquid interfaces. The following study probes the impact that ions have on the local polarity about a solute at a water/alkane interface.

5.2. Motivation and Background

Motivation for this work stems from the aforementioned conflicting observations of simple ion surface activity as well as the observation that interfacial polarity appears to depend on the charge of ionic surfactant headgroups.^{15,16} In previous work,^{15,17-20} we described the use of molecular rulers to assess quantitatively the interfacial widths of various liquid/liquid interfaces. Resonance-enhanced second harmonic generation (SHG) is used to measure the effective excitation energy of a chromophore within the interfacial

region and thus infer the interfacial polarity. Observing changes in the solvatochromic probe response as a function of alkyl chain length provides a means to measure the interfacial dipolar width, the distance required for solvent polarity to converge to the bulk organic limit. When the probe samples a polarity corresponding to that of the bulk organic solvent, the headgroup-probe separation sets an upper limit to the interfacial dipolar width.

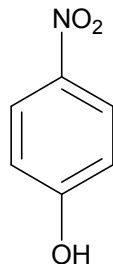
The interfacial polarity sampled by an anionic ruler adsorbed to the water/cyclohexane interface approaches the bulk cyclohexane limit from an environment of intermediate polarity between that of bulk water and bulk cyclohexane.¹⁷ However, when cationic surfactants are used, the observed behavior is quite different.¹⁵ The SHG spectrum for the shortest cationic ruler surfactant lies at a wavelength corresponding to the wavelength maximum of the chromophore's absorbance spectrum in bulk cyclohexane. For the *p*-nitroanisole-based probe in molecular rulers, a blue shift in the absorbance spectrum typically corresponds to solvation in a less polar environment suggesting that the interfacial polarity sampled by the shortest cationic ruler appears to be of similar polarity to that of the adjoining bulk cyclohexane phase. This result could arise from several different sources,¹⁵ although the most likely cause is a change in the electronic structure of the chromophore rather than a decrease in interfacial polarity.¹⁶ Specifically, coupling between the cationic headgroup and the electron-rich aromatic ring would reduce the change in dipole moment accompanying electronic excitation of the molecule and would result in a shift to shorter wavelength in the electronic absorbance spectrum relative to a neutral analogue with no intramolecular association.¹⁵

Evidence for such intramolecular association in bulk solution stems from nuclear Overhauser enhancement nuclear magnetic resonance (NMR) experiments where cationic molecular ruler samples in D₂O were irradiated at the chemical shift corresponding to the methyl groups of the quaternary trimethylammonium headgroup.¹⁵ A small but significant enhancement in the integrated intensity of peaks corresponding to the protons situated “meta” to the nitro group indicates a through-space interaction between these protons and those of the methyl protons in the headgroup as depicted in Figure 3.4. This intramolecular coupling between the cationic headgroup and the aromatic ring is most pronounced for the shortest surfactants and is not observable in NMR experiments for surfactants having four methylene spacers or more (Figure 3.5).¹⁵ No such intramolecular interaction is observed for anionic molecular rulers of any length.

To examine whether or not simple anions could inhibit the intramolecular interactions described above, SHG spectra were collected for cationic molecular rulers adsorbed to the liquid/vapor interface of aqueous solutions saturated with 1-octanol in the presence of simple salts.¹⁶ Such an interface captures the solvation properties of a weakly associating water/organic interface due to the self-assembly of an alkyl monolayer at the liquid/vapor boundary.^{16,18,20-22} This 1-octanol in water system has been used as a convenient mimic of the water/alkane boundary.¹⁶ When short cationic molecular rulers are adsorbed to this liquid/vapor surface, the SHG spectra again shift to shorter wavelengths relative to the spectra of anionic rulers, similar to the behavior of cationic rulers adsorbed to the water/cyclohexane interface. However, the addition of sodium iodide to the aqueous solution leads to a spectral red shift in the SHG spectrum, and at iodide concentrations greater than 1 mM, the cationic and anionic surface spectra are

indistinguishable. The spectral shift to anionic ruler behavior is attributed to a weakening of the charge-dipole interactions proposed for cationic molecular rulers. Screening of this association occurs due to Coulombic interactions between the iodide anion and the quaternary trimethylammonium cationic headgroup of the surfactant. Inhibition of the intramolecular association would inhibit the reduction of the change in dipole moment associated with electronic excitation. Consequently, the cationic surfactant would exhibit behavior similar to that of the anionic molecular ruler.¹⁶

In order to explore further surface charge-probe coupling, experiments described in this work attempt to decouple the probe from the charge by using a neutral surfactant, *p*-nitrophenol (PNP) (Figure 5.1), and adding simple salts at various concentrations to the solutions. The use of a neutral surfactant also allows us to control closely the ionic strength of each system, a condition that is difficult to manage when using molecular rulers due to ionic contaminants. Based on results presented below, we conclude that, in the absence of direct correlation between the charged species and a probe molecule, charges have a similar influence on interfacial solvation of neutral organic species such as PNP as they do on bulk solution solvation. An analysis of the surface distribution of PNP and the conjugate base, *p*-nitrophenoxide (PNP⁻) suggests that adsorption of PNP is favored over PNP⁻ adsorption by a factor of ten, giving rise to an equilibrium surface distribution that is an order of magnitude greater than that found in bulk solution. These findings indicate that the amount of PNP⁻ at the surface in an aqueous solution of 10 mM PNP is negligible.



p-nitrophenol
(PNP)

Figure 5.1. Molecular structure of *p*-nitrophenol (PNP). This molecule is used to determine the effects of charge on interfacial solvation.

5.3. Results and Discussion

Surface Solvation of PNP with Electrolyte Solutions

To observe the solvation environment of a solute adsorbed to a liquid/liquid interface, we utilize resonance-enhanced SHG. Figure 5.2 shows SHG spectra for PNP at the water/cyclohexane interface where the aqueous phase contains different salts and a variety of bulk salt concentrations. With the exception of the spectrum for the salt-free system, each spectrum shown reflects a composite of at least three and up to nine individual spectra that have been normalized and averaged together. The salt-free sample was used as a benchmark to assess the consistency of the experimental setup. Consequently, the corresponding spectrum shown in Figure 5.2 is a composite of 17 spectra. Since increasing the number of spectra incorporated into a composite reduces the uncertainty in the SHG wavelength maximum, the spectrum for the salt-free system is much less noisy than the other spectra shown in Figure 5.2.

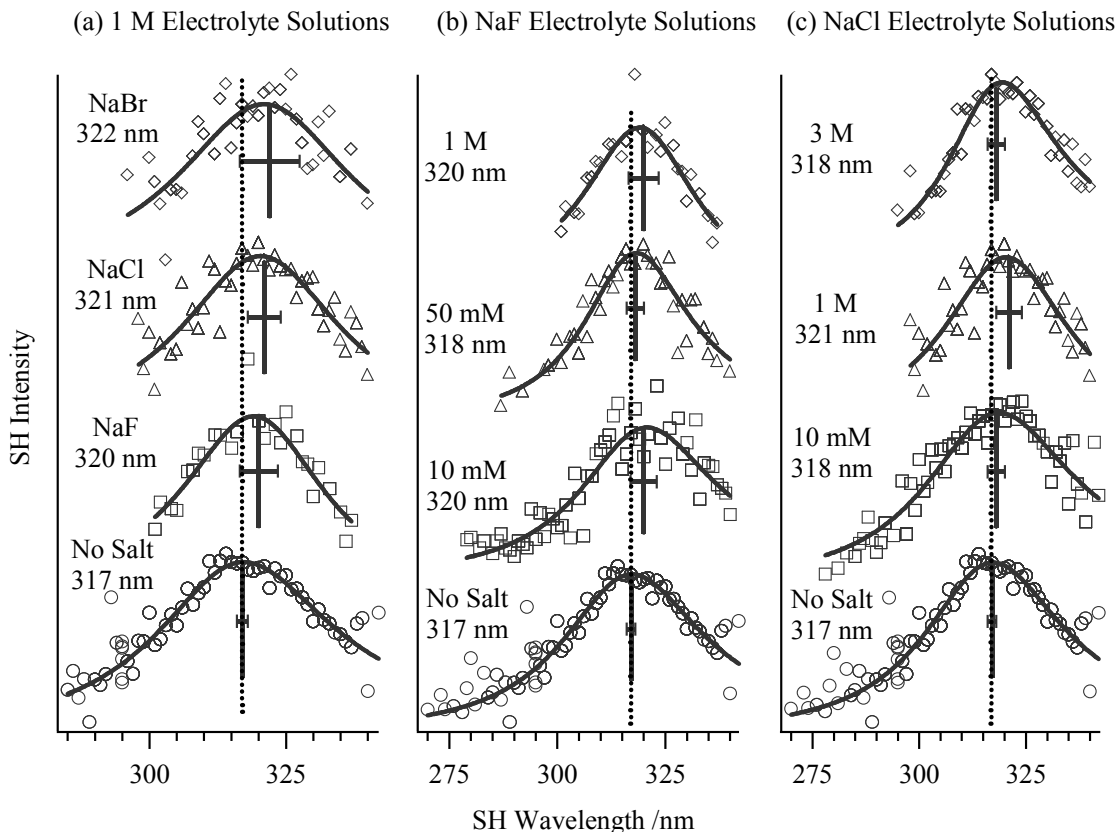


Figure 5.2. SHG spectra of PNP at the aqueous/cyclohexane interface where the electrolyte solutions are (a) 1 M NaF, 1 M NaCl, and 1 M NaBr, (b) 10 mM NaF, 50 mM NaF, and 1 M NaF, and (c) 10 mM NaCl, 1 M NaCl, and 3 M NaCl. Solid lines represent fits of the data to Eqs. 2.5-2.7. Dotted lines show interfacial wavelength maxima of PNP in the presence of the indicated salt resulting from Eq. 2.7. Dashed vertical lines correspond to interfacial maximum of PNP at the salt-free water/cyclohexane interface. Note that SH maxima do not necessarily coincide with spectral intensity maxima due to the nonresonant term in Eq. 2.6. The uncertainty $\delta\lambda_{\max}(\text{SHG})$ is indicated by horizontal error bars and ranges from ± 1 nm (salt-free PNP solution) to ± 5.5 nm (1 M NaBr system) with an average uncertainty of ± 3 nm.

Data for each spectrum were fit using Eqs. 2.5-2.7. With constant salt concentrations of 1 M, the SHG spectra appear to shift to longer wavelength as the salt's anion size increases from fluoride to chloride to bromide (Figure 5.2a). In the absence of salt, the SHG spectrum for PNP lies at 317 nm, but the spectrum shifts as much as +5 nm when NaBr is added, the most extreme case. However, such a large shift is within the window of uncertainty, $\delta\lambda_{\text{SH}}$, as shown in Table 5.1. Therefore, such a shift may not be

significant. Solutions containing NaI were omitted from this study since any results attributed to the presence of anionic species cannot be assigned solely to the effects of Γ^- , but must also consider the presence of I_3^- . A closer inspection of spectral trends shows no dependence for either NaF or NaCl systems on bulk salt concentration (Figure 5.2b-c). The second harmonic wavelength maximum shifts anywhere from 1 to 4 nanometers to the red, independently of salt concentration, a shift that remains within our windows of uncertainty.

Table 5.1. Comparisons of wavelength maxima for bulk and interface electrolyte solution spectra of PNP.

Sample	$\lambda_{\max}(\text{SHG})$	$\lambda_{\max}(\text{bulk})^a$	$\Delta\lambda_{\max}^b$	$\delta\lambda_{\max}(\text{SHG})^c$
No Salt	317 nm	317.3 nm	0 nm	± 1 nm
1 M NaF	320 nm	320.1 nm	0 nm	± 3.5 nm
1 M NaCl	321 nm	318.4 nm	3 nm	± 3 nm
1 M NaBr	322 nm	318.5 nm	4 nm	± 5.5 nm
3 M NaCl	318 nm	319.6 nm	2 nm	± 2 nm

^a Reported values are averages of several measurements. Bulk solution measurements were made using 0.5 nm resolution. Therefore, uncertainty in these measurements is ± 0.5 nm. ^b $\Delta\lambda_{\max} = \lambda_{\max}(\text{SHG}) - \lambda_{\max}(\text{bulk})$. ^c $\delta\lambda_{\max}(\text{SHG})$ represents the uncertainty in the wavelength maximum of the SHG measurement using a 95% confidence interval.

To interpret the apparent spectral red shift observed for changes in ion identity at 1 M concentrations, we compared SHG spectra to bulk aqueous electrolyte solution absorbance spectra. As shown in Figure 5.3, the solute's electronic excitation shifts to longer wavelength as bulk salt concentration increases, and the magnitude of the observed red shift correlates to ion size and hydration energy. With the exception of the fluoride ion, the red shift is more dramatic for larger ions, both cationic and anionic. For both potassium and sodium salts, the red shift is greater for a bromide counterion than a

chloride counterion. If anion identity is maintained, the red shift is greater for a potassium counterion than a sodium counterion.

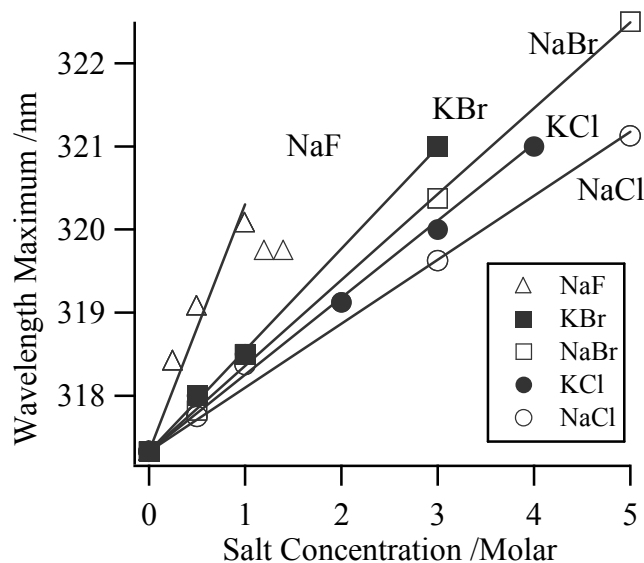


Figure 5.3. Wavelength maxima for electronic absorbance spectra of PNP in bulk electrolyte solutions. The resolution of the spectrophotometer yields an uncertainty in each data point of ± 0.5 nm. Measurements for NaF deviate from linearity as salt concentration approaches the solubility limit. Therefore the fit for this data includes only the first four data points.

This shift in bulk electrolyte solution spectra could arise from either a change in the solvent's bulk dielectric properties *or* specific ion-solute interactions. However, the static dielectric constant of a solvent generally *diminishes* upon the addition of electrolytes due to excluded volume effects and the screening of solvent dipoles by ions, which lead to a decrease in dipole-dipole correlations.²³⁻²⁷ For PNP, a decrease in the solvent's dielectric constant would lead to a *blue* shift in the absorbance spectrum. Consequently, the observed *red* shift must be attributed to specific ion-solute interactions that increase the solute's ground state dipole moment relative to the dipole moment of the excited state. A previous report has suggested that the arrangement of water molecules around a PNP molecule is similar to that of water around cations.²⁸ The authors claim that

the competition for hydration between PNP and cations weakens the solvation of PNP. The solvation of PNP is weakened further by cations with more negative enthalpies of hydration. The solvatochromic behavior of PNP indicates that a more strongly bound solvation shell around the solute causes a red shift in the electronic absorbance spectrum. Consequently, PNP in electrolyte solutions containing larger cations (K^+ vs. Na^+ in this case) will show a larger positive deviation (= red shift) from the salt-free absorbance wavelength maximum.²⁹

Conversely, anions will tend to enhance the solvation of PNP molecules in solution. Enhanced solvation of PNP is most pronounced for weakly hydrated anions. Therefore, one expects to see a more prominent red shift from the salt-free absorbance wavelength for larger, less solvated anions. The expected results are consistent with data presented in this work, although we are as yet unable to explain the behavior of fluoride-containing solutions. (Fluoride salts were not used in the work cited above.²⁹)

As summarized in Table 5.1, the observed spectral shifts of PNP adsorbed to aqueous electrolyte/cyclohexane interfaces closely tracks changes in the solute's electronic structure in bulk aqueous electrolyte solutions as a function of salt concentration and identity. For 1 M NaF measurements, the SHG maximum is identical to the bulk solution absorbance maximum. The slight red shift from bulk solution measurements for 1 M NaCl and 1 M NaBr (+3 nm and +4 nm, respectively) lie within the uncertainty associated with the SHG measurements (see Table 5.1). Even if the apparent spectral red shift observed for adsorbed PNP as a function of ion identity is real, given the small magnitude of the shift from bulk electrolyte solution limits *and* the absence of any systematic spectral shift as a function of salt concentration

(Figure 5.2b-c), we can attribute the observed red shift in surface spectra entirely to effects similar to those in bulk electrolyte solutions rather than specific, surface charge effects. However, given the magnitude and uncertainty in $\lambda_{\text{max}}(\text{SHG})$, any effects of ions on surface solvation cannot differ significantly from bulk solution interactions.

This conclusion that simple salts affect both water/cyclohexane interfacial polarity and bulk solution solvation of PNP in the same way is somewhat surprising given the previously discussed results for cationic and anionic molecular rulers. Probe-headgroup interactions for cationic rulers were thought to significantly perturb the response of the solvatochromic chromophore whereas anionic headgroups showed no evidence of such interaction.^{15,16} Furthermore, given recent molecular dynamics simulations⁵ that indicate a significantly higher surface activity for bromide ions than fluoride ions, we would expect a marked difference in SHG spectra for NaF and NaBr systems. However, surface spectra of both systems are indistinguishable from their respective bulk solution limits. To reconcile previous findings^{5,15,16} with the results presented above, we suggest that the effects of charge on surface solvation are important only when the charge and the solute are closely coupled (as they are in cationic surfactants).

Distribution of PNP and PNP^- at the Aqueous/Cyclohexane Interface

In our efforts to study effects of electrolytes on surface solvation, we carefully controlled the aqueous phase ionic strength. Using a neutral surfactant, PNP, as opposed to the charged molecular rulers helps minimize the amount of unwanted charged species in solution. However, PNP presents a unique source of ions through its equilibrium with the conjugate base, PNP^- ($\text{pK}_a = 7.15$,³⁰ Figure 5.4a). To ensure that the liquid/liquid

interface was not “contaminated” by this ionic solute, the surface distribution of PNP and PNP^- in a solution containing 10 mM PNP was determined.

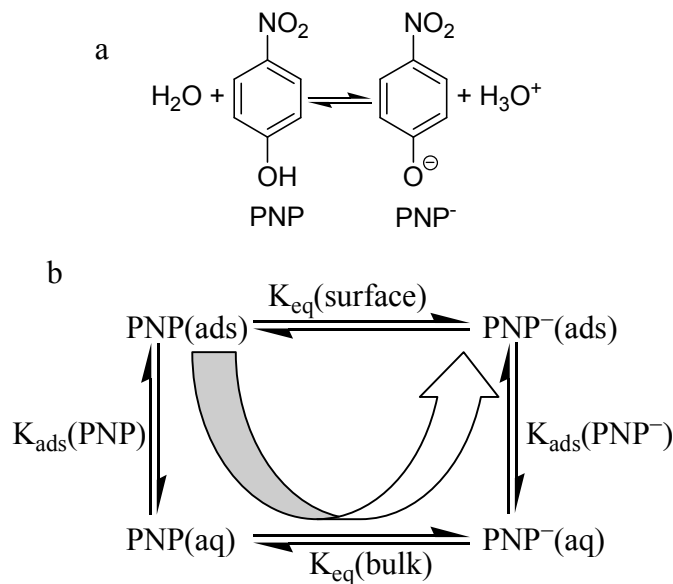


Figure 5.4. Equilibrium equations governing the distribution of PNP and PNP^- in bulk solution (a) and at the water/cyclohexane interface (b).

Since the change in Gibbs free energy is a state function and is related to the equilibrium constant describing PNP/PNP^- partitioning, we can determine the surface distribution of these two species by taking a stepwise path as shown in Figure 5.4b. The equilibrium distribution for PNP and PNP^- in bulk solution ($K_{\text{eq}}(\text{bulk})$) is known, and the equilibrium constants for the adsorption of PNP ($K_{\text{ads}}(\text{PNP})$) and PNP^- ($K_{\text{ads}}(\text{PNP}^-)$) in 10 mM solutions were calculated from adsorption isotherms at the water/cyclohexane interface of PNP under acidic conditions and NaPNP, respectively.

Figure 5.5 shows the surface pressure isotherms for these two systems acquired using the Wilhelmy plate method.³¹ Excess surface concentration was determined by

fitting the data to the Gibbs equation (Eq. 2.3)³¹ where the interfacial area is in cm^2 , the interfacial pressure is in J/cm^2 , and the surface excess is in moles. R , the gas constant is $8.314 \text{ Jmol}^{-1}\text{K}^{-1}$, and the temperature is $295 \pm 1.5 \text{ K}$. Since measurements are taken at millimolar concentrations, we approximate the solute activity with the bulk concentration, c using molL^{-1} . The surface excess concentrations of PNP and PNP^- were calculated using Eq. 2.4. From 10 mM solutions of acidic PNP and NaPNP, Γ/A is $2.04 \times 10^{-10} \text{ mol}/\text{cm}^2$ for PNP and $2.06 \times 10^{-11} \text{ mol}/\text{cm}^2$ for PNP^- , a difference of one order of magnitude.

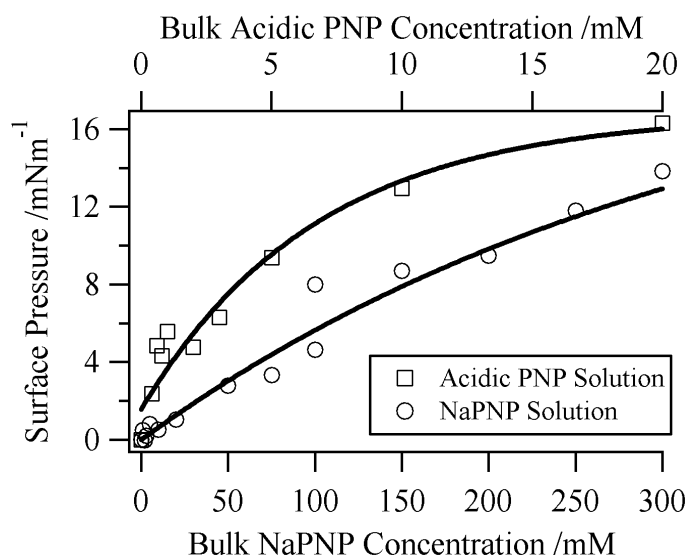


Figure 5.5. Surface pressure isotherms for PNP and PNP^- . Surface pressure data was fit using the Gibbs isotherm (Eq. 2.3). Uncertainty (2σ) ranges from $1\text{-}6 \text{ mNm}^{-1}$ for acidic PNP measurements (squares, top axis) and $0.1\text{-}0.8 \text{ mNm}^{-1}$ for NaPNP measurements (circles, bottom axis). Data from acidic PNP solutions indicate PNP adsorption while data from NaPNP correspond to PNP^- adsorption.

Determining the equilibrium constant for an adsorption process is difficult because there exists no well-defined standard state for the surface excess concentration. In these calculations, a mole fraction of 1 was used as the standard state for each species

at the surface and in bulk solution. Given that the surface orientation of PNP is 55° off normal³² and the volume occupied by one PNP molecule, as determined through geometric considerations, is $\sim 57 \text{ \AA}^3$, we estimate that, using the room temperature density of water, each surface molecule of PNP or PNP^- replaces about two water molecules. Defining the depth of the adsorbed monolayer to be $\sim 3.3 \text{ \AA}$ (according to the size of a PNP molecule with the appropriate orientation) allows us to calculate the mole fraction of adsorbed surfactant, X_i^{ads} , where i represents either PNP or PNP^- . The mole fraction of adsorbed PNP was calculated to be 0.12 using the isotherm for PNP under acidic conditions (pH ~ 3) and that of PNP^- was determined to be 0.01 using the isotherm for NaPNP, assuming total dissociation of NaPNP into Na^+ and PNP^- . We then calculate the mole fraction of the solute in bulk solution X_i by multiplying the molar concentration (0.01 M) by the molar volume of water, 0.018 Lmol^{-1} . (This calculation assumes that there is no change in the molar volume of water from that of pure water for such dilute solutions.) For a 10 mM solution, X_i is 1.8×10^{-4} . The equilibrium constant for adsorption of species i , $K_{\text{ads}}(i)$, is simply $[X_i^{\text{ads}}/X_i]$. Given the surface excess concentrations of PNP and PNP^- (stated above), the equilibrium constants are calculated to be 680 for $K_{\text{ads}}(\text{PNP})$ and 61 for $K_{\text{ads}}(\text{PNP}^-)$.

The surface distribution of PNP and PNP^- in a 10 mM solution, $K_{\text{eq}}(\text{surface})$, can now be determined according to the following equation

$$K_{\text{eq}}(\text{surface}) = K_{\text{eq}}(\text{bulk}) * K_{\text{ads}}(\text{PNP}^-) / K_{\text{ads}}(\text{PNP}) \quad (5.1)$$

where $K_{\text{eq}}(\text{bulk})$ represents the equilibrium distribution of PNP and PNP^- in bulk solution. Here, we have neglected any contributions from the hydronium ion to the equilibrium constant. The bulk solution dissociation reaction is defined simply as

PNP(aq) \leftrightarrow PNP⁻ (aq), and the equilibrium constant, $K_{\text{eq}}(\text{bulk})$ is defined accordingly for a 10 mM solution. Under these conditions, $K_{\text{eq}}(\text{bulk})$ is 2.6×10^{-3} . The equilibrium surface distribution, $K_{\text{eq}}(\text{surface})$, of PNP and PNP⁻ is $\sim 2.4 \times 10^{-4}$. Compared to the amount in bulk solution, there is even less PNP⁻ at the surface of a 10 mM solution of PNP. We conclude that since only about 0.02% of the surface molecules are PNP⁻, there is very little “contamination” of the surface by this ionic species, and therefore, any spectral changes produced by ions come from simple salts rather than the equilibrium between PNP and PNP⁻.

5.4. Conclusions

Previous experiments using SHG for surfactants adsorbed to the water/cyclohexane interface suggested that cationic molecular rulers are solvated by a less polar interfacial environment than analogous anionic rulers at the same interface. SHG studies of a neutral surfactant, PNP, adsorbed to the water/cyclohexane interface were performed to further explore the role of charges in interfacial solvation. Results indicate that, compared to bulk solution absorbance spectra, there is no dependence of SHG spectra on charge identity or concentration when the simple salts NaF, NaCl, and NaBr are added to the aqueous phase. These seemingly contradictory results are resolved by the following conclusions: (1) charges at the water/cyclohexane interface influence the interfacial solvation of a solute in the same way that bulk solution solvation is affected by the addition of electrolytes, and (2) the spectral shift of adsorbed cationic molecular rulers (relative to anionic molecular rulers) suggests a nonpolar interfacial environment but is actually a result of a change in the solute’s electronic structure due to an unshielded probe-headgroup interaction. Additionally, a surface tension study of a 10 mM PNP

solution in equilibrium with an organic cyclohexane phase was carried out. Results indicate that the partitioning of PNP and PNP^- at the surface favors PNP adsorption over PNP^- adsorption by a factor of ten. This equilibrium distribution is one order of magnitude greater than that found in bulk solution, demonstrating that the amount of PNP^- present at the water/cyclohexane interface of a 10 mM PNP solution is negligible.

References

- (1) Gouy. *J. Phys. IV* **1910**, 9, 457.
- (2) Stern, O. *Z. Elektrochem.* **1924**, 30, 508.
- (3) Randles, J. E. B. *Phys. Chem. Liq.* **1977**, 7, 107.
- (4) Weissenborn, P. K.; Pugh, R. J. *J. Colloid Interface Sci.* **1996**, 184, 550.
- (5) Jungwirth, P.; Tobias, D. J. *J. Phys. Chem. B* **2002**, 106, 6361.
- (6) Petersen, P. B.; Saykally, R. J. *Chem. Phys. Lett.* **2004**, 397, 51.
- (7) Raymond, E. A.; Richmond, G. L. *J. Phys. Chem. B* **2004**, 108, 5051.
- (8) Liu, D.; Ma, G.; Levering, L. M.; Allen, H. C. *J. Phys. Chem. B* **2004**, 108, 2252.
- (9) Ghosal, S.; Hemminger, J. C.; Bluhm, H.; Mun, B. S.; Hebenstreit, E. L. D.; Ketteler, G.; Ogletree, D. F.; Requejo, F. G.; Salmeron, M. *Science* **2005**, 307, 563.
- (10) Onsager, L.; Samaras, N. N. T. *J. Chem. Phys.* **1934**, 2, 528.
- (11) Adam, N. K. *The Physics and Chemistry of Surfaces*; Oxford University Press: London, 1941.

- (12) Bikerman, J. J. *Surface Chemistry: Theory and Applications*; Academic Press: New York, 1958.
- (13) Chatteraj, D. K.; Birdi, K. S. *Adsorption and the Gibbs Surface Excess*; Plenum: New York, 1984.
- (14) Aveyard, R.; Saleem, S. M. *J. Chem. Soc., Faraday Trans. 1* **1976**, *72*, 1609.
- (15) Beildeck, C. L.; Steel, W. H.; Walker, R. A. *Langmuir* **2003**, *19*, 4933.
- (16) Beildeck, C. L.; Steel, W. H.; Walker, R. A. *Faraday Discuss.* **2005**, *129*, 69.
- (17) Steel, W. H.; Damkaci, F.; Nolan, R.; Walker, R. A. *J. Am. Chem. Soc.* **2002**, *124*, 4824.
- (18) Steel, W. H.; Walker, R. A. *Nature* **2003**, *424*, 296.
- (19) Steel, W. H.; Lau, Y. Y.; Beildeck, C. L.; Walker, R. A. *J. Phys. Chem. B* **2004**, *108*, 13370.
- (20) Steel, W. H.; Beildeck, C. L.; Walker, R. A. *J. Phys. Chem. B* **2004**, *108*, 16107.
- (21) Esenturk, O.; Walker, R. A. "Vibrational Studies of Alcohol Films: Molecular Structure Vs. Long-Range Order"; 227th ACS National Meeting, 2004, Anaheim, CA.
- (22) Esenturk, O.; Mago, D.; Walker, R. A. *In preparation* **2005**.
- (23) Levesque, D.; Weis, J. J.; Patey, G. N. *J. Chem. Phys.* **1980**, *72*, 1887.

- (24) Patey, G. N.; Carnie, S. L. *J. Chem. Phys.* **1983**, 78, 5183.
- (25) Kusalik, P. G.; Patey, G. N. *J. Chem. Phys.* **1988**, 88, 7715.
- (26) Barthel, J. M. G.; Krienke, H.; Kunz, W. *Top. Phys. Chem.* **1998**, 5, 1.
- (27) Bockris, J. O. M.; Reddy, A. K. N. *Modern Electrochemistry, 2nd Ed.*; Plenum: New York, 1998; Vol. 1.
- (28) Nikol'skii, B. P.; Yudovich, E. E.; Pal'chevskii, V. V.; Spevak, V. N. *Zh. Obshch. Khim.* **1969**, 39, 1673.
- (29) Nikol'skii, B. P.; Yudovich, E. E.; Pal'chevskii, V. V.; Spevak, V. N. *Zh. Fiz. Khim.* **1970**, 44, 709.
- (30) *CRC Handbook of Chemistry and Physics*; 77th ed.; Lide, D. R., Ed.; CRC Press: Boca Raton, Florida, 1996.
- (31) Adamson, A. W. *Physical Chemistry of Surfaces*; John Wiley & Sons: New York, 1990.
- (32) Steel, W. H.; Walker, R. A. *J. Am. Chem. Soc.* **2003**, 125, 1132.

Chapter 6. Conclusions and Future Directions

6.1. Conclusions

The purpose of this work was to characterize solvation at liquid/liquid interfaces through the study of interfacial solvent polarity. Through the use of specially designed surfactants, interfacial solvent polarity is profiled to determine the dipolar width of the liquid/liquid boundary. The surface activity of simple ions has been debated for decades, and, given recent simulations that suggest that polarizable ions partition to the air/water surface, we surmise that aqueous solution ionic strength may play a significant role in the interfacial solvation of solutes. This idea is investigated by monitoring interfacial polarity as a function of bulk solution ionic strength using both molecular ruler surfactants and a neutral probe molecule.

Cationic Molecular Ruler Development and Characterization

A new family of cationic, solvent-sensitive surfactants has been synthesized and characterized. The surfactants consist of a solvatochromic, hydrophobic chromophore connected to a quaternized ammonium headgroup by short alkyl spacers of varying lengths. The chromophore is based on *p*-nitroanisole (pNAs), a simple aromatic probe whose first electronic excitation wavelength shifts more than 20 nm as the local dielectric environment varies between nonpolar and polar limits. Given that pNAs is 20 times more soluble in cyclohexane than in water, lengthening the separation between the chromophore and the charged headgroup enables the chromophore to extend further into the organic phase when surfactants adsorb to an aqueous/organic interface. Thus, these surfactants can function as molecular rulers by measuring the distance required for

solvent polarity to converge from an aqueous to an organic limit across different liquid/liquid boundaries. Resonance-enhanced second harmonic generation (SHG) can be used to measure effective excitation spectra of surfactants adsorbed to an aqueous/cyclohexane interface. In bulk solution, short-chain surfactants appear to self-associate through a charge-dipole interaction between the charged headgroup and the probe's aromatic ring. This behavior manifests itself as diminished solvatochromic activity as well as through-space coupling in nuclear Overhauser enhancement spectra. The strength of intramolecular association diminishes with increasing alkyl spacer length and disappears completely with alkyl chains having six methylene groups.

Cationic Rulers and Simple Salts at Liquid/Liquid and Model Liquid/Liquid Interfaces

SHG coupled with molecular rulers has been used to explore solvation across liquid/liquid interfaces in the presence of excess charge in the aqueous phase. Interfacial dipolar width is monitored as a function of chromophore-headgroup separation. Data show that cationic and anionic surfactants of equivalent lengths sample very different environments across a water/cyclohexane interface. The effective excitation wavelength of the cationic surfactants are consistent with those of the solutes in bulk cyclohexane while anionic surfactants sample an environment that converges smoothly from the aqueous to the organic limit with increasing spacer length. To further evaluate the effect of surface charge on interfacial solvation, SHG was used to probe the environment surrounding molecular ruler chromophores adsorbed to the liquid/vapor interface of water saturated with 1-octanol. The densely packed monolayer of 1-octanol that forms on the water surface has been shown to reproduce qualitatively many of the features associated with bulk water/alkane interfaces and are logistically easier to assemble. Changing the

ionic strength of the underlying aqueous subphase drives cationic molecular rulers to adopt anionic ruler-like behavior. SHG results suggest that alterations of the electronic structure of the cationic ruler probe at salt-free interfaces are due to headgroup-probe interactions rather than properties of the surrounding nonpolar environment.

Interfacial Solvation of PNP as a Function of Ionic Strength and Salt Identity

SHG was used to study the interfacial solvation of a neutral surfactant, PNP, adsorbed to the water/cyclohexane interface in the presence of simple salts at varying salt concentrations. The purpose of this work was to determine what relationship (if any) exists between interfacial polarity and bulk solution ionic strength. Data show an apparent red shift in SHG spectra with an increase in salt anion size from fluoride to chloride to bromide at 1 M salt concentrations. A spectral red shift of the PNP electronic excitation implies an increase in local polarity. Within experimental limits, however, these observed interfacial spectral shifts mimic shifts in absorbance spectra observed for PNP in bulk electrolyte solutions. Given the similarities between bulk and surface behavior, we conclude that observed shifts in SHG spectra are attributed to effects similar to those found in bulk solution. Additionally, the surface adsorption of PNP to the water/cyclohexane interface was studied to determine the surface distribution of PNP and the conjugate base, *p*-nitrophenoxide (PNP^-) for a 10 mM PNP solution. PNP adsorption is favored over PNP^- adsorption by a factor of ten, giving rise to an equilibrium surface distribution that is an order of magnitude greater than that found in bulk solution. These findings indicate that the amount of PNP^- at the surface in an aqueous solution of 10 mM PNP is negligible.

6.2. Future Directions

Molecular rulers, both anionic and cationic, have proven to be useful probes for studying solvation at liquid/liquid interfaces. While anionic rulers have been used extensively to determine dipolar widths of several weakly- and strongly-associating liquid/liquid interfaces, cationic rulers have just “scratched the surface” when it comes to monitoring interfacial polarity as a function of ionic strength. These studies have focused on measuring interfacial solvation using simple salts and varying anion identity, since highly polarizable anions (e.g. Br^-) are predicted to have a higher affinity for the air/water surface. Recent simulations suggest that, given their role in the hydrogen-bonding network of water, positively charged hydronium ions may also be attracted to the air/water surface. Future studies will involve molecular rulers and other simple electrolyte solutions to profile interfacial polarity as a function of cation identity including the hydronium ion. Other, more complex salts (including organic salts) will be used to see if cations with a greater affinity for the organic phase (due to their relative hydrophobic nature) influence interfacial solvation to a greater degree than inorganic salts. Since the cationic headgroup is a trimethyl ammonium ion, the use of organic ions in solution is important to further distinguish between the anionic and cationic ruler headgroup effects observed at the water/cyclohexane interface.

Changing the ionic strength of a solution is only one way to alter the surface free energy (i.e. surface tension) of a liquid/liquid system. Countless studies have shown that adsorbed monolayers lower the interfacial tension, and the dynamics of such adsorption are well understood. However, little is known about how the presence of a monolayer affects interfacial polarity. Charged monolayers formed by molecular rulers at the

liquid/liquid interface are ideal candidates for answering these questions. While the interfacial polarity of several liquid/liquid systems has been profiled using anionic or cationic molecular rulers, experiments involving mixed monolayers have not yet been attempted. Given that cationic and anionic molecular rulers yield such contrasting results for the weakly-associating water/cyclohexane interface, predicting how mixed monolayers of these charged species would affect interfacial solvation is not trivial.

Another way to regulate surface energy (and structure) is with temperature. While temperature-dependent studies are limited to a relatively small range due to the freezing and boiling points of solvents, changes in molecular structure may be observable. Phase changes involving the order or disorder of alkyl chains of the molecular rulers and packing densities of solvents are two examples of structural changes that will likely impact interfacial solvation. Also, according to the Gibbs relation, as temperature increases, surface tension decreases. Changes in the surface free energy play an important role in the adsorption of surfactants to liquid/liquid interfaces. As more or less surfactants exist at a surface, the ability of the neighboring molecules to solvate the surfactant may change. Understanding such phenomena will lead to inferences about the influence of molecular structure and surface free energy on interfacial solvation. While temperature-controlled studies that use molecular rulers to probe interfacial solvation are planned, significant alterations to the experimental setup are required. In particular, a new temperature-regulated cell must be designed and constructed while maintaining the important features of the current system.

Finally, as work continues on the study of interfacial solvation, new molecular rulers will be designed. Many have suggested that, to have better control over the position

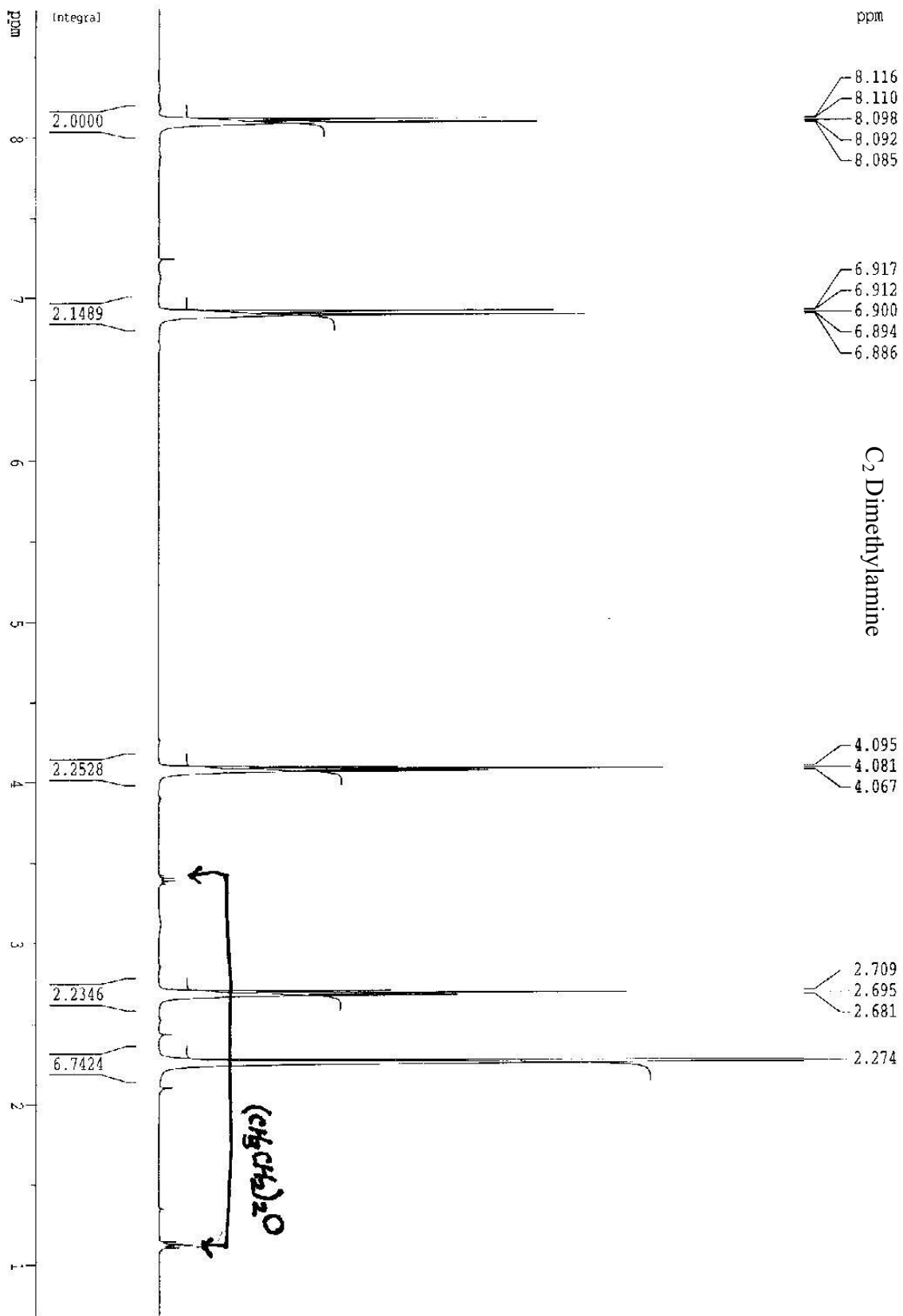
of the chromophore within the interfacial region, molecular rulers should have a more rigid structure in contrast to the flexible nature of the methylene chain currently being used. Incorporation of double or triple bonds into the alkyl spacer architecture may achieve this purpose and possibly weaken or even prevent the intramolecular charge-dipole interactions observed for short-chain cationic molecular rulers. While conjugated chains may be significantly more reactive, another possibility would be to incorporate fused rings such as cyclohexane to form a decalin-type “rigid rod” spacer. Additional modifications may call for a change in the identity of the charged headgroup. Perhaps a more hydrophilic cationic headgroup like a simple ammonium could shift the behavior of the cationic molecular rulers closer to that of the anionic species by avoiding complications introduced by “float depth.”

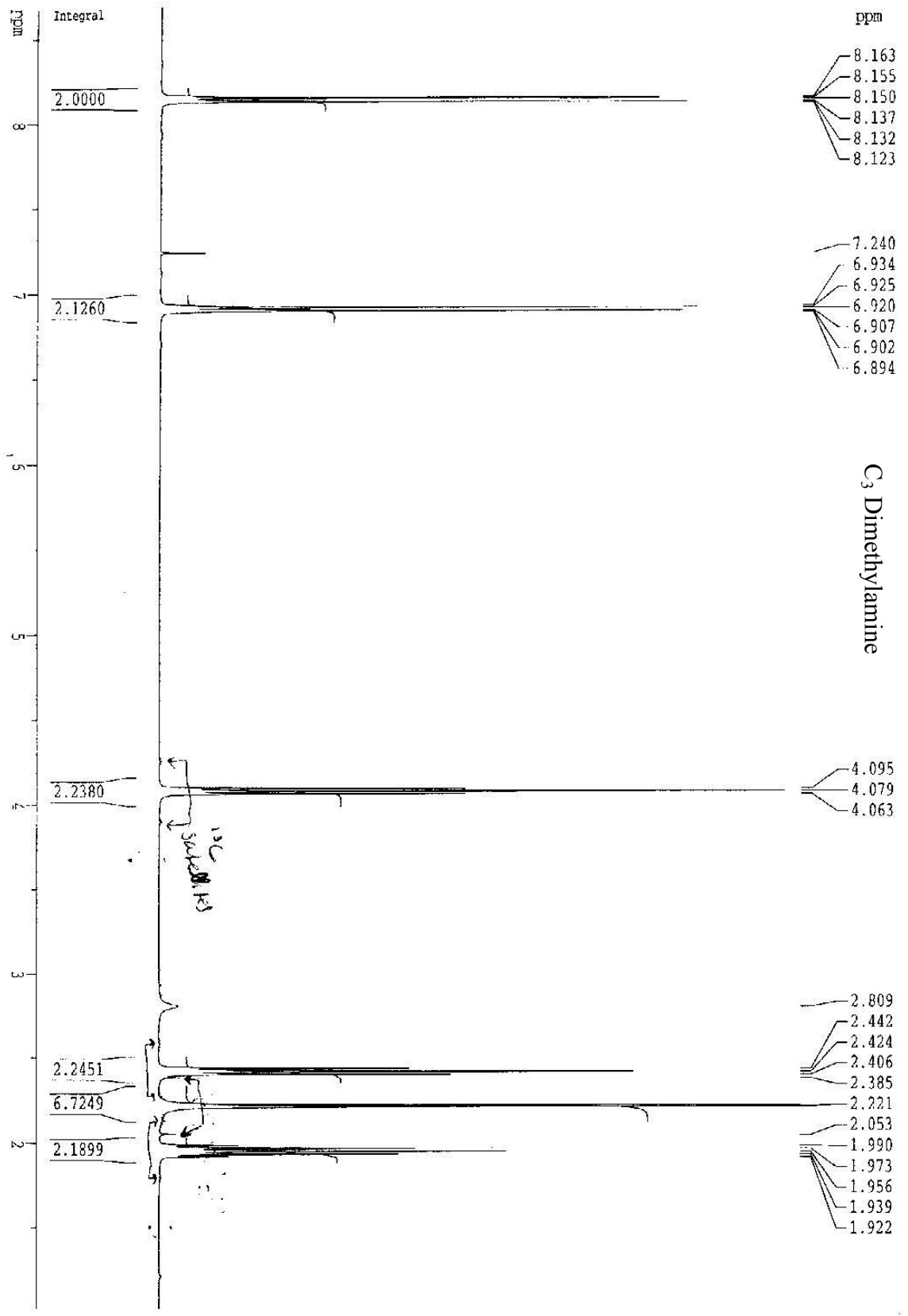
New rulers that have hydrogen-bonding capabilities are currently being designed in our lab. Recent studies from our group show that indoline has unique solvatochromic behavior that depends not on solvent polarity but on the hydrogen-bonding capacity of the solvent. Incorporating this probe structure into a molecular ruler architecture will hopefully lead to a better understanding of specific solvation forces at liquid/liquid interfaces.

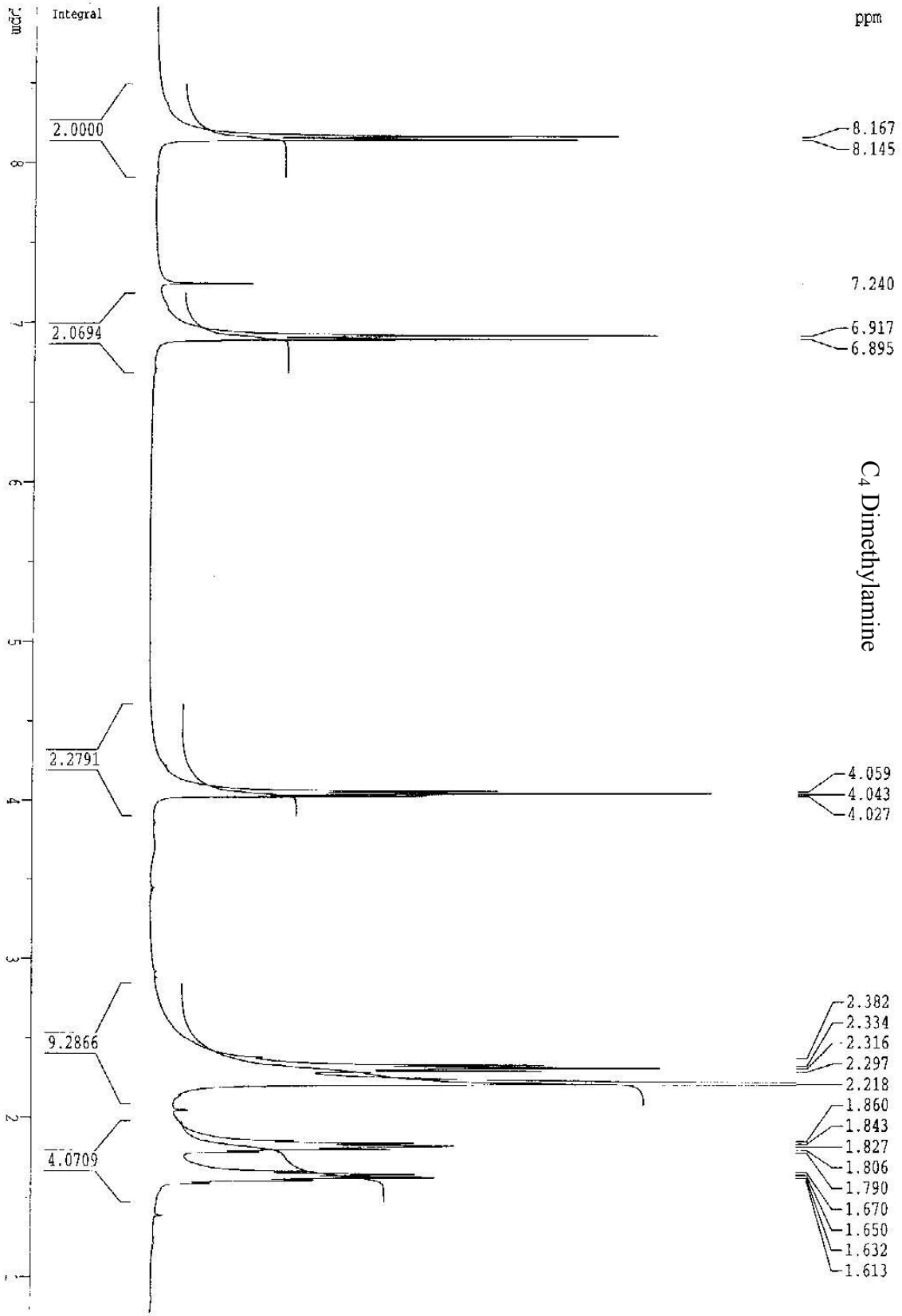
While this work has initiated an understanding of the influence of ionic strength on interfacial polarity, many unanswered questions regarding solvation at liquid/liquid interfaces remain. Studies will continue to ascertain the role of bulk solution ions on interfacial polarity and dipolar width, and future work on the development of new molecular rulers will continue to unravel the properties governing solvation at liquid/liquid interfaces.

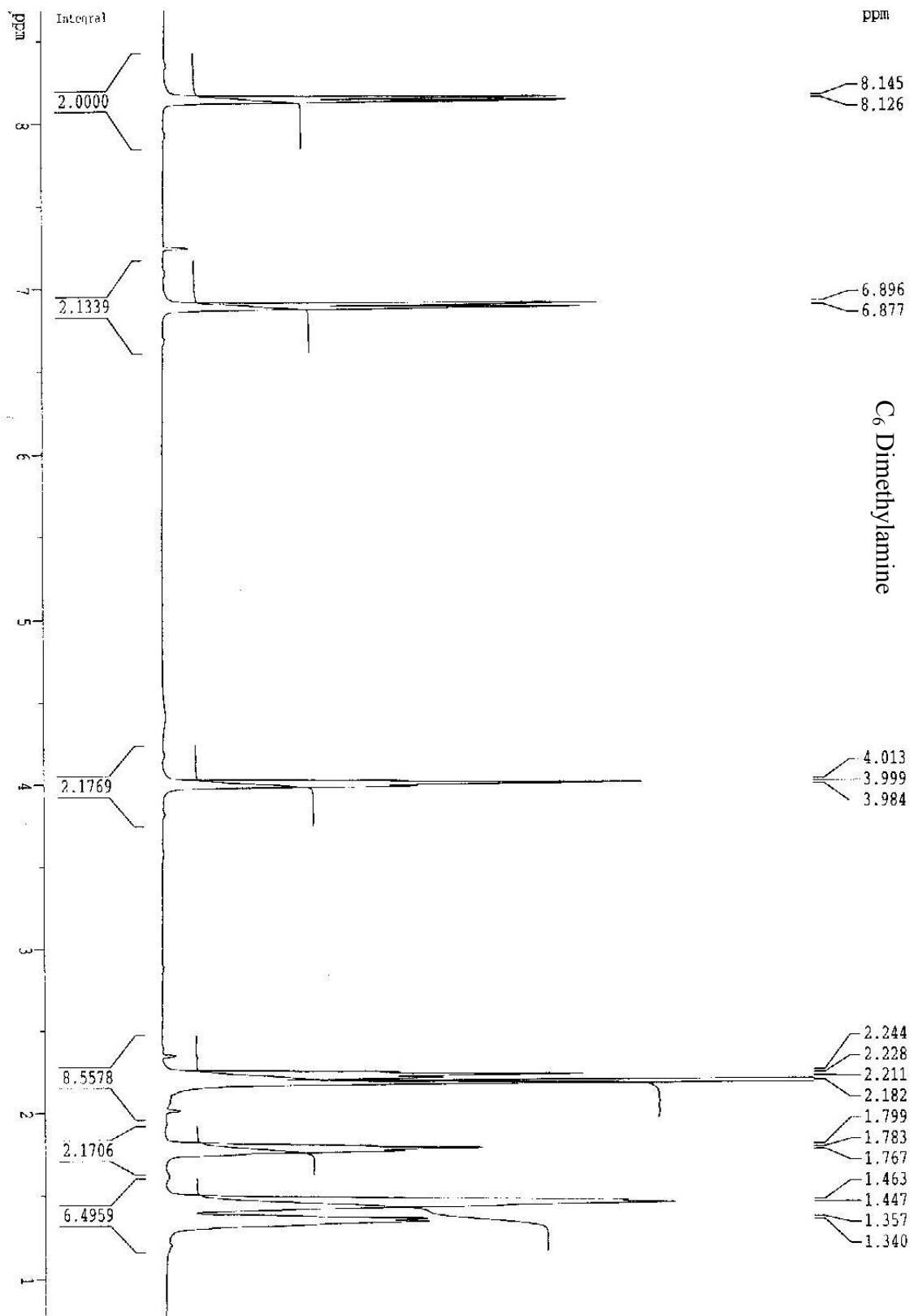
Appendix A. Characterization of Cationic Molecular Rulers

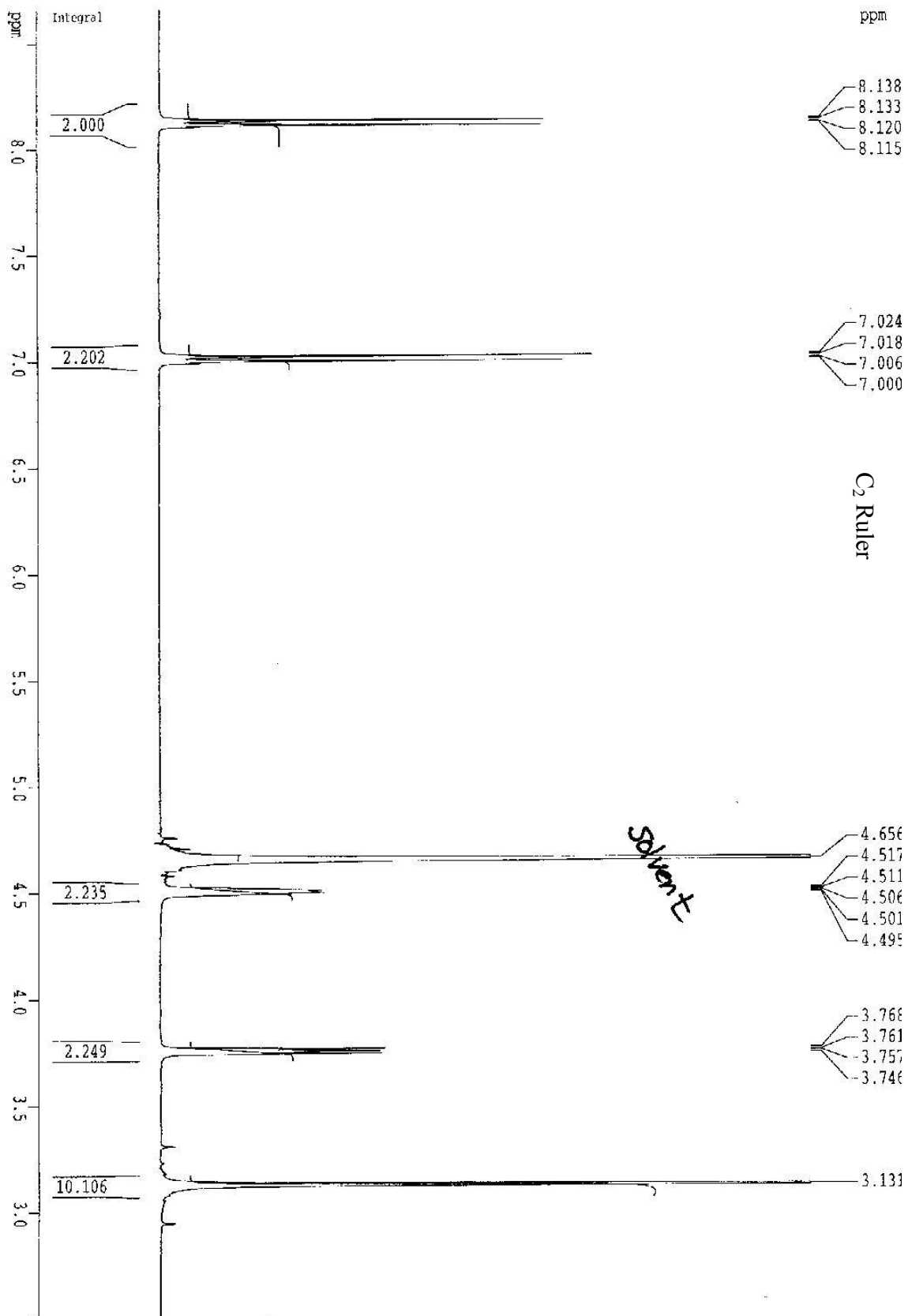
The data in this section is considered to be supporting information. It includes NMR and mass spectra recorded for all neutral and cationic molecular ruler species; NOE NMR spectra for all neutral species and the C₆ cationic ruler; and surface pressure isotherms for the C₃ and C₄ cationic rulers. When data for both neutral and cationic species are presented, that of the neutral species is presented first. When both a FAB and an EI mass spectrum are available, the FAB spectrum is displayed first. All NMR spectra of neutral species were collected in CDCl₃ while those of the cationic species were collected in D₂O. The NOE spectra display a ¹H NMR spectrum on the bottom and the enhancement spectrum on the top.

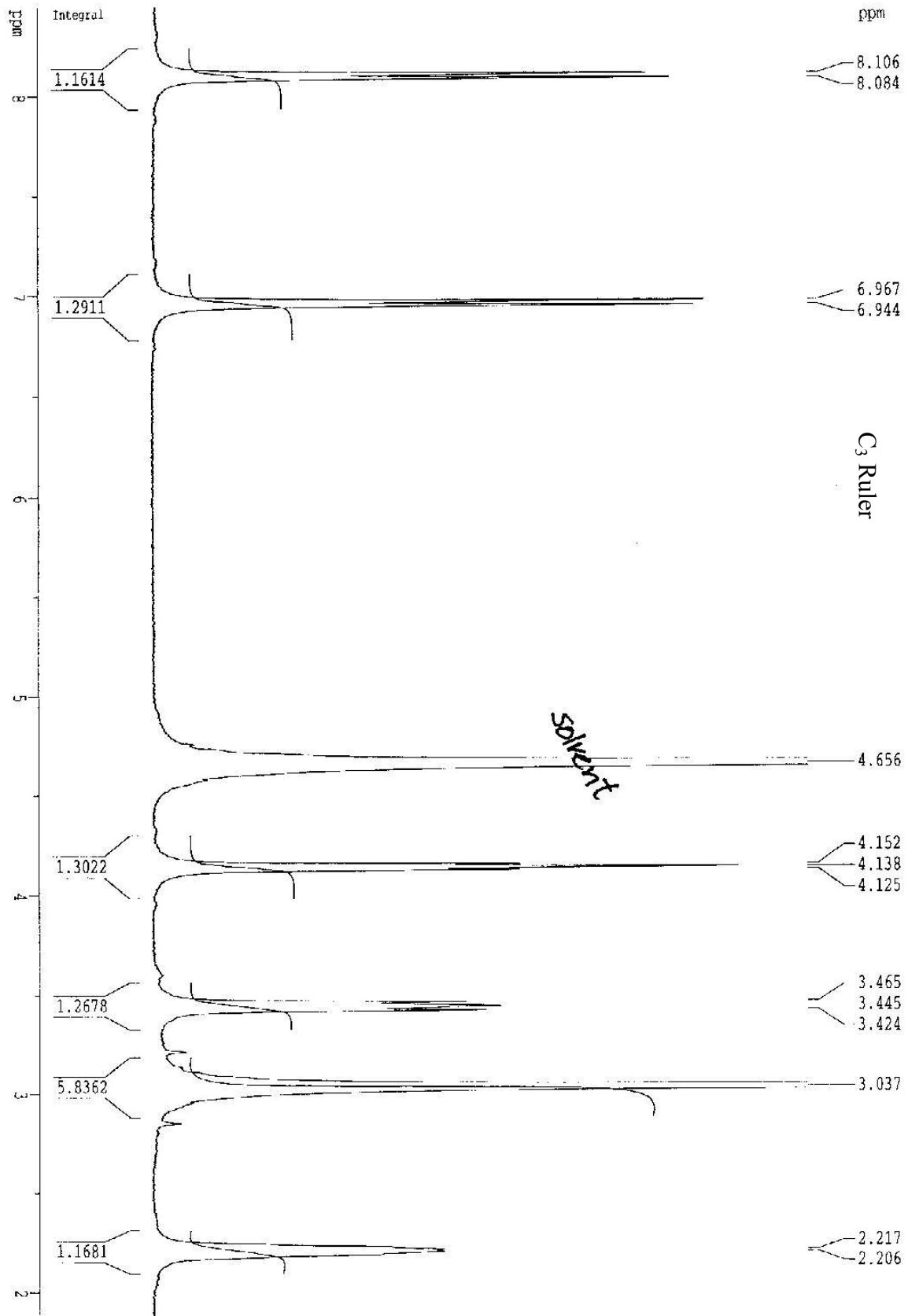


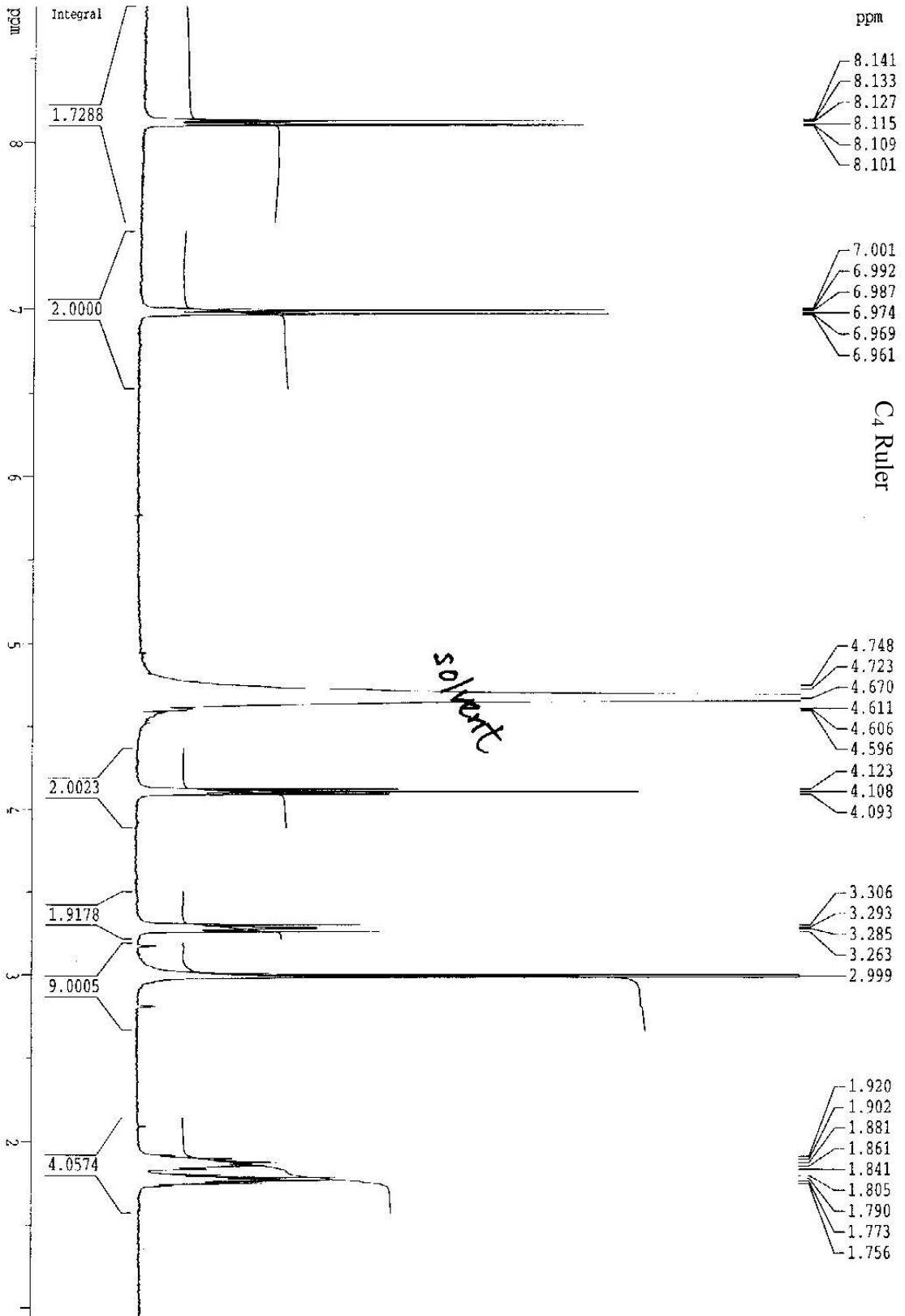


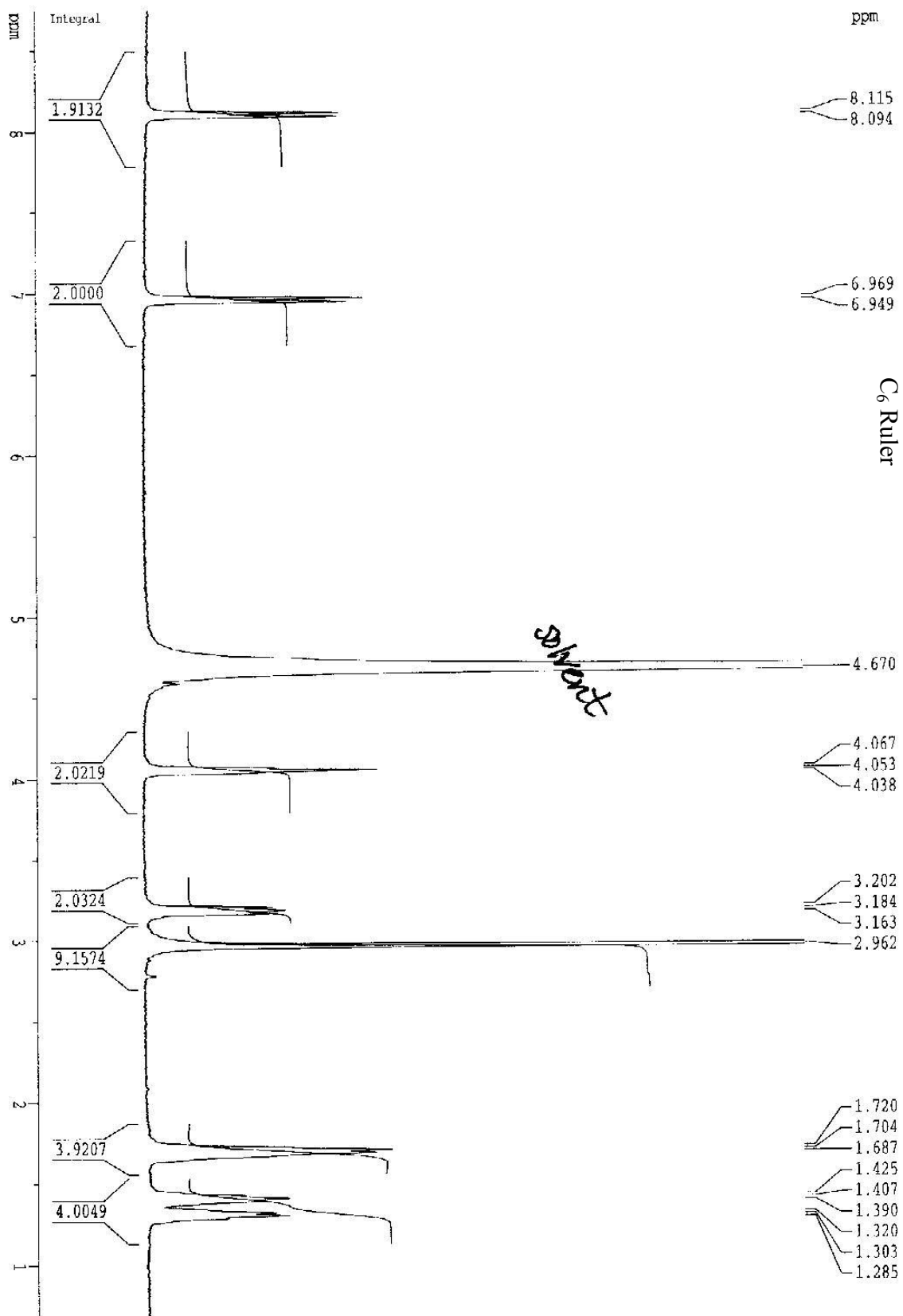


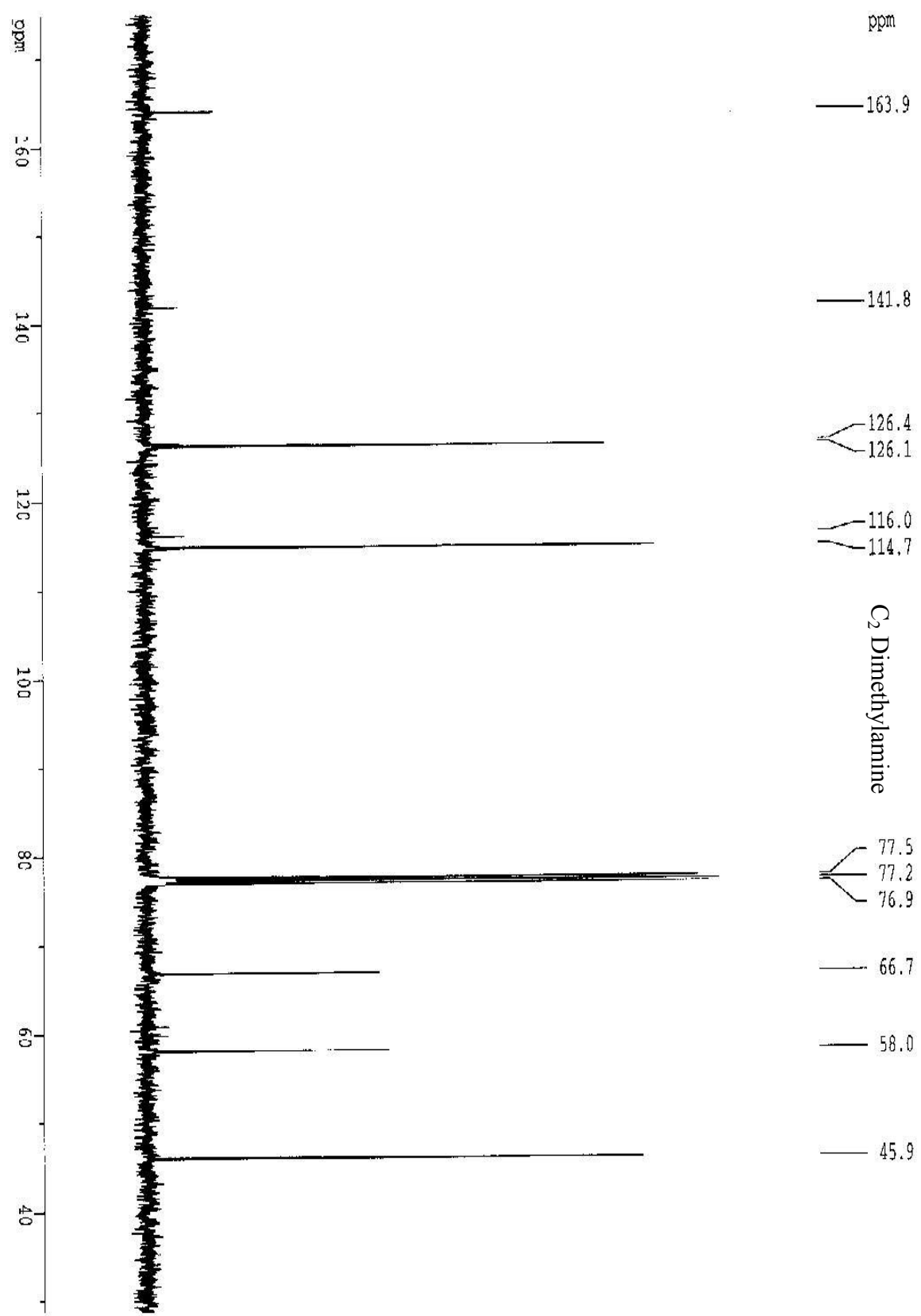


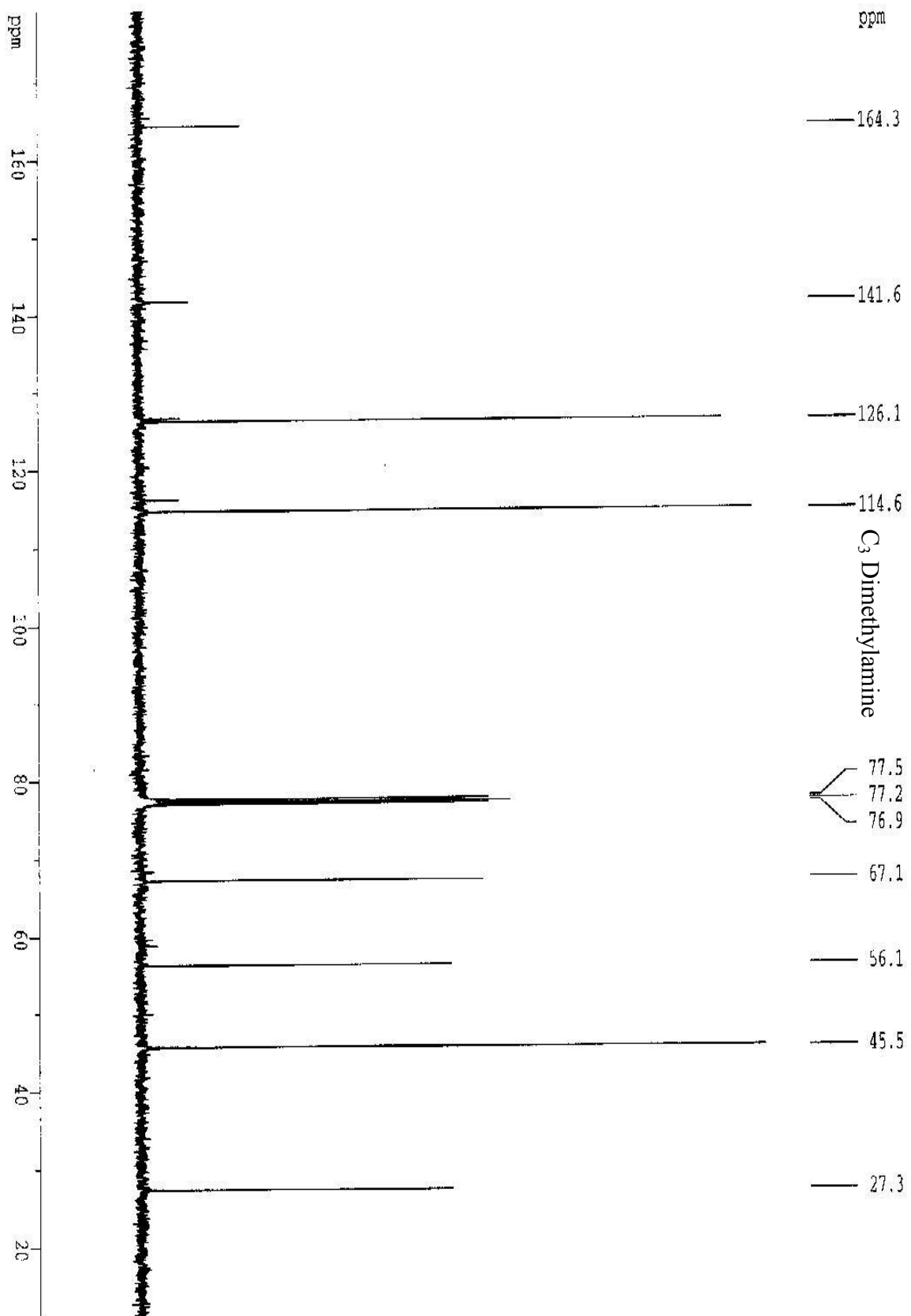


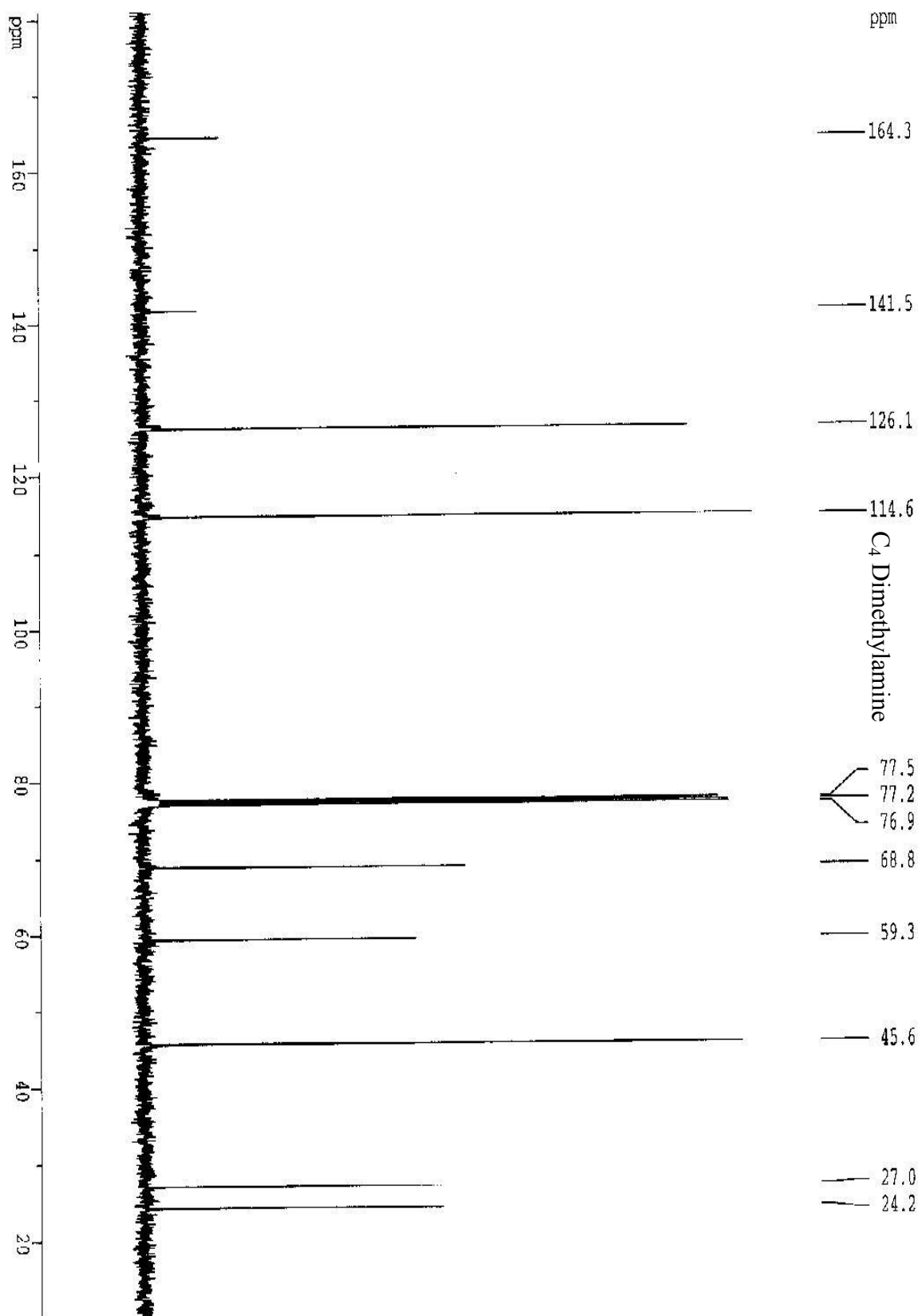


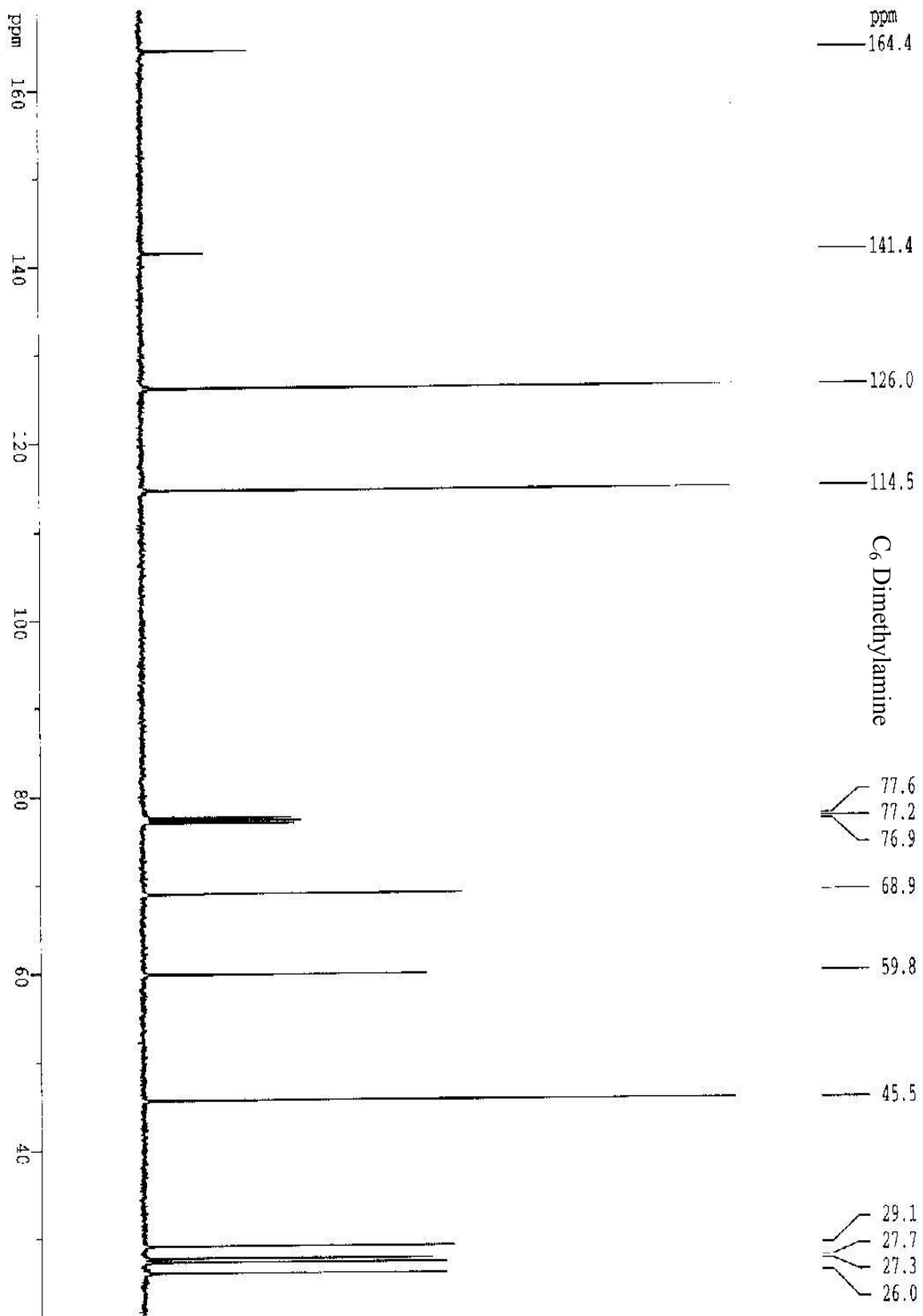




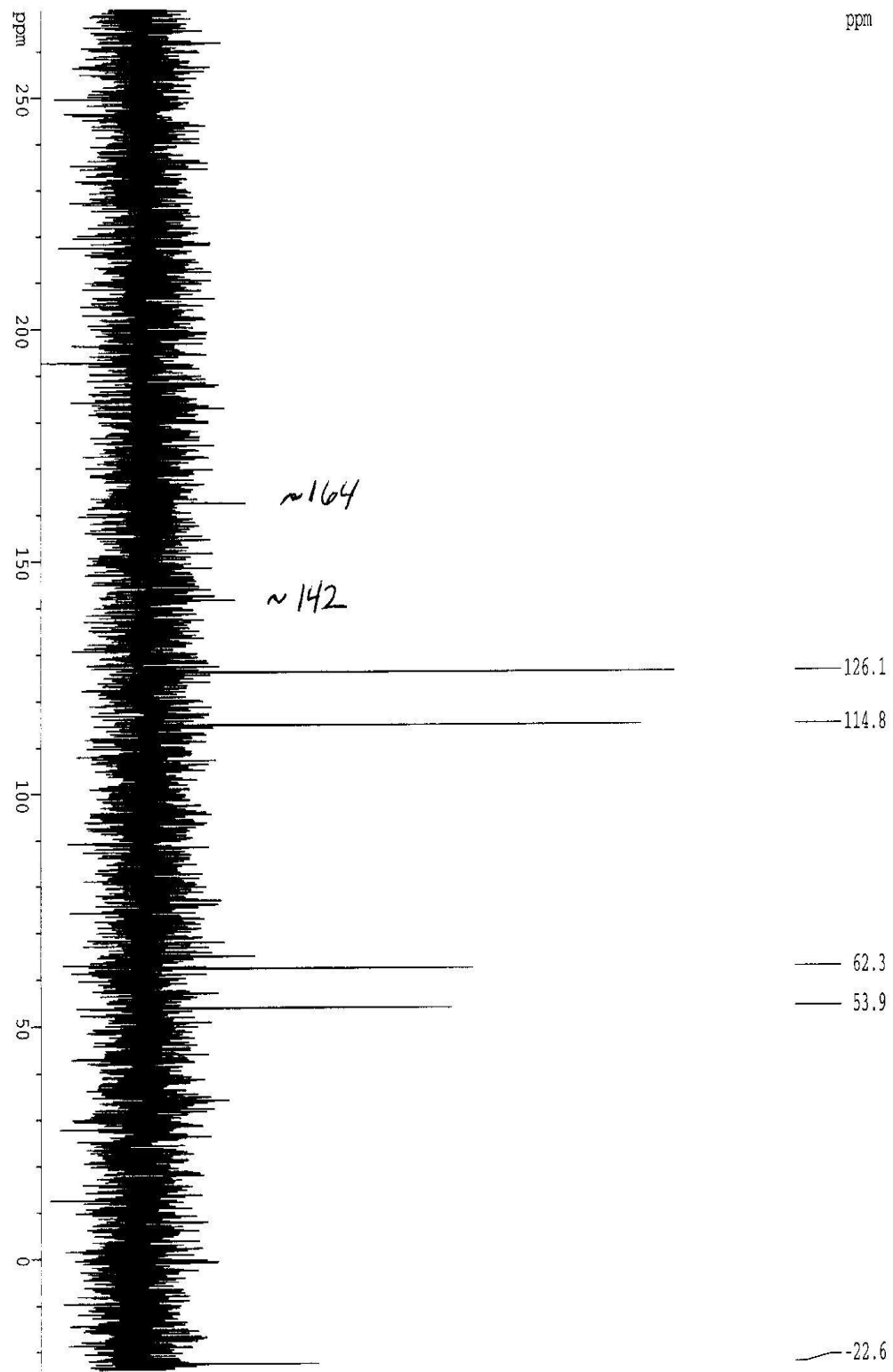




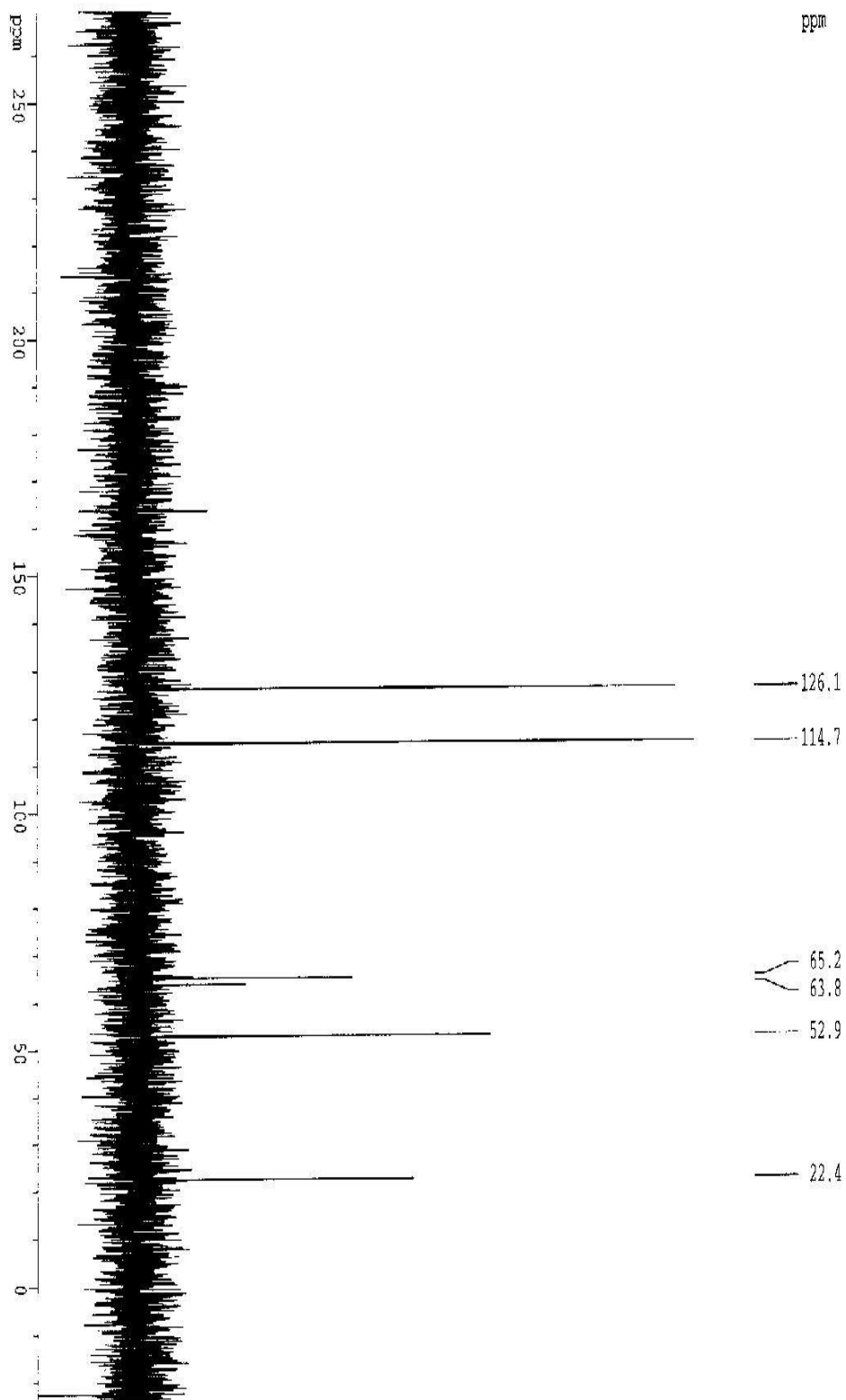




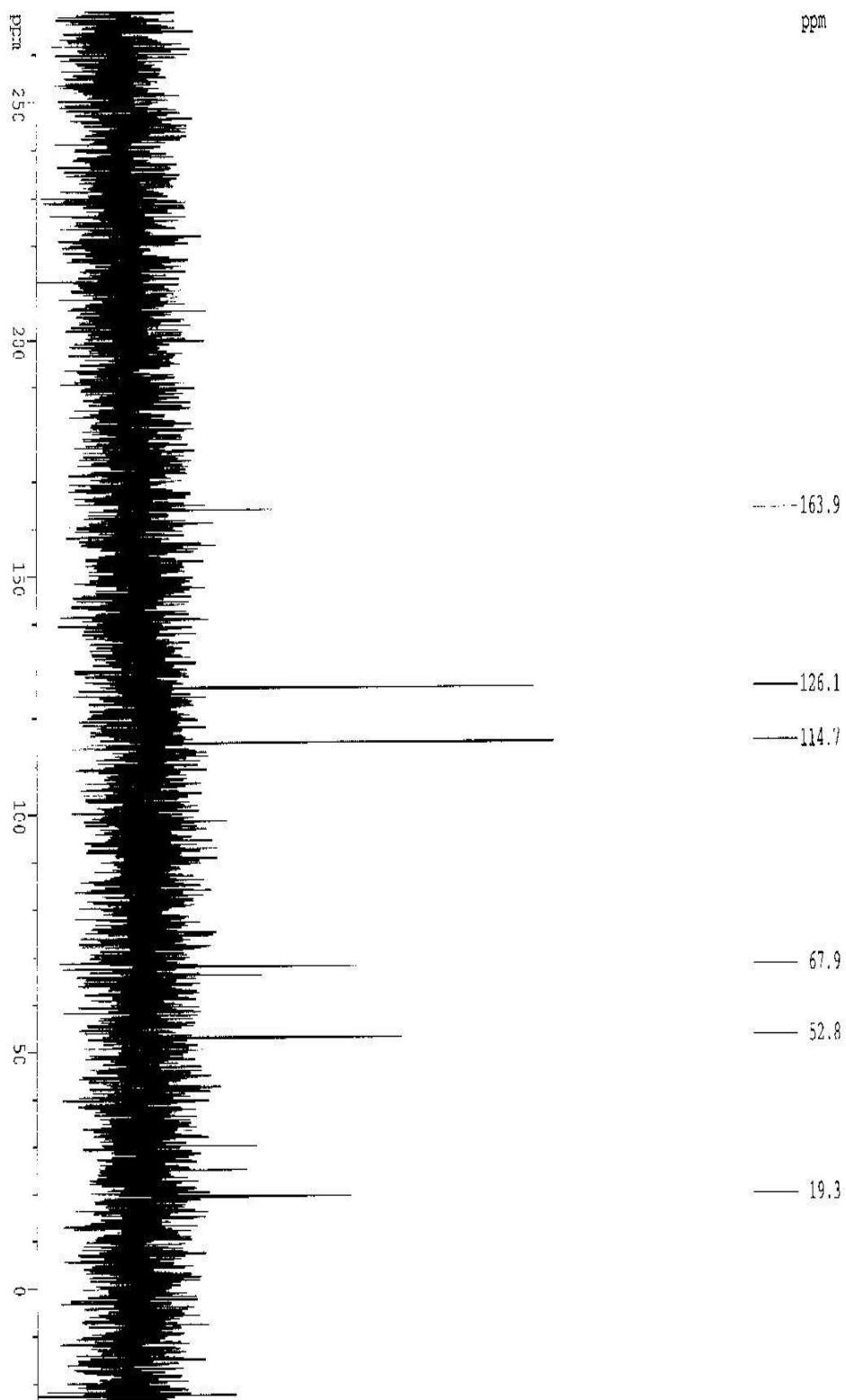
C₂ Ruler



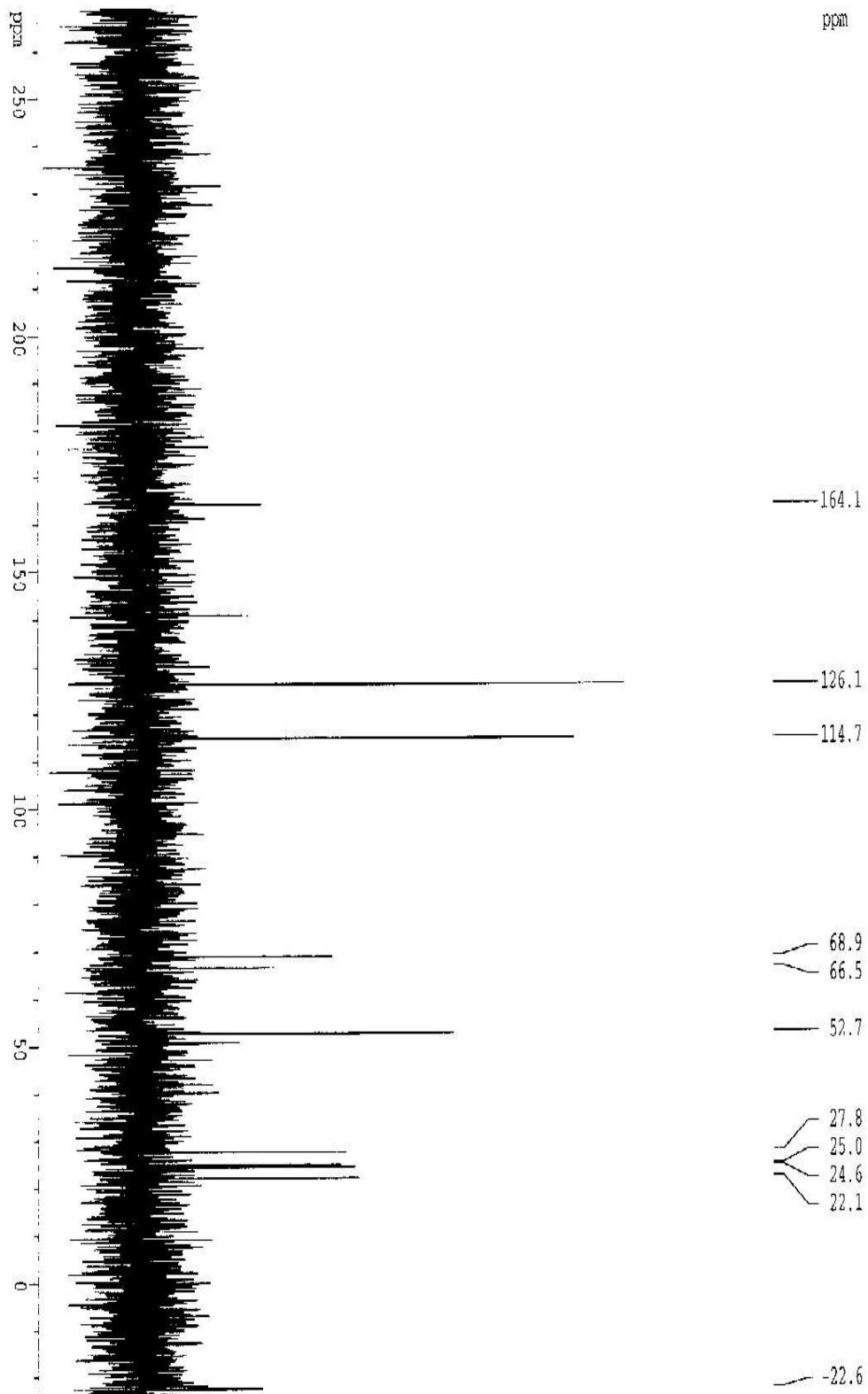
C₃ Ruler



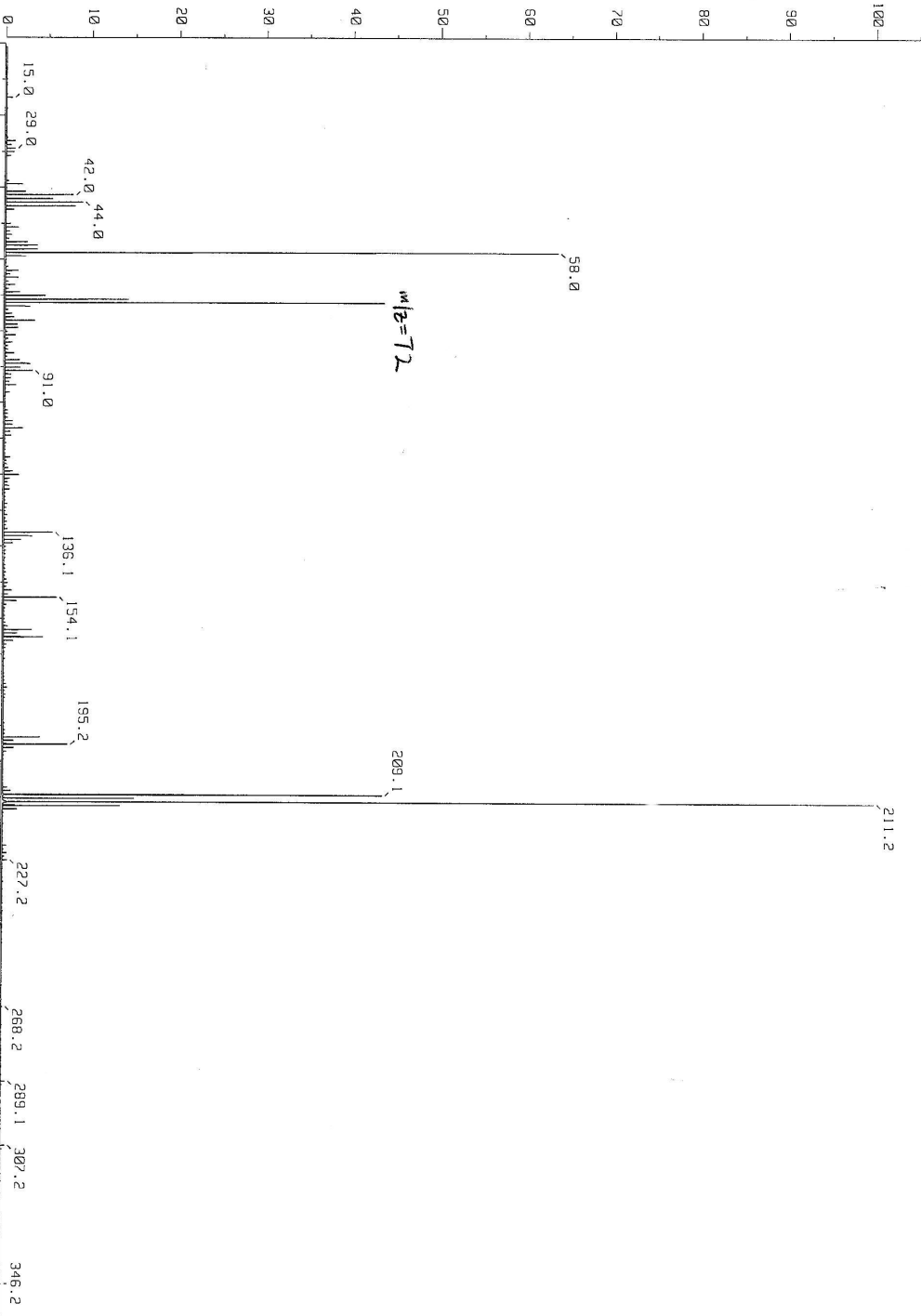
C₄ Ruler



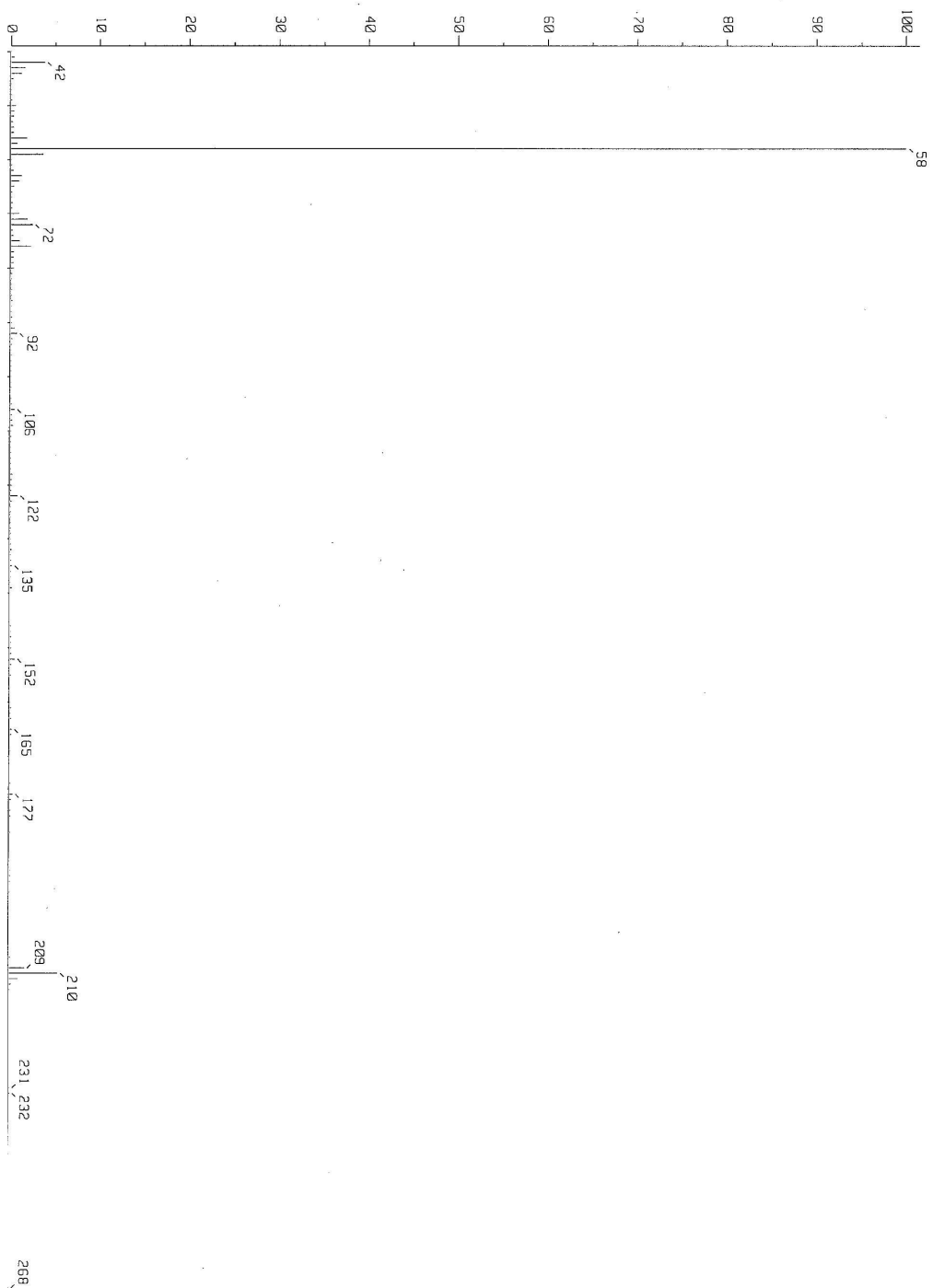
C₆ Ruler



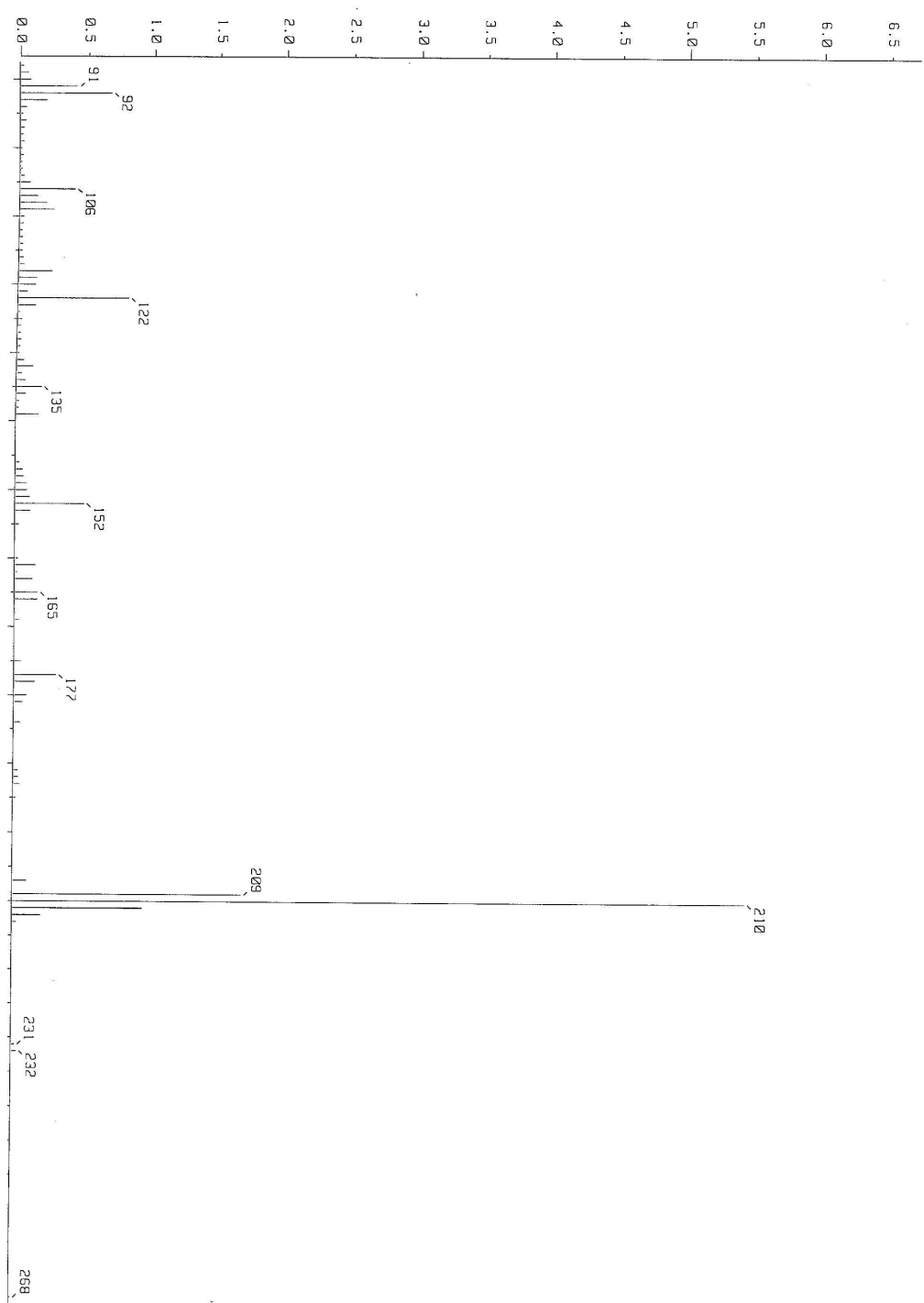
C₂ Dimethylamine



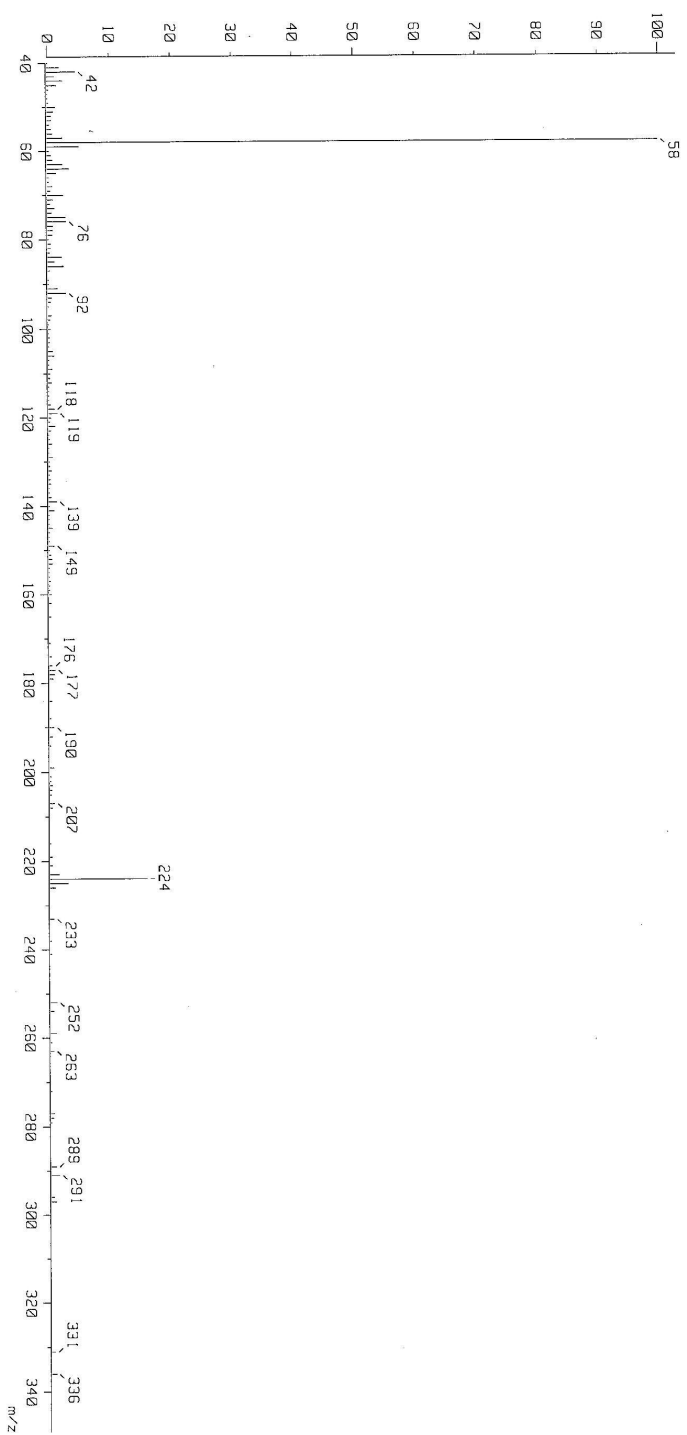
C₂ Dimethylamine



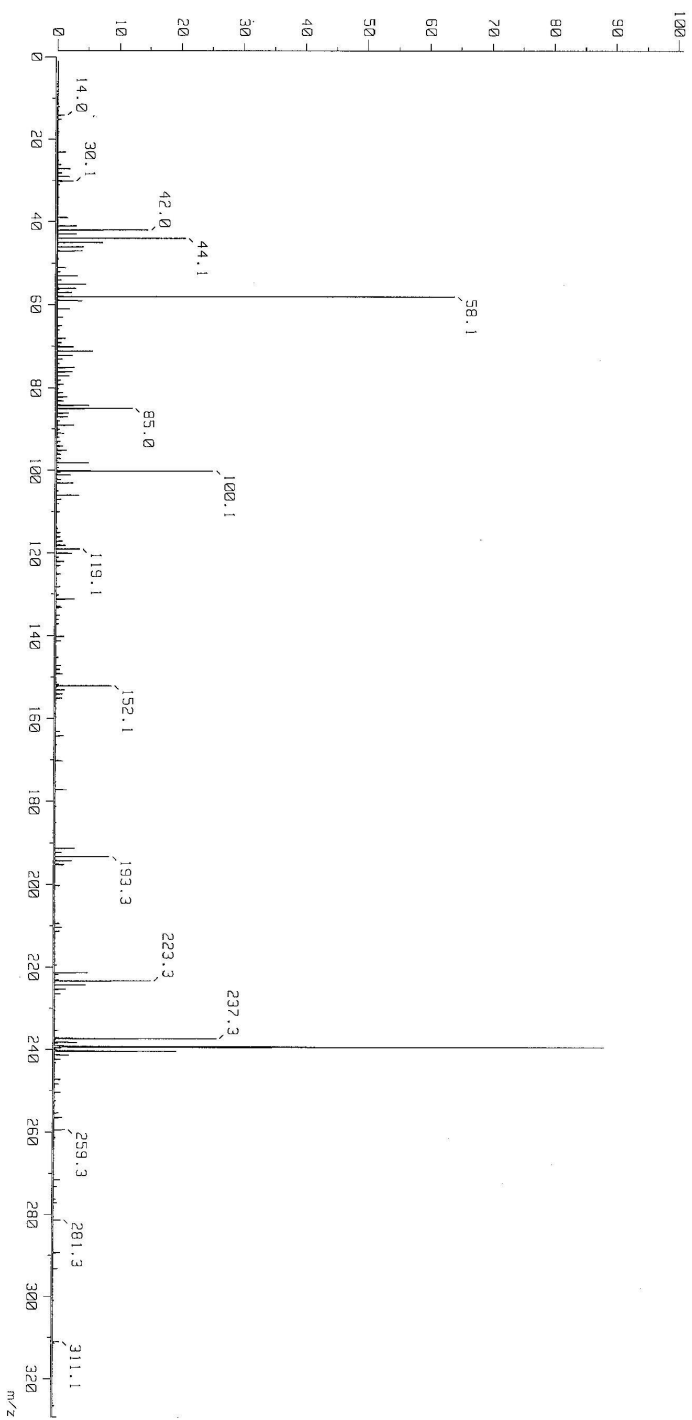
C₂ Dimethylamine



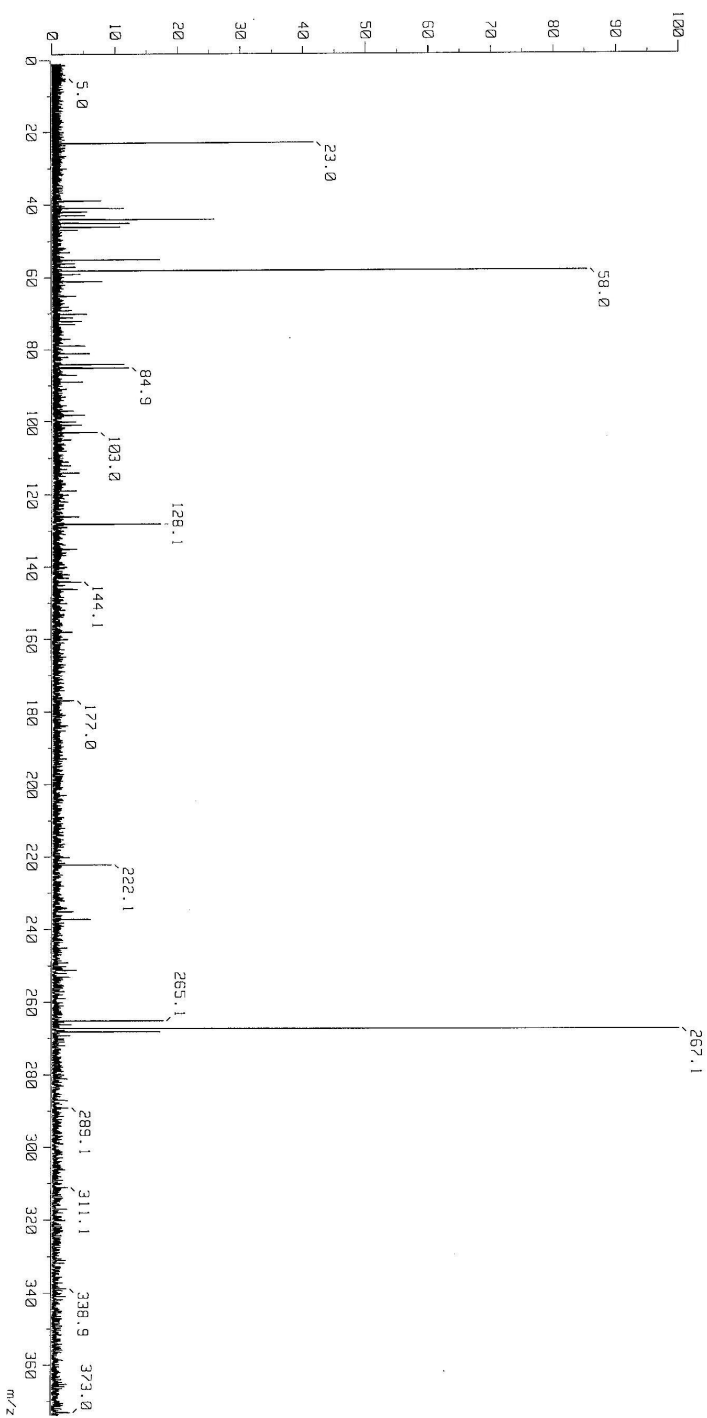
C₃ Dimethylamine



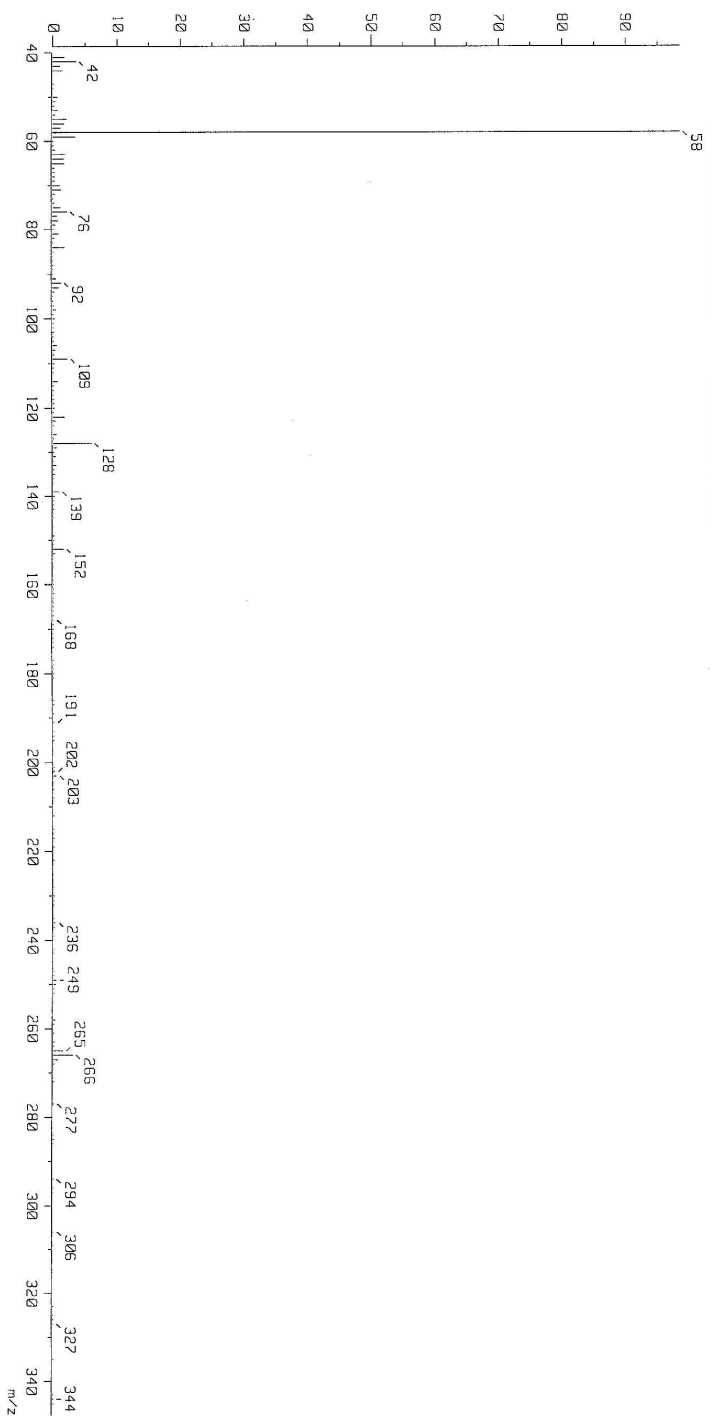
C₄ Dimethylamine



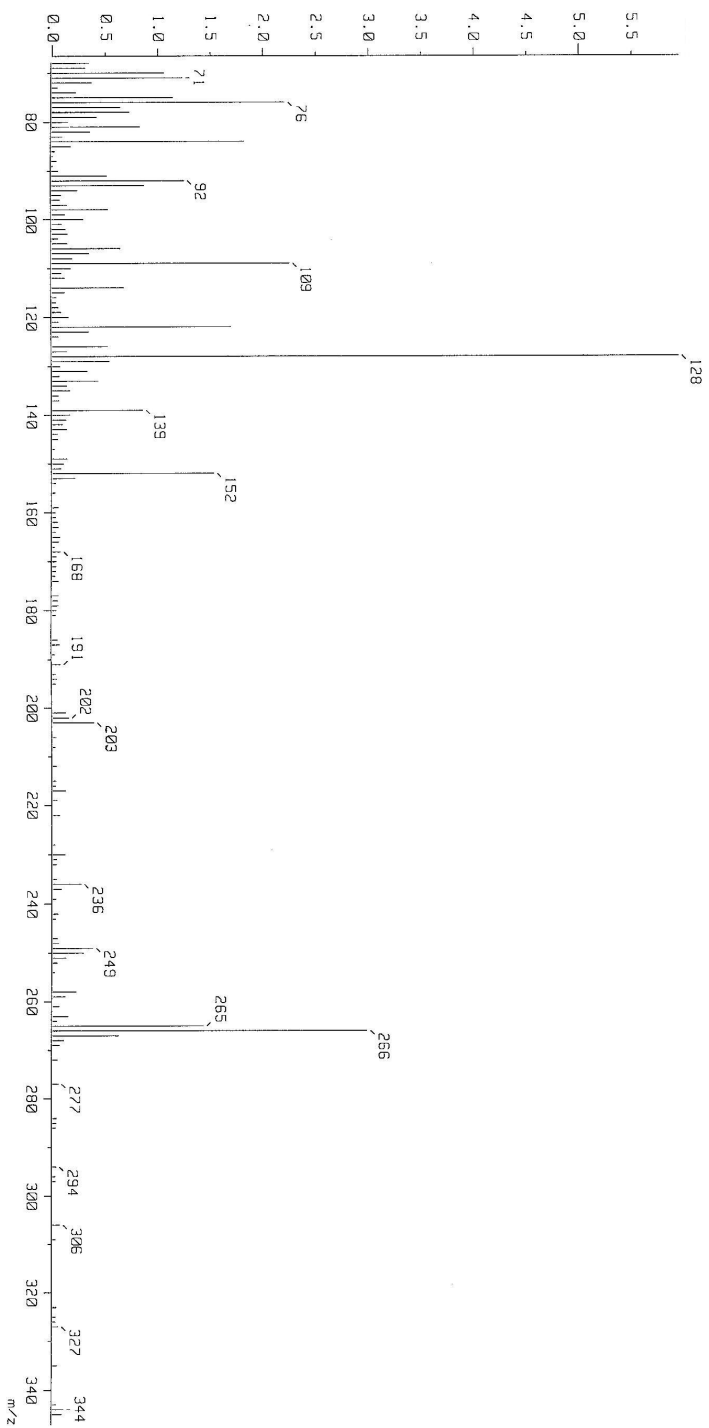
C₆ Dimethylamine



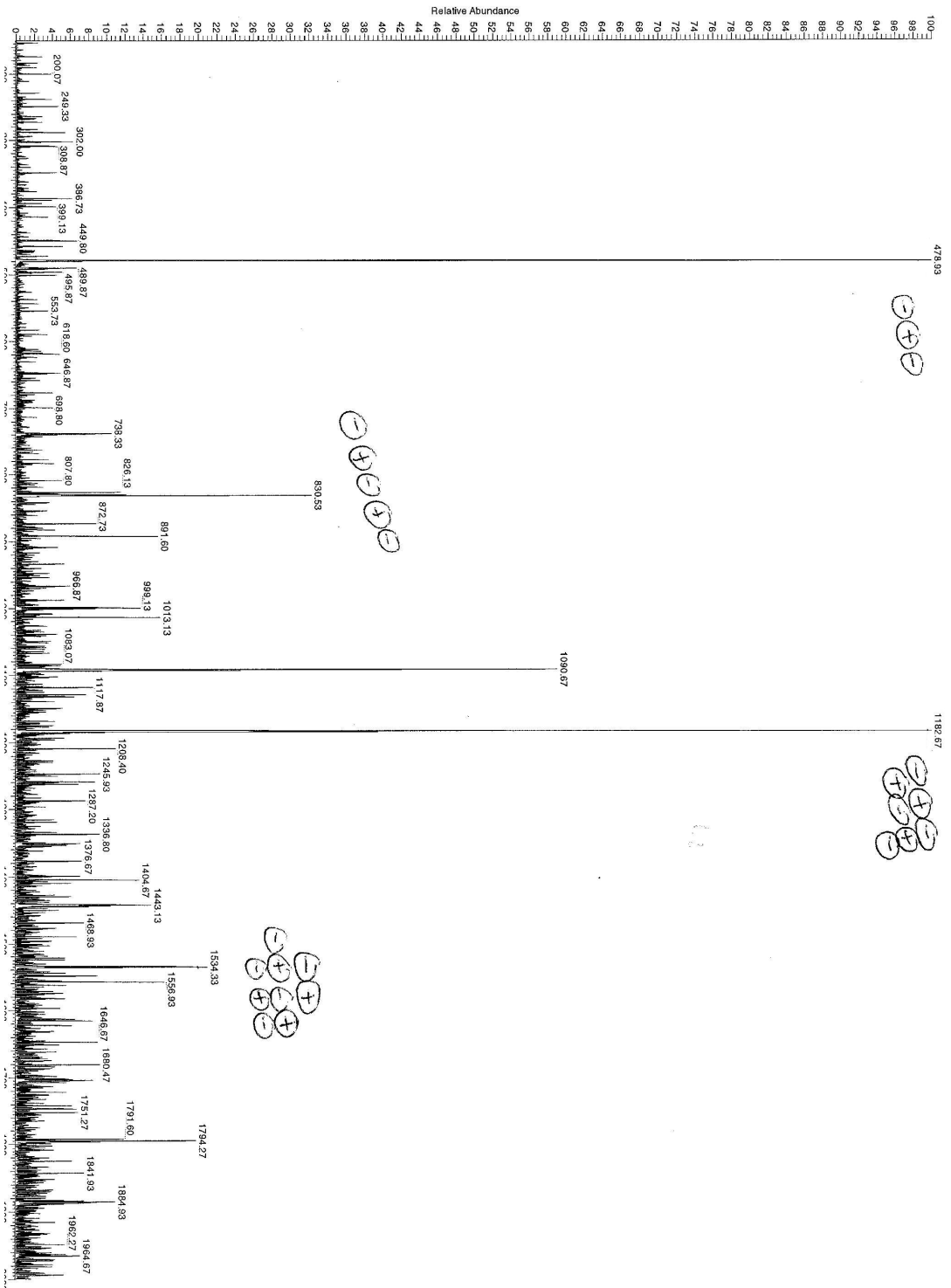
C₆ Dimethylamine



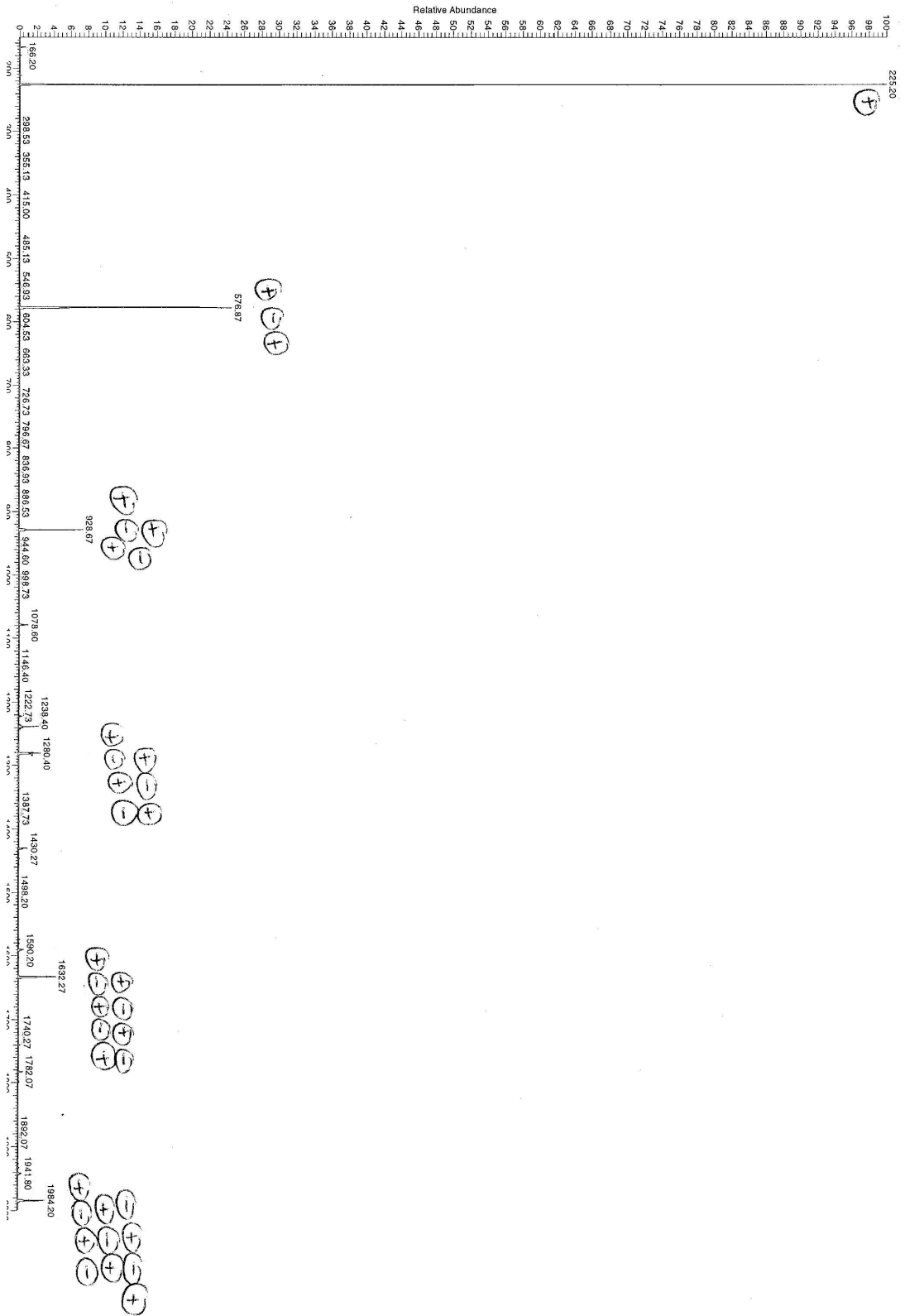
C₆ Dimethylamine



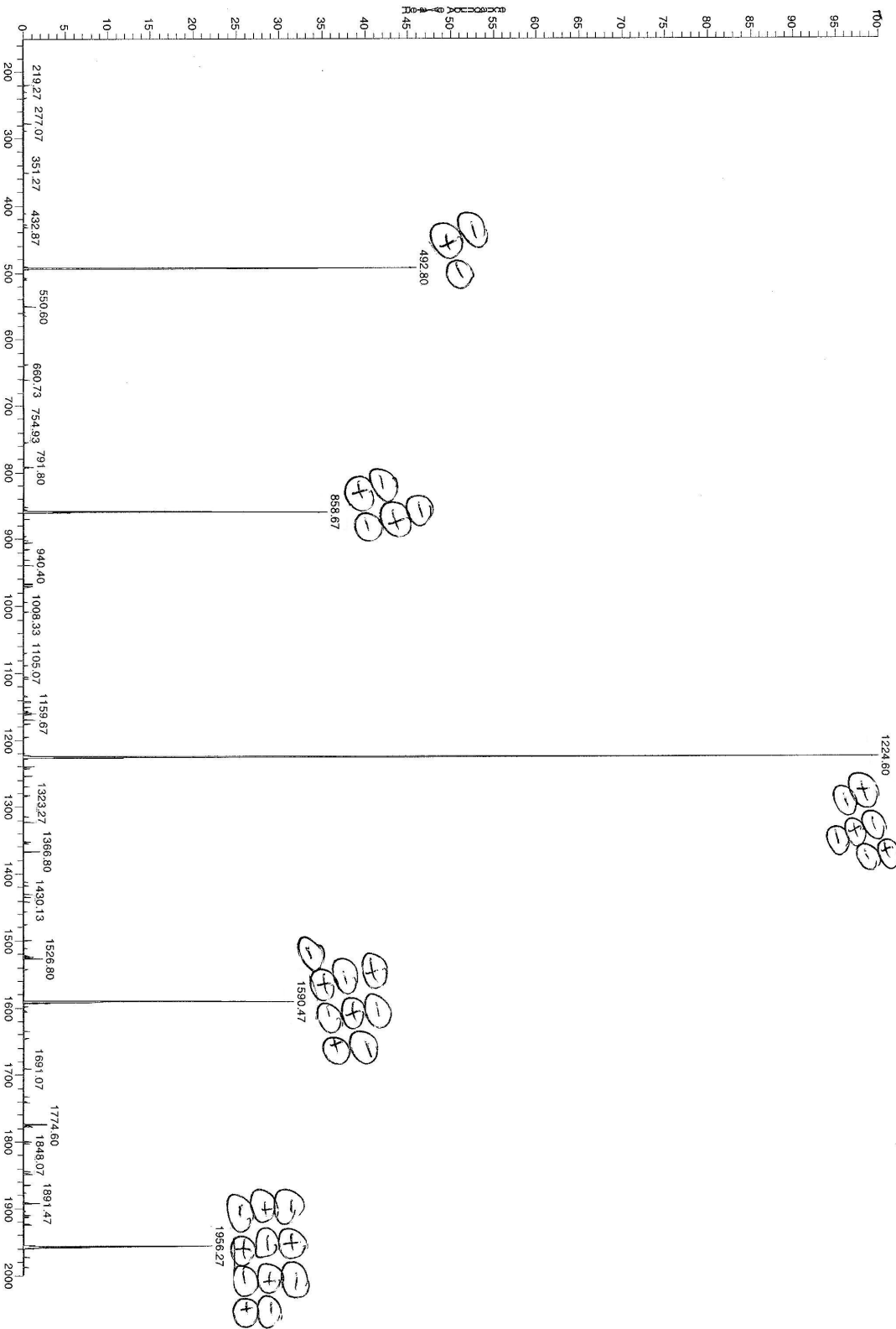
C₂ Ruler



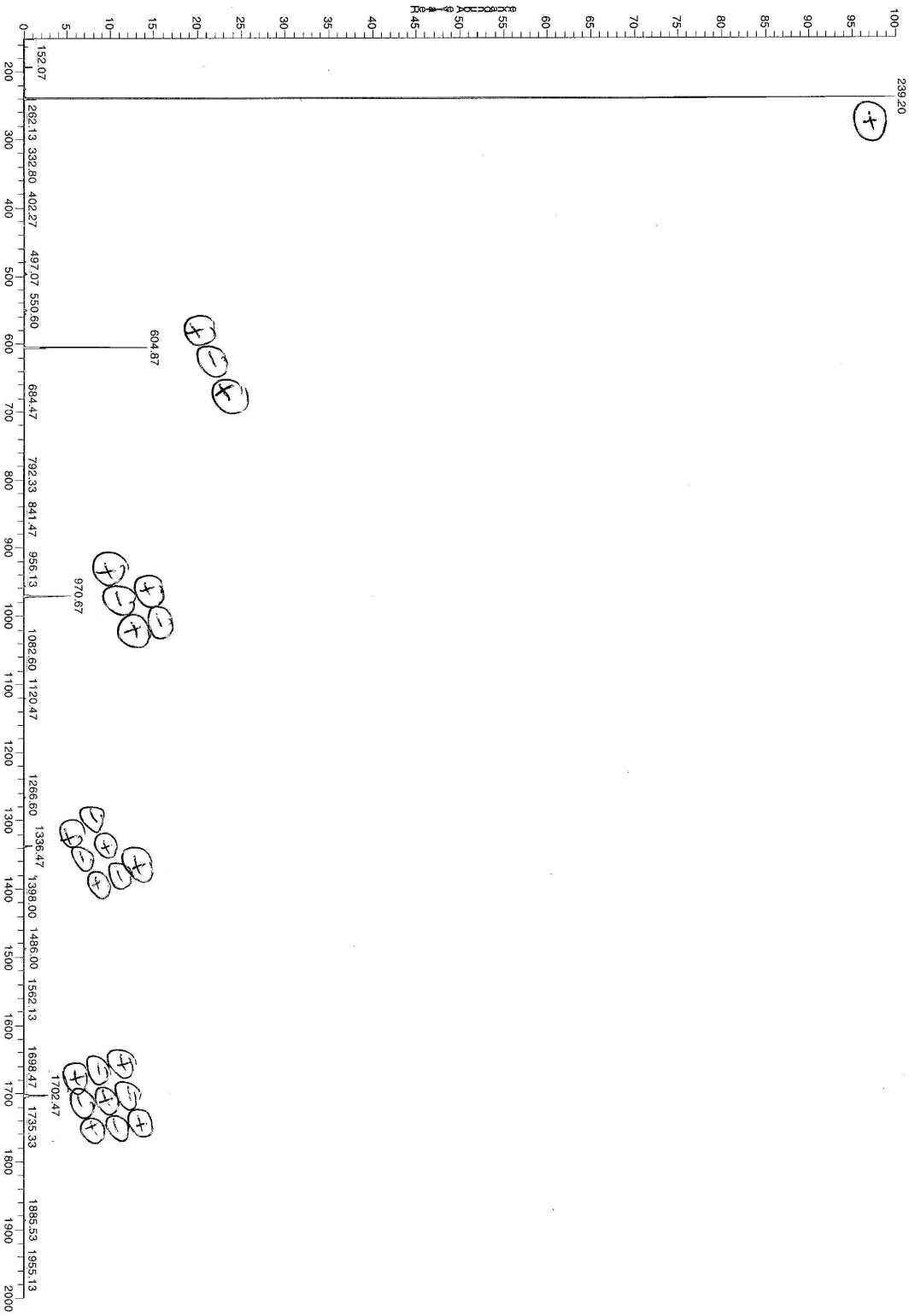
C₂ Ruler

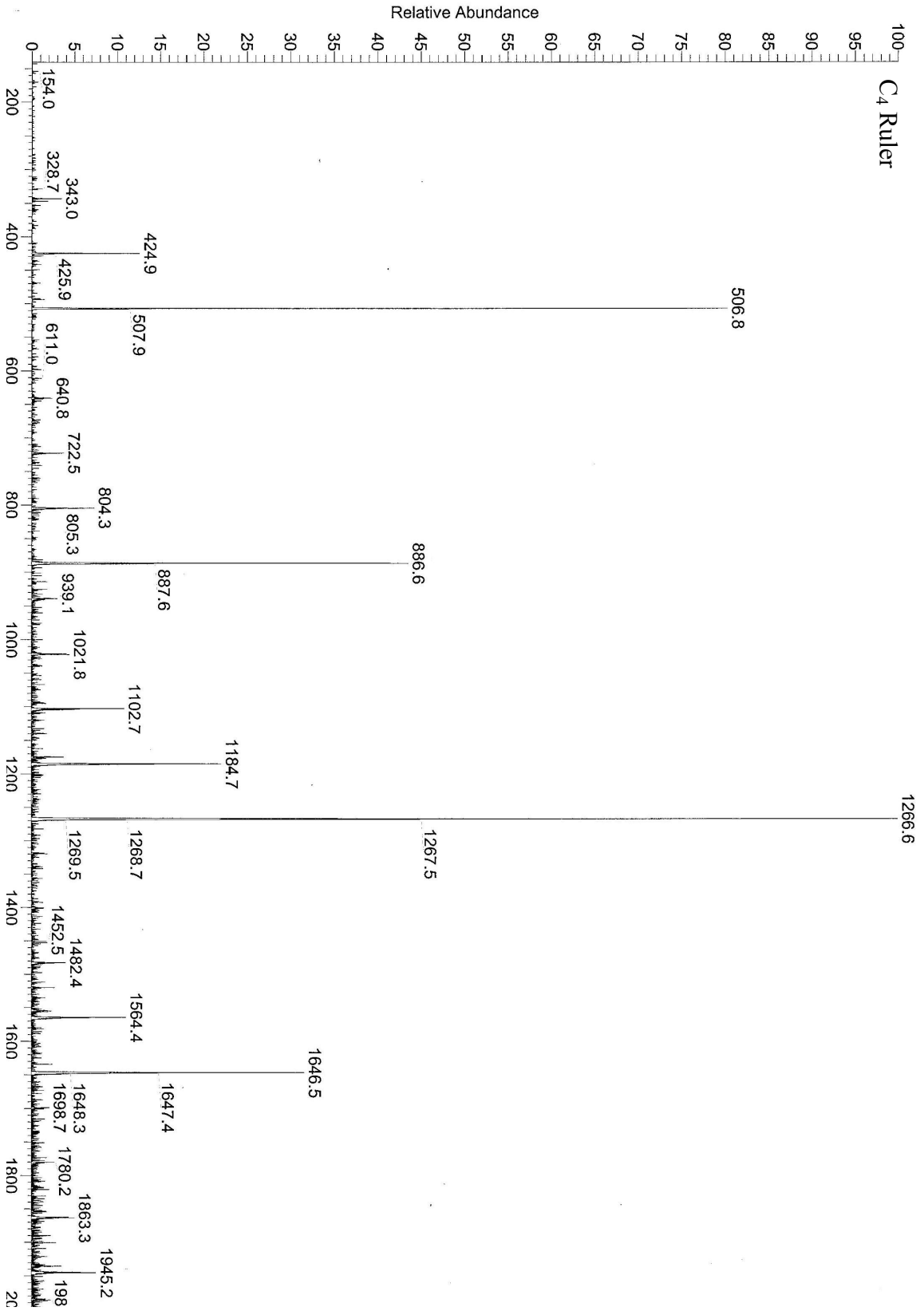


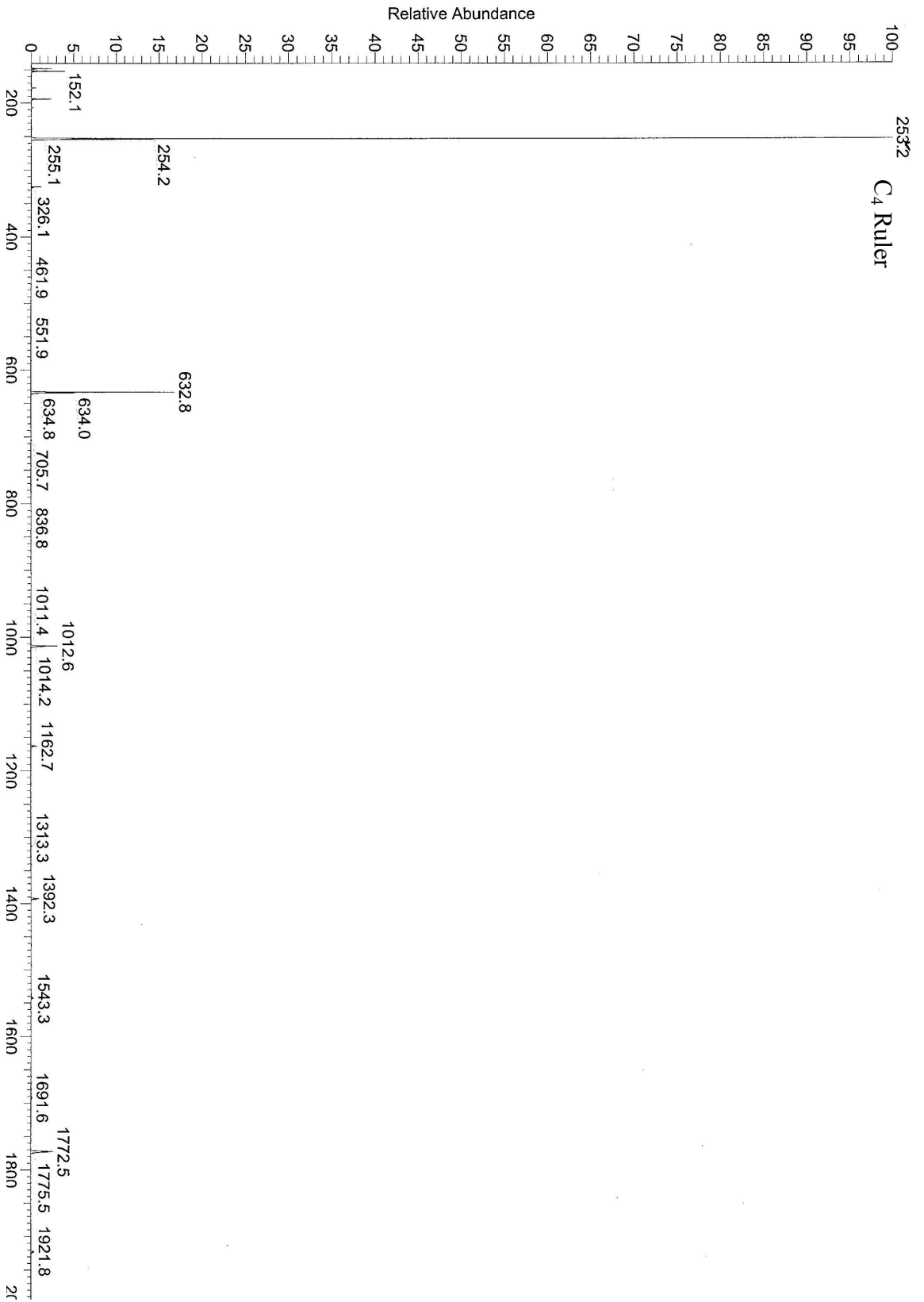
C₃ Ruler



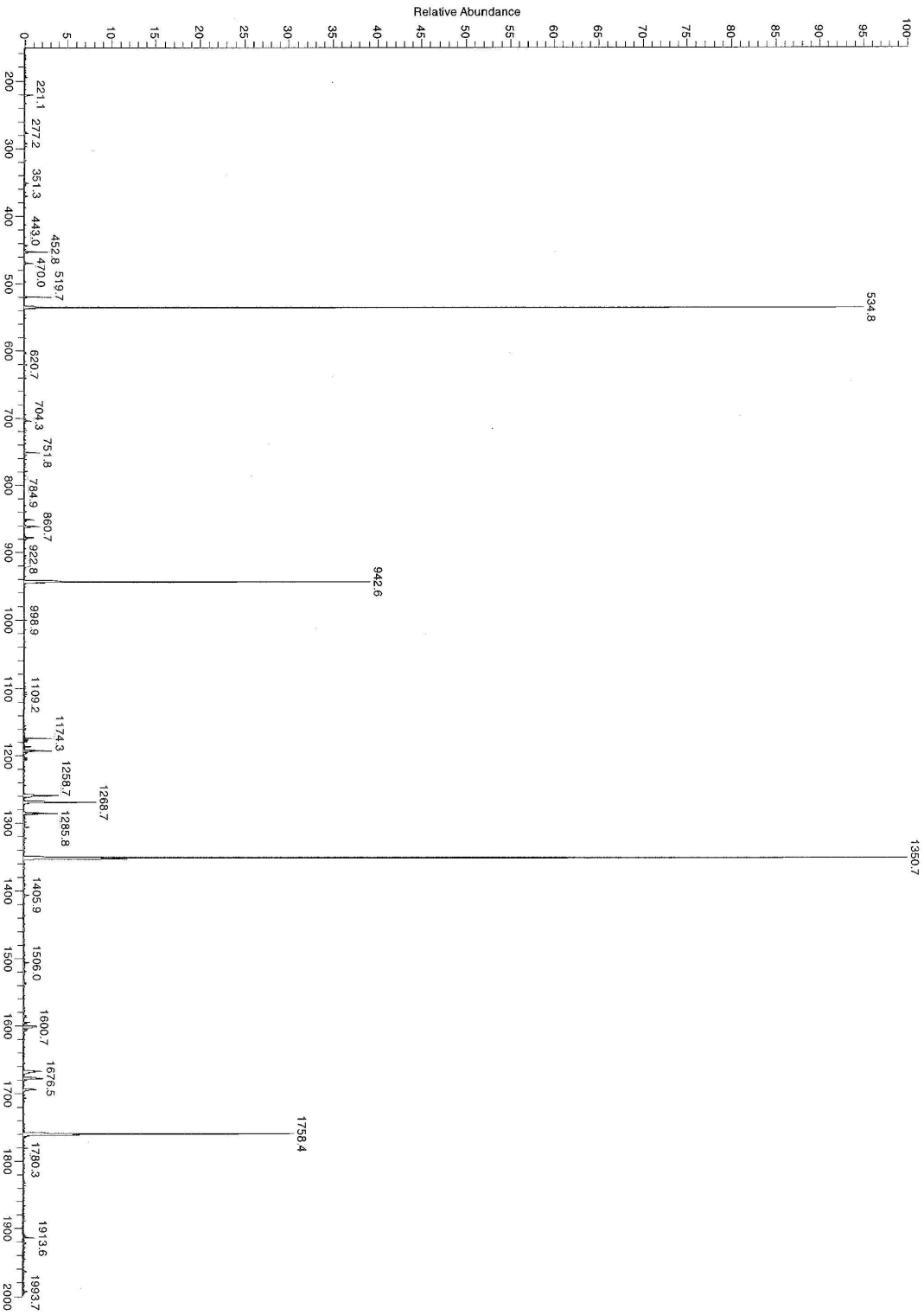
C₃ Ruler



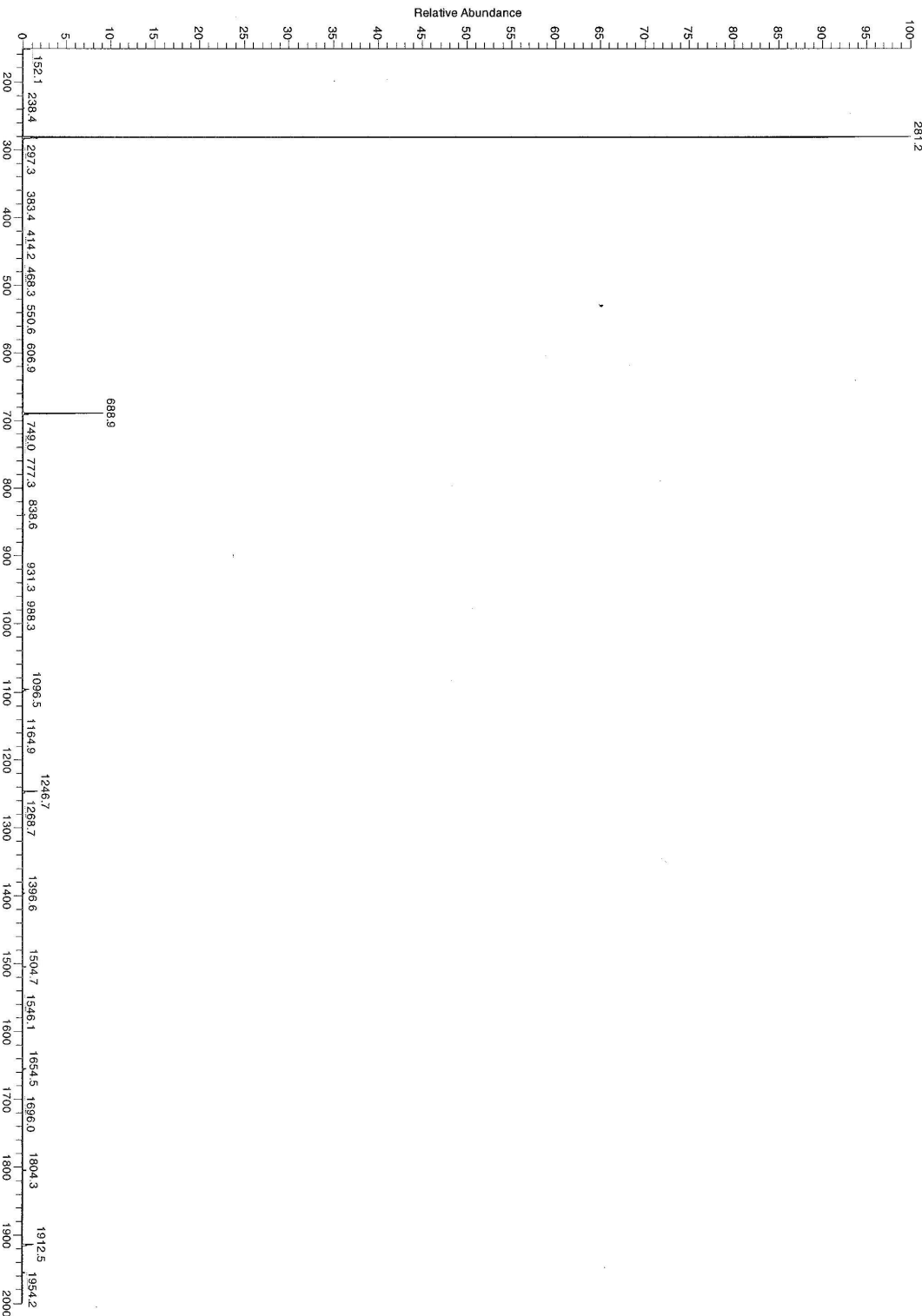




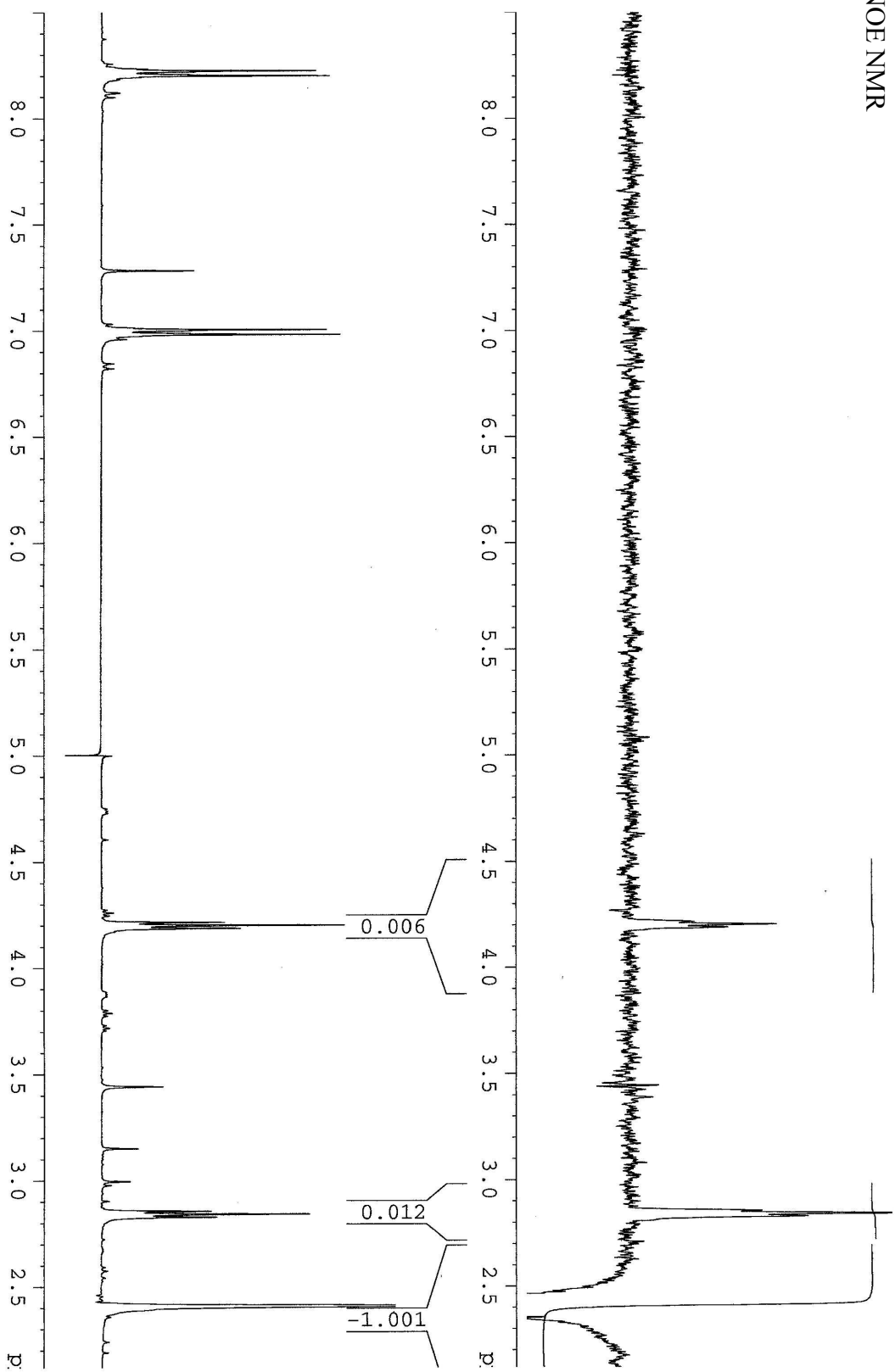
C₆ Ruler



C₆ Ruler

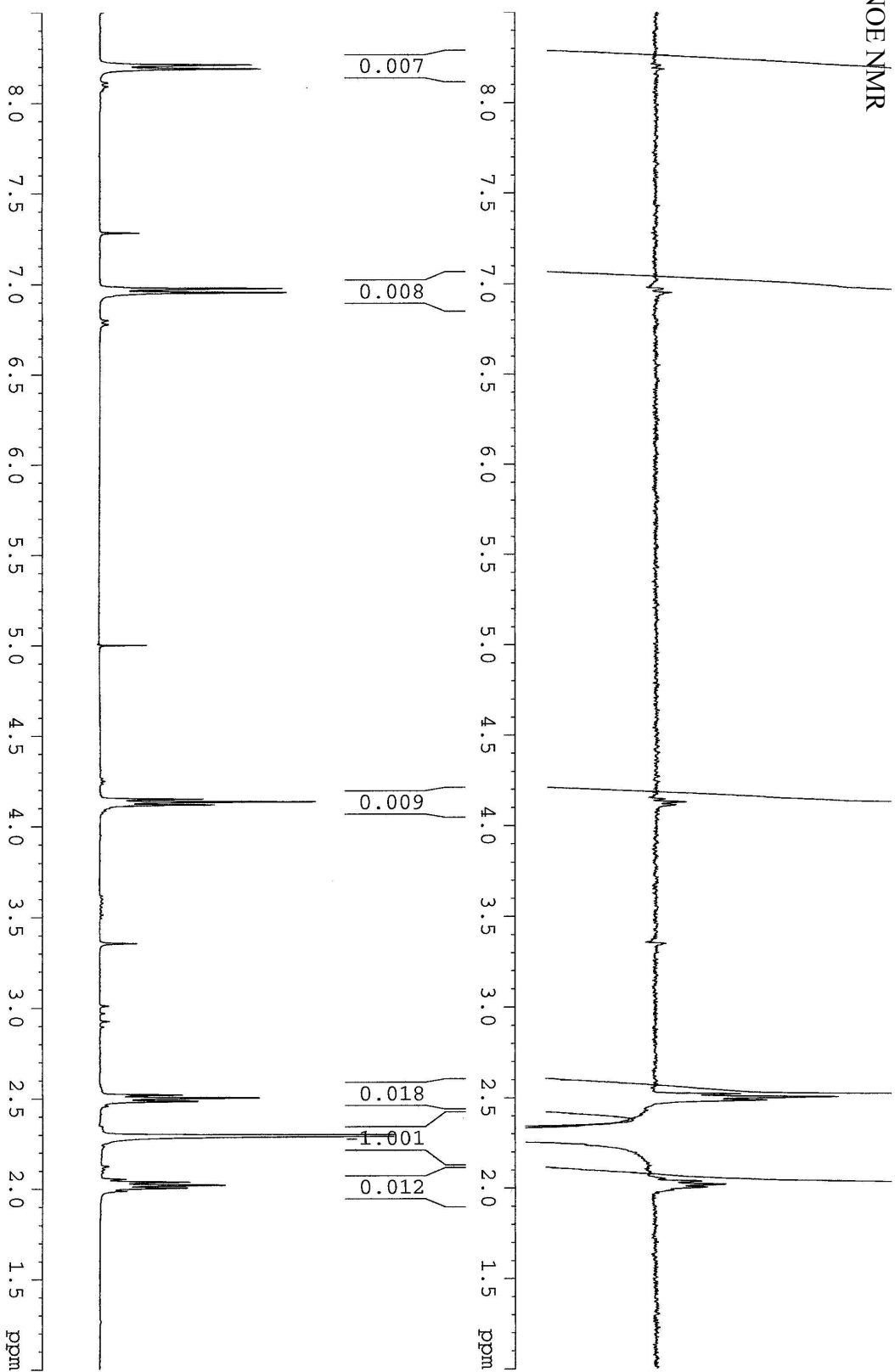


C₂ Dimethylamine
NOE NMR



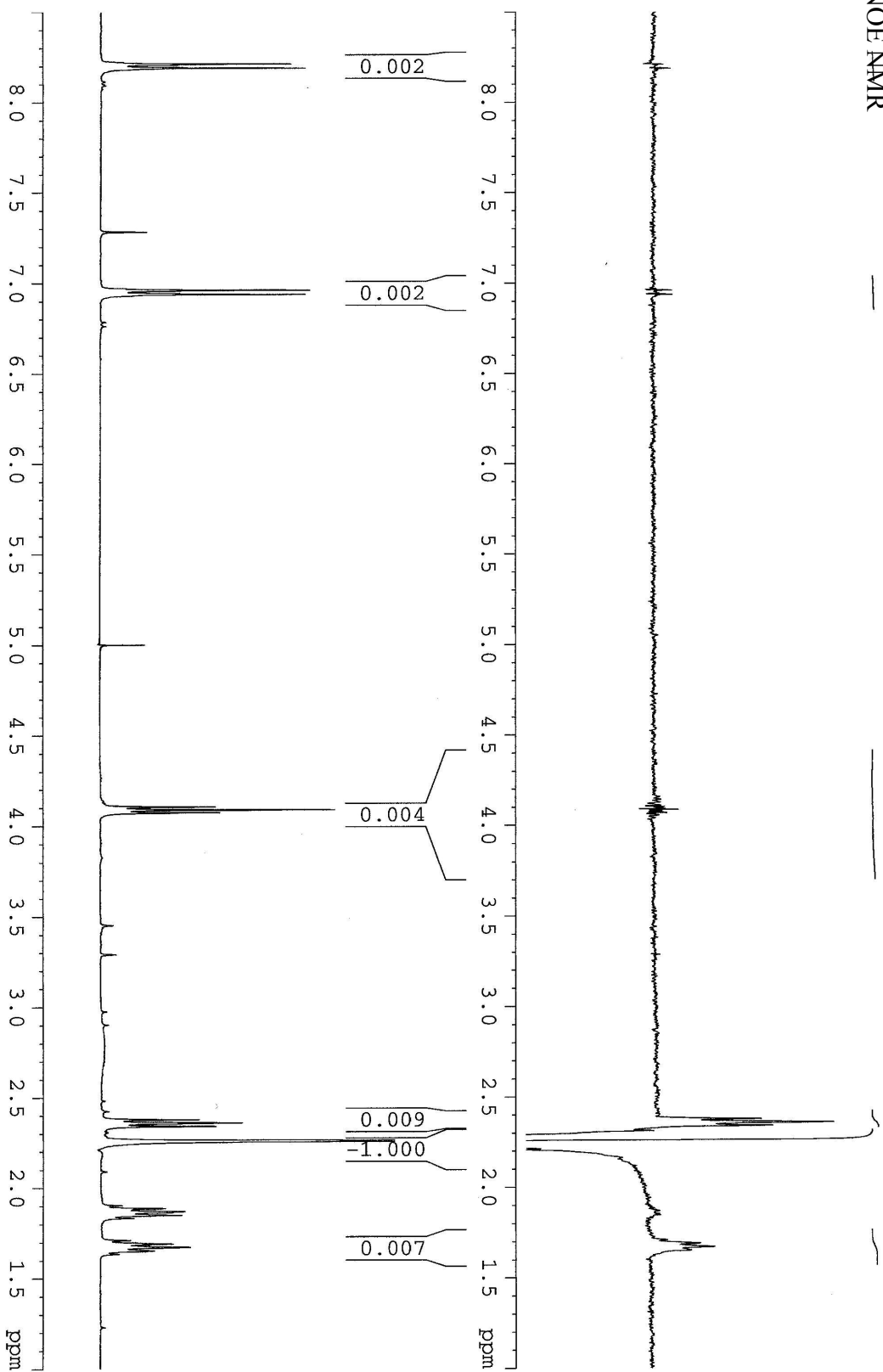
C₃ Dimethylamine

NOE NMR



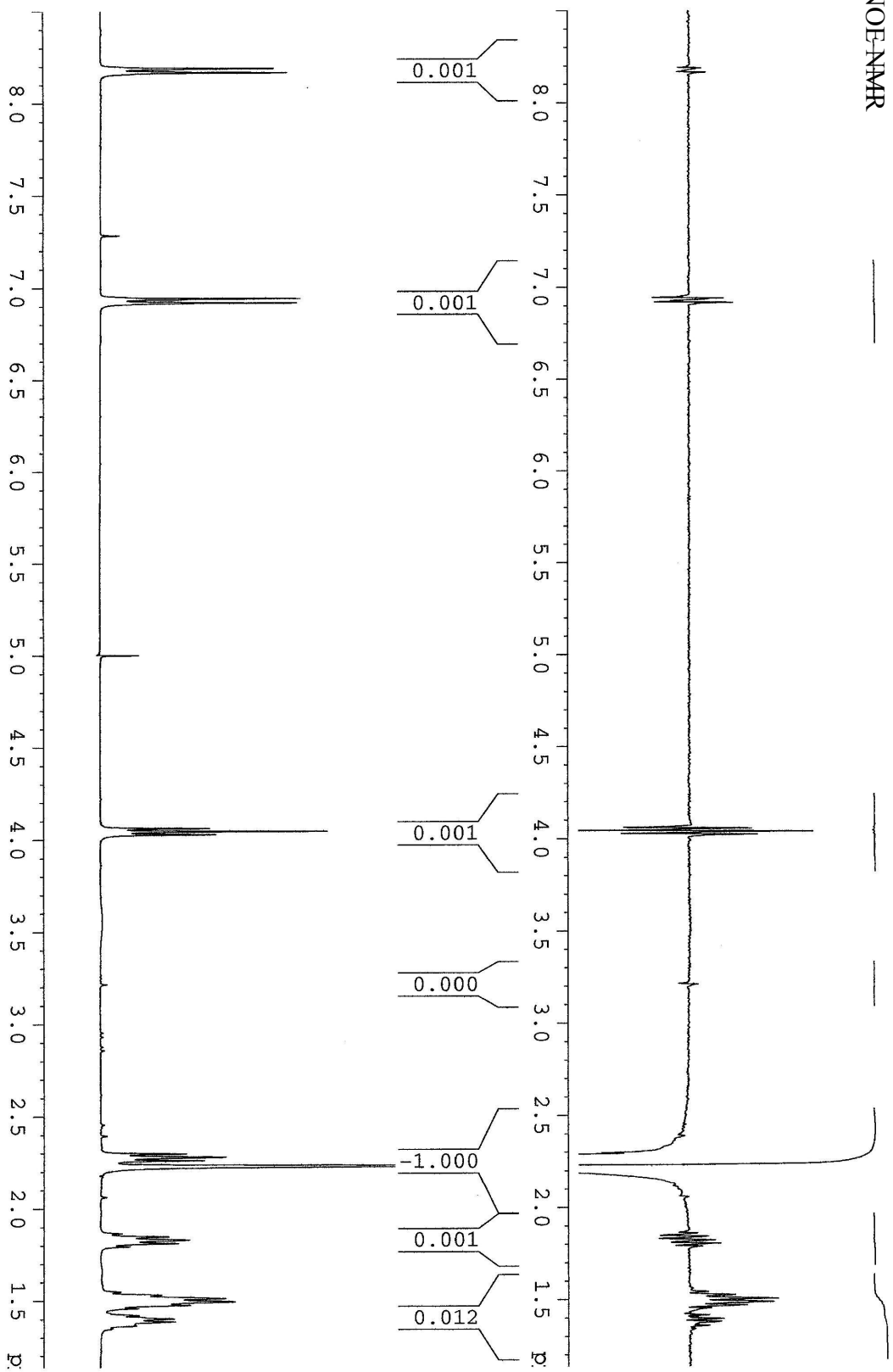
C₄ Dimethylamine

NOE AMR

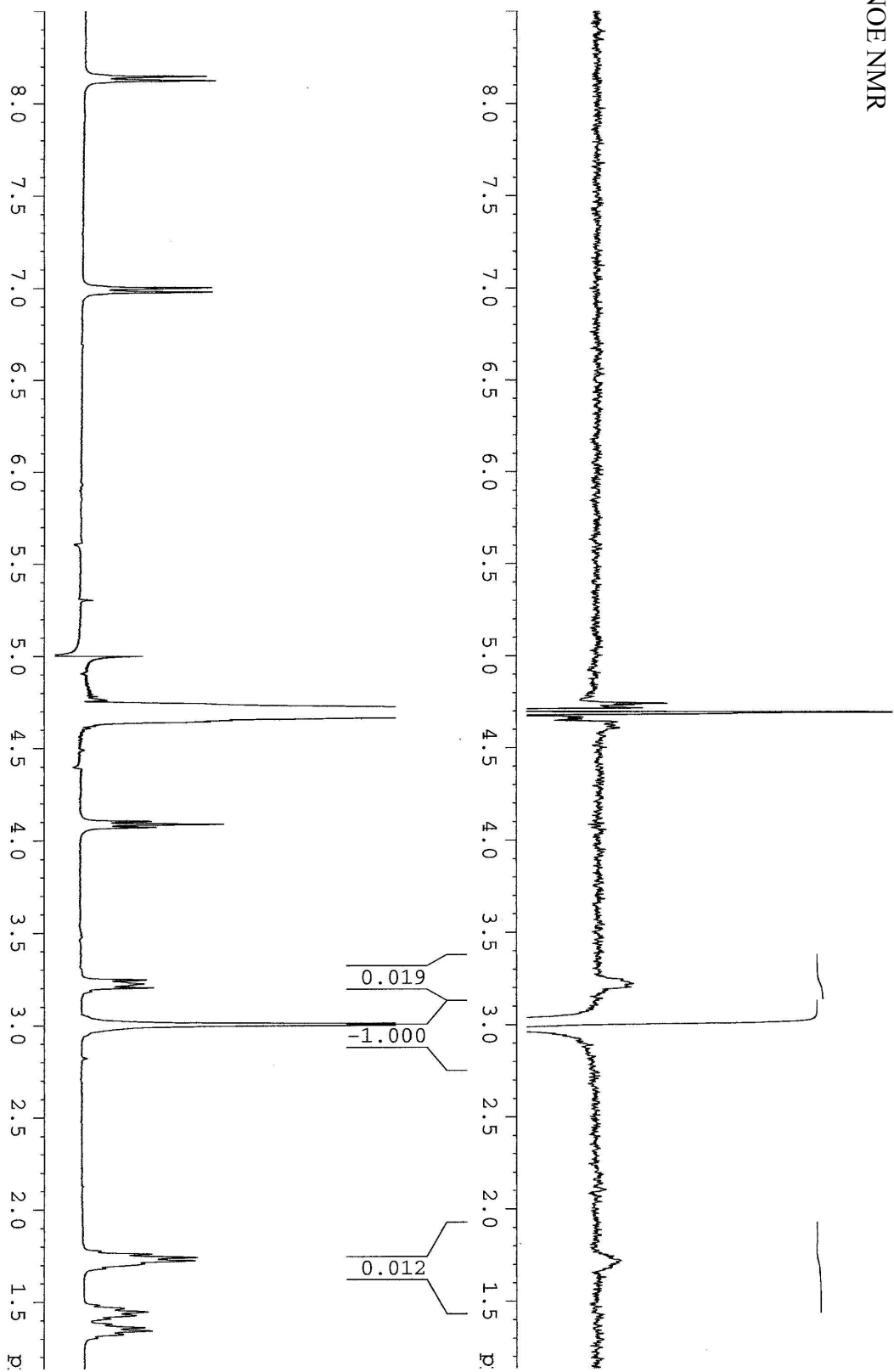


C₆ Dimethylamine

NOE-NMR

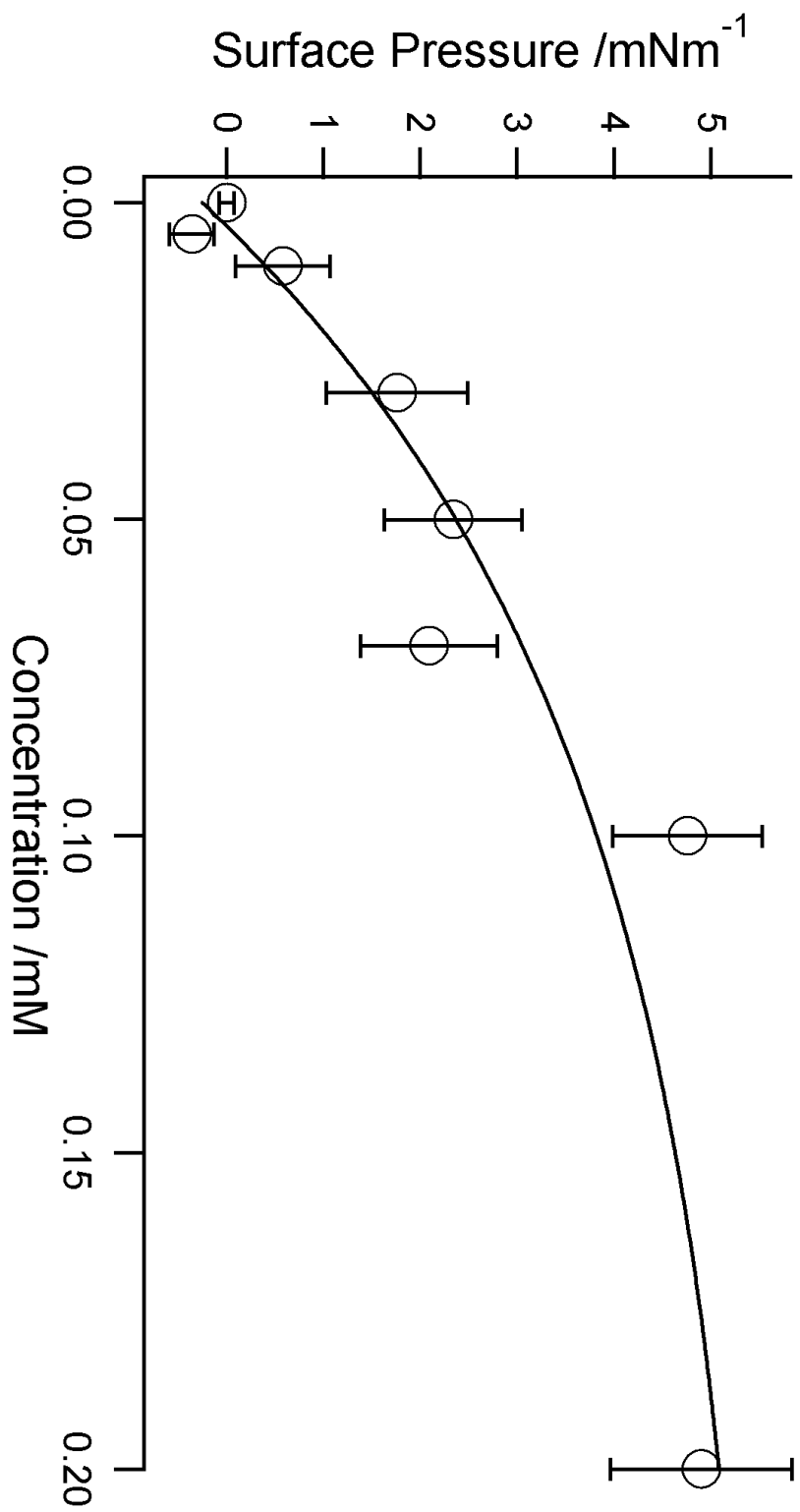


C₆ Ruler
NOE NMR



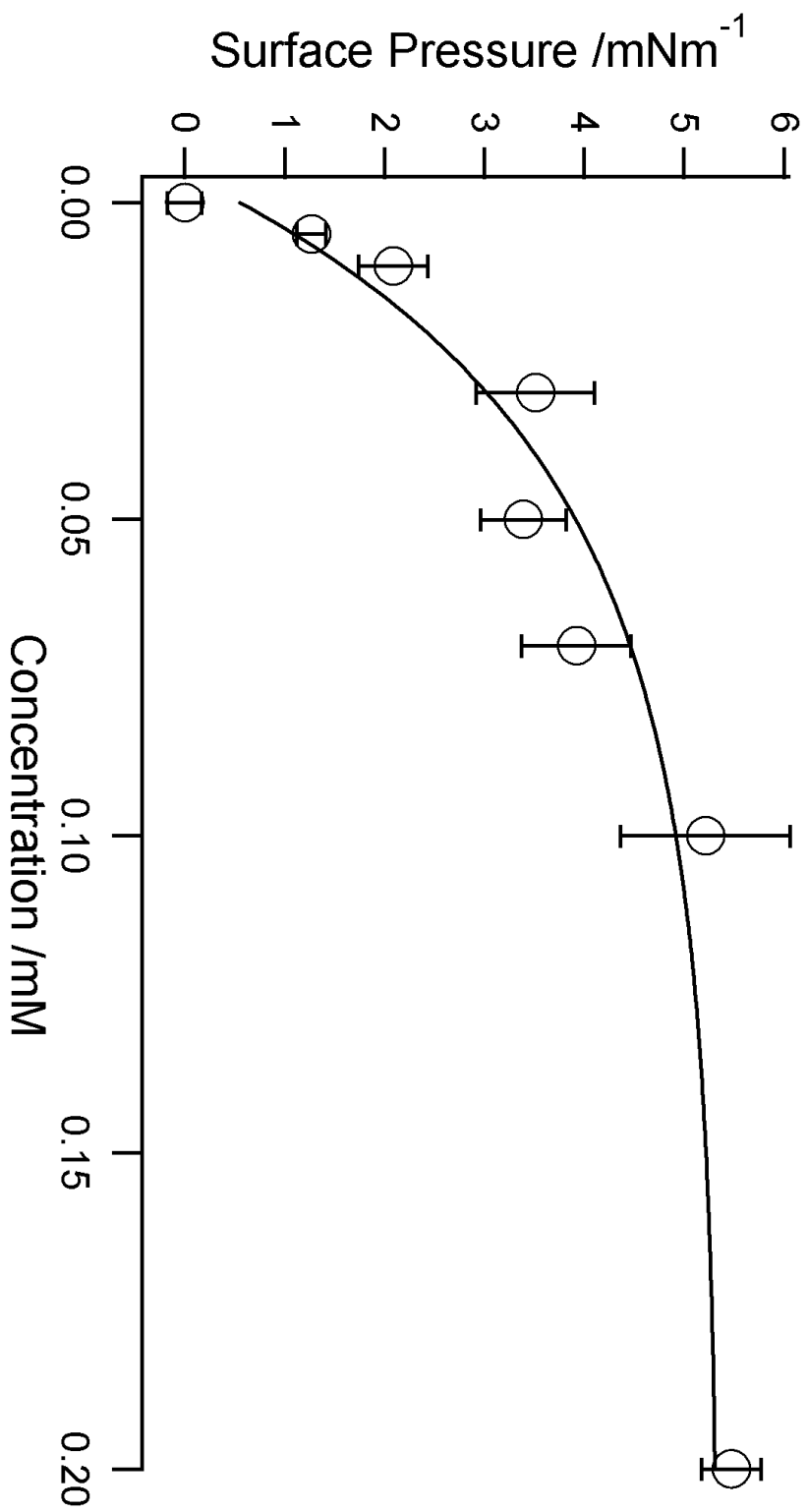
C₃ Ruler

Surface Pressure Isotherm



C₄ Ruler

Surface Pressure Isotherm



Appendix B. Error Analysis of SHG Data

The acquisition of SHG data is a rather tedious process as described in Chapter 2. After aligning the system to ensure that the second harmonic signal is reaching the detector and before collecting any data, the monochromator is tuned “off-resonance” and a background signal is collected. The intensity of the background signal usually ranges from 2-10 photon counts per 10-s interval. Since the power of the incident beam is controlled to keep the second harmonic signal between 100 and 300 counts per 10-s interval, this background amounts to <5% of the total signal. For future measurements, the number of counts determined from the background check is then subtracted from the average number of photons detected in four 10-s intervals.

Once the incident beam has been tuned to a particular wavelength using the optical parametric amplifier, the wavelength of the second harmonic signal is manually selected using a monochromator. Additionally, the height of the sample must be slightly adjusted so that the second harmonic signal is focused onto the slit of the photomultiplier tube. This height adjustment is to account for small changes in the wavelength dependent refractive indices of the quartz prism and the solvents. Both of these fine-tuning steps introduce random error into the data acquisition process. Once the setup has been optimized (as determined by the number of photon counts delivered by the photomultiplier tube to the gated photon counting electronics), the number of photon counts in each of four 10-s intervals is recorded. An average number of photons collected in a 10-s interval is determined, and a statistical uncertainty is associated with this value.

For example, in the spectrum of *p*-nitrophenol at the water/cyclohexane interface collected on 09/20/2004 shown in Figure B.1, the number of photon counts collected in

the four 10-s intervals for the 311 nm data point are 255, 236, 248, and 241. The average number of photon counts is 245, and the standard deviation is 8, a 3% uncertainty. The recordings of the background for this particular sample were 2, 3, 3, 6, and 4, yielding an average of 4 with a standard deviation of 2. Since the uncertainties in these two quantities, the total number of counts δT and the number of counts attributed to the background δB , are independent and random, we can determine the uncertainty in our final measurement by adding them in quadrature. The uncertainty in the signal δS is given by

$$\delta S = \sqrt{(\delta T)^2 + (\delta B)^2} = \sqrt{64 + 4} = 8.2 \approx 8 \quad (\text{B.1})$$

Our final value of the number of photon counts at 311 nm is 241 ± 8 .

Since the power of the incident beam depends on the wavelength, it varies from point to point. While the power can be controlled using neutral density filters to keep the photon counts within an appropriate range, subtle differences in the power can have a large impact on the intensity of the signal since the second harmonic signal depends quadratically on the intensity (power) of the incident beam (Eq. 2.5). To compensate for the variation in the power of the incident beam, we normalize the number of photon counts by the square of the incident power. The power is determined using a joule-meter and is given in μJ per unit time. Since the time (a femtosecond pulse) is constant for each measurement, we simply divide the number of counts by the square of the “power” given in μJ . For the example given above, the incident power was $0.038 \mu\text{J}$. So the SH intensity is $241/(0.038)^2 = 166898$ as depicted in the graph (Figure B.1). Just as we normalized the number of photon counts, we can normalize the uncertainty since multiplication of a

measured quantity by an exact number changes the uncertainty proportionally. Our final value for the SH intensity at 311 nm is 166898 ± 5540 as indicated by the error bars in the graph in Figure B.1.

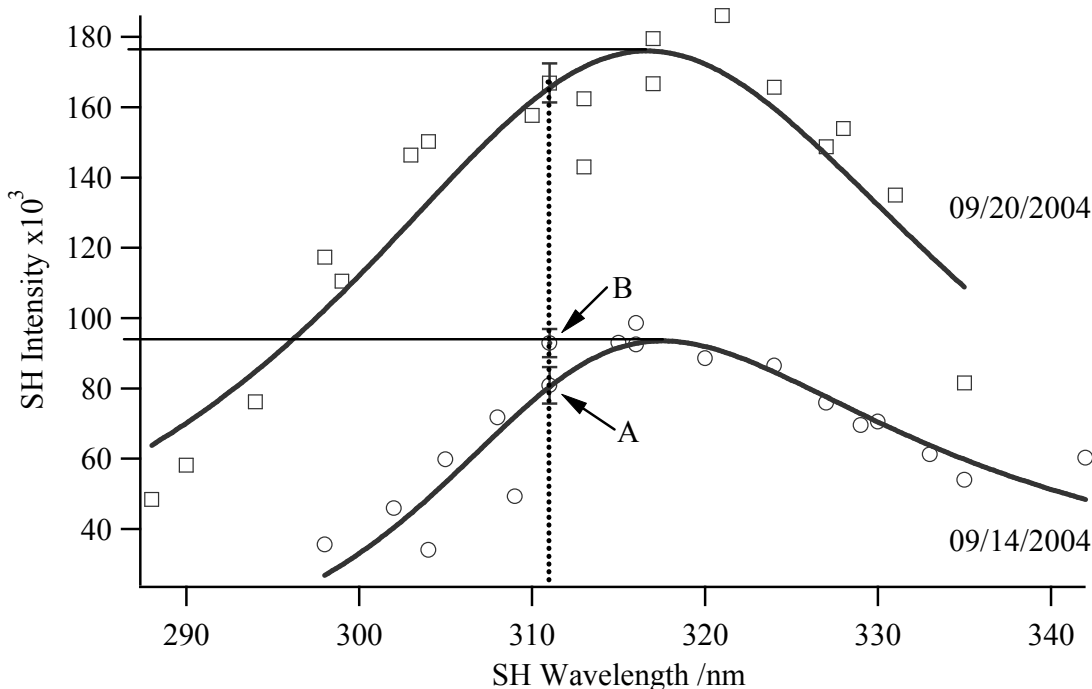


Figure B.1. SHG spectra of *p*-nitrophenol collected on two different days. Each spectrum has one or two data points corresponding to the SH intensity at 311 nm.

At times during a data collection period, we may sample the SH intensity of a certain wavelength more than once. This is shown in the spectrum of *p*-nitrophenol at the water/cyclohexane interface collected on 09/14/2004 in Figure B.1. The procedure described above is used to determine the SH intensity of each point separately. The background is again 4 ± 2 . The values T_i in Table B.1 give the number of photon counts in a 10-s interval (i), and T_{ave} is the average value. By normalizing with the power of the

incident beam, we have determined that the SH intensity of point A is 80899 ± 5178 and the SH intensity of point B is 92900 ± 4000 .

Table B.1. Data used to calculate the normalized intensity of points A and B from Figure B.1.

Point	T₁	T₂	T₃	T₄	T_{ave}	Power/ μJ	Normalized Intensity
A	240	221	223	207	223 ± 14	0.052	80899 ± 5178
B	255	236	248	241	236 ± 10	0.038	92900 ± 4000

Rather than use an individual spectrum with a limited number of data points to draw conclusions about interfacial polarity, we use composites of several spectra to fully analyze a particular system. To make a composite, each spectrum must be normalized. In Figure B.1 each data set has a different maximum value. These spectra are normalized to 1 by dividing the SH intensity of each point by the maximum value of the fit from Eqs. 2.5-2.7. As in the case of normalizing an individual data point to the incident power, multiplication of a measured quantity by an exact number changes the uncertainty proportionally. For the spectrum acquired on 09/14/2004, SH intensities (and their uncertainties) are divided by 93493, yielding intensities of 0.87 ± 0.06 and 0.99 ± 0.04 for the two points at 311 nm. Similarly, SH intensities acquired on 09/20/2004 are divided by 176000, resulting in an SH intensity of 0.95 ± 0.03 for the 311 nm point.

In the composite spectrum, multiple points at the same wavelength are averaged together and weighted accordingly. If there are three points corresponding to one wavelength, as in our example, the averaged SH intensity is reported three times when determining the fit to Eqs. 2.5-2.7. The composite of these two spectra is shown in

Figure B.2. The SH intensity of the point at 311 nm is the average of 0.87, 0.99, and 0.95, and the uncertainty associated with this number is the standard deviation: 0.94 ± 0.06 .

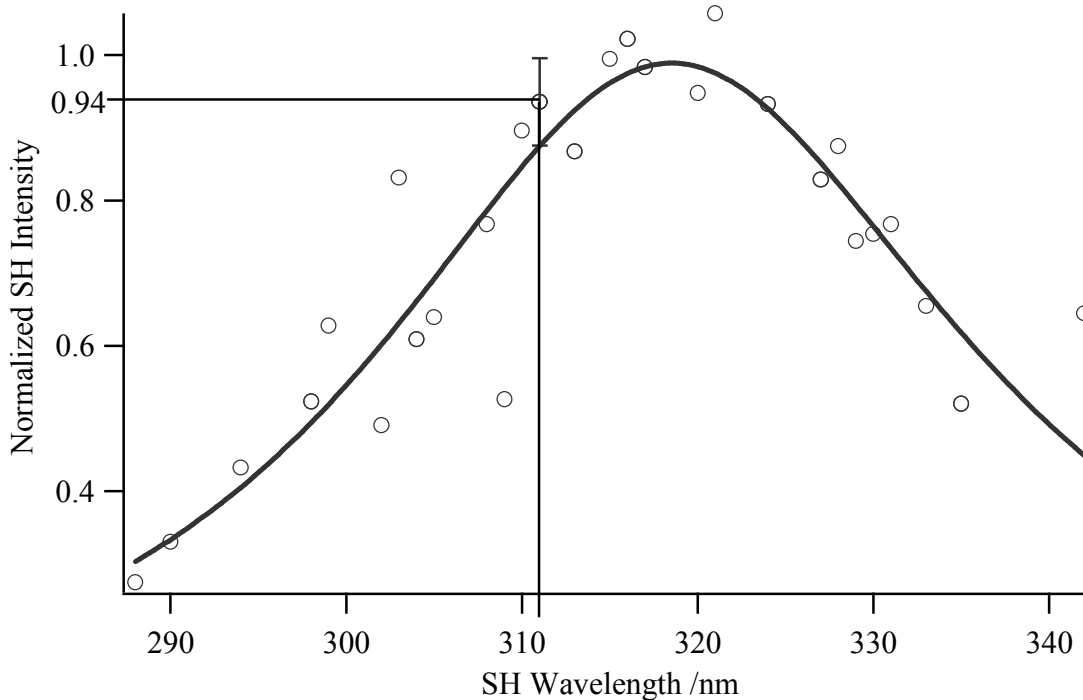


Figure B.2. Composite spectrum of *p*-nitrophenol at the water/cyclohexane interface using the individual spectra collected on 09/14/2004 and 09/20/2004. The SH intensity of the point at 311 nm has been calculated to be 0.94 ± 0.06 .

Bibliography

- (1) Adam, N. K. *The Physics and Chemistry of Surfaces*; Oxford University Press: London, 1941.
- (2) Adamson, A. W. *Physical Chemistry of Surfaces*; John Wiley & Sons: New York, 1990.
- (3) Als-Nielsen, J.; Jacquemain, D.; Kjaer, K.; Leveiller, F.; Lahav, M.; Leiserowitz, L. *Phys. Rep.* **1994**, *246*, 251.
- (4) Antoine, R.; Bianchi, F.; Brevet, P. F.; Girault, H. H. *J. Chem. Soc., Faraday Trans.* **1997**, *93*, 3833.
- (5) Aveyard, R.; Saleem, S. M. *J. Chem. Soc., Faraday Trans. 1* **1976**, *72*, 1609.
- (6) Bardeen, C. J.; Rosenthal, S. J.; Shank, C. V. *J. Phys. Chem. A* **1999**, *103*, 10506.
- (7) Barthel, J. M. G.; Krienke, H.; Kunz, W. *Top. Phys. Chem.* **1998**, *5*, 1.
- (8) Becraft, K. A.; Moore, F. G.; Richmond, G. L. *Phys. Chem. Chem. Phys.* **2004**, *6*, 1880.
- (9) Beildeck, C. L.; Steel, W. H.; Walker, R. A. *Faraday Discuss.* **2005**, *129*, 69.
- (10) Beildeck, C. L.; Steel, W. H.; Walker, R. A. *Langmuir* **2003**, *19*, 4933.
- (11) Bell, G. R.; Li, Z. X.; Bain, C. D.; Fischer, P.; Duffy, D. C. *J. Phys. Chem. B* **1998**, *102*, 9461.
- (12) Benjamin, I. *J. Phys. Chem. A* **1998**, *102*, 9500.
- (13) Bentley, T. W.; Llewellyn, G. *Prog. Phys. Org. Chem.* **1990**, *17*, 121.

- (14) Bentley, T. W.; Schleyer, P. v. R. *Adv. Phys. Org. Chem.* **1977**, *14*, 1.
- (15) Bikerman, J. J. *Surface Chemistry: Theory and Applications*; Academic Press: New York, 1958.
- (16) Bockris, J. O. M.; Reddy, A. K. N. *Modern Electrochemistry, 2nd Ed.*; Plenum: New York, 1998; Vol. 1.
- (17) Böttcher, C. J. F. *Theory of Electric Polarization*; Elsevier: New York, 1973; Vol. 1: Dielectrics in Static Fields.
- (18) Chattoraj, D. K.; Birdi, K. S. *Adsorption and the Gibbs Surface Excess*; Plenum: New York, 1984.
- (19) Chipot, C.; Wilson, M. A.; Pohorille, A. *J. Phys. Chem. B* **1997**, *101*, 782.
- (20) Cosgrove, T.; Phipps, J. S.; Richardson, R. M. *Colloids Surf.* **1992**, *62*, 199.
- (21) Cramb, D. T.; Wallace, S. C. *J. Phys. Chem. B* **1997**, *101*, 2741.
- (22) *CRC Handbook of Chemistry and Physics*; 77th ed.; Lide, D. R., Ed.; CRC Press: Boca Raton, Florida, 1996.
- (23) Dang, L. X. *J. Phys. Chem. B* **1999**, *103*, 8195.
- (24) Dang, L. X. *J. Phys. Chem. B* **2001**, *105*, 804.
- (25) Dang, L. X.; Chang, T.-M. *J. Phys. Chem. B* **2002**, *106*, 235.
- (26) Davies, J. T. *Proc. R. Soc. London* **1951**, *A208*, 224.
- (27) Davies, J. T. *Trans. Faraday Soc.* **1952**, *48*, 1052.
- (28) Debye, P. *Phys. Z.* **1924**, *25*, 97.
- (29) Debye, P.; Hückel, E. *Phys. Z.* **1923**, *24*, 185.

- (30) Dimroth, K.; Reichardt, C.; Siepmann, T.; Bohlmann, F. *Ann.* **1963**, *661*, 1.
- (31) Dominguez, H. *J. Phys. Chem. B* **2002**, *106*, 5915.
- (32) Dominguez, H.; Berkowitz, M. L. *J. Phys. Chem. B* **2000**, *104*, 5302.
- (33) Eisenthal, K. B. *J. Phys. Chem.* **1996**, *100*, 12997.
- (34) Esenturk, O.; Mago, D.; Walker, R. A. *In preparation* **2005**.
- (35) Esenturk, O.; Walker, R. A. "Vibrational Studies of Alcohol Films: Molecular Structure Vs. Long-Range Order"; 227th ACS National Meeting, 2004, Anaheim, CA.
- (36) Fainberg, A. H.; Winstein, S. *J. Am. Chem. Soc.* **1956**, *78*, 2770.
- (37) Fleming, G. R.; Cho, M. *Annu. Rev. Phys. Chem.* **1996**, *47*, 109.
- (38) Fonseca, T.; Kim, H. J.; Hynes, J. T. *J. Photochem. Photobiol., A* **1994**, *82*, 67.
- (39) Fragneto-Cusani, G. *J. Phys.: Condens. Matter* **2001**, *13*, 4973.
- (40) Gaines, G. L., Jr. *Insoluble Monolayers at Liquid-Gas Interfaces*; Interscience Publishers: New York, 1966.
- (41) Gang, O.; Wu, X. Z.; Ocko, B. M.; Sirota, E. B.; Deutsch, M. *Phys. Rev. E: Stat. Phys., Plasmas, Fluids, Relat. Interdiscip. Top.* **1998**, *58*, 6086.
- (42) Ghosal, S.; Hemminger, J. C.; Bluhm, H.; Mun, B. S.; Hebenstreit, E. L. D.; Ketteler, G.; Ogletree, D. F.; Requejo, F. G.; Salmeron, M. *Science* **2005**, *307*, 563.
- (43) Gouy, G. *Ann. Phys.* **1917**, *7*, 129.
- (44) Gouy, J. *J. Phys. IV* **1910**, *9*, 457.
- (45) Grunwald, E.; Winstein, S. *J. Am. Chem. Soc.* **1948**, *70*, 846.

- (46) Hao, C.; March, R. E. *J. Mass Spectrom.* **2001**, *36*, 509.
- (47) Haverd, V. E.; Warr, G. G. *Langmuir* **2000**, *16*, 157.
- (48) Hicks, J. M.; Vandersall, M. T.; Sitzmann, E. V.; Eisenthal, K. B. *Chem. Phys. Lett.* **1987**, *135*, 413.
- (49) Higgins, D. A.; Abrams, M. B.; Byerly, S. K.; Corn, R. M. *Langmuir* **1992**, *8*, 1994.
- (50) Horng, M. L.; Gardecki, J. A.; Papazyan, A.; Maroncelli, M. *J. Phys. Chem.* **1995**, *99*, 17311.
- (51) Ishizaka, S.; Habuchi, S.; Kim, H. B.; Kitamura, N. *Anal. Chem.* **1999**, *71*, 3382.
- (52) Ishizaka, S.; Kim, H. B.; Kitamura, N. *Anal. Chem.* **2001**, *73*, 2421.
- (53) Israelachvili, J. N. *Intermolecular and Surface Forces*, 2nd ed.; Academic Press: London, 1992.
- (54) Jungwirth, P.; Tobias, D. J. *J. Phys. Chem. B* **2002**, *106*, 6361.
- (55) Kamlet, M. J.; Abboud, J. L. M.; Taft, R. W. *Prog. Phys. Org. Chem.* **1981**, *13*, 485.
- (56) Katritzky, A. R.; Fara, D. C.; Yang, H.; Taemm, K.; Tamm, T.; Karelson, M. *Chem. Rev.* **2004**, *104*, 175.
- (57) Katz, S. N.; Spence, J. E.; O'Brien, M. J.; Skiff, R. H.; Vogel, G. J.; Prasad, R. Decaffeination of Coffee Green Beans with Supercritical Carbon Dioxide; General Foods Corp.: U.S., 1990; pp 11.

- (58) Kessler, H.; Oschkinat, H.; Griesinger, C.; Bermel, W. *J. Magn. Reson., Ser.* **1986**, *70*, 106.
- (59) Kosower, E. M. *J. Am. Chem. Soc.* **1958**, *80*, 3253.
- (60) Kovaleski, J. M.; Wirth, M. J. *J. Phys. Chem.* **1995**, *99*, 4091.
- (61) Kusalik, P. G.; Patey, G. N. *J. Chem. Phys.* **1988**, *88*, 7715.
- (62) Langan, J. G.; Sitzmann, E. V.; Eisenthal, K. B. *Chem. Phys. Lett.* **1984**, *110*, 521.
- (63) Laurence, C.; Nicolet, P.; Dalati, M. T.; Abboud, J.-L. M.; Notario, R. *J. Phys. Chem.* **1994**, *98*, 5807.
- (64) Lee, E. M.; Simister, E. A.; Thomas, R. K. *Mol. Cryst. Liq. Cryst.* **1990**, *179*, 151.
- (65) Levesque, D.; Weis, J. J.; Patey, G. N. *J. Chem. Phys.* **1980**, *72*, 1887.
- (66) Li, M.; Tikhonov, A. M.; Schlossman, M. L. *Europhys. Lett.* **2002**, *58*, 80.
- (67) Li, Z. X.; Bain, C. D.; Thomas, R. K.; Duffy, D. C.; Penfold, J. *J. Phys. Chem. B* **1998**, *102*, 9473.
- (68) *Liquid Interfaces in Chemical, Biological, and Pharmaceutical Applications*; Volkov, A. G., Ed.; Marcel Dekker, Inc.: New York, 2001; Vol. 95, pp 853.
- (69) Liu, D.; Ma, G.; Levering, L. M.; Allen, H. C. *J. Phys. Chem. B* **2004**, *108*, 2252.
- (70) Lu, J. R.; Su, T. J.; Li, Z. X.; Thomas, R. K.; Staples, E. J.; Tucker, I.; Penfold, J. *J. Phys. Chem. B* **1997**, *101*, 10332.
- (71) Ma, G.; Liu, D.; Allen, H. C. *Langmuir* **2004**, *20*, 11620.

- (72) Magid, L. J.; Han, Z.; Warr, G. G.; Cassidy, M. A.; Butler, P. D.; Hamilton, W. A. *J. Phys. Chem. B* **1997**, *101*, 7919.
- (73) Majewski, J.; Kuhl, T. L.; Wong, J. Y.; Smith, G. S. *Rev. Molec. Biotech.* **2000**, *74*, 207.
- (74) Makov, G.; Nitzan, A. *J. Phys. Chem.* **1994**, *98*, 3459.
- (75) Michael, D.; Benjamin, I. *J. Chem. Phys.* **1997**, *107*, 5684.
- (76) Michael, D.; Benjamin, I. *J. Chem. Phys.* **2001**, *114*, 2817.
- (77) Michael, D.; Benjamin, I. *J. Phys. Chem.* **1995**, *99*, 16810.
- (78) Michael, D.; Benjamin, I. *J. Phys. Chem. B* **1998**, *102*, 5145.
- (79) Mitrinovic, D. M.; Tikhonov, A. M.; Li, M.; Huang, Z. Q.; Schlossman, M. L. *Phys. Rev. Lett.* **2000**, *85*, 582.
- (80) Mitrinovic, D. M.; Williams, S. M.; Schlossman, M. L. *Phys. Rev. E: Stat. Phys., Plasmas, Fluids, Relat. Interdiscip. Top.* **2001**, *6302*, art. no. 021601.
- (81) Mitrinovic, D. M.; Zhang, Z. J.; Williams, S. M.; Huang, Z. Q.; Schlossman, M. L. *J. Phys. Chem. B* **1999**, *103*, 1779.
- (82) Nakatani, K.; Ishizaka, S.; Kitamura, N. *Anal. Sci.* **1996**, *12*, 701.
- (83) Neuhaus, D.; Williamson, M. P. *The Nuclear Overhauser Effect in Structural and Conformational Analysis*, 2nd ed., 2000.
- (84) Nikol'skii, B. P.; Yudovich, E. E.; Pal'chevskii, V. V.; Spevak, V. N. *Zh. Fiz. Khim.* **1970**, *44*, 709.
- (85) Nikol'skii, B. P.; Yudovich, E. E.; Pal'chevskii, V. V.; Spevak, V. N. *Zh. Obshch. Khim.* **1969**, *39*, 1673.

- (86) Noggle, J. H.; Schirner, R. E. *The Nuclear Overhauser Effect: Chemical Applications*, 1971.
- (87) Onsager, L. *J. Am. Chem. Soc.* **1936**, *58*, 1486.
- (88) Onsager, L.; Samaras, N. N. T. *J. Chem. Phys.* **1934**, *2*, 528.
- (89) Patey, G. N.; Carnie, S. L. *J. Chem. Phys.* **1983**, *78*, 5183.
- (90) Penfold, J.; Richardson, R. M.; Zarbakhsh, A.; Webster, J. R. P.; Bucknall, D. G.; Rennie, A. R.; Jones, R. A. L.; Cosgrove, T.; Thomas, R. K.; Higgins, J. S.; Fletcher, P. D. I.; Dickinson, E.; Roser, S. J.; McLure, I. A.; Hillman, A. R.; Richards, R. W.; Staples, E. J.; Burgess, A. N.; Simister, E. A.; White, J. W. *J. Chem. Soc., Faraday Trans.* **1997**, *93*, 3899.
- (91) Petersen, P. B.; Saykally, R. J. *Chem. Phys. Lett.* **2004**, *397*, 51.
- (92) Pratt, L. R. *J. Phys. Chem.* **1992**, *96*, 25.
- (93) Pratt, L. R.; Tawa, G. J.; Hummer, G.; Garcia, A. E.; Corcelli, S. A. *Int. J. Quantum Chem.* **1997**, *64*, 121.
- (94) *Principles of Colloid and Surface Chemistry*; 3rd ed.; Hiemenz, P. C.; Rajagopalan, R., Eds.; Marcel Dekker: New York, 1997, pp 688.
- (95) Purcell, I. P.; Thomas, R. K.; Penfold, J.; Howe, A. M. *Colloids Surf., A* **1995**, *94*, 125.
- (96) Randles, J. E. B. *Phys. Chem. Liq.* **1977**, *7*, 107.
- (97) Rarick, M. J.; Brewster, R. Q.; Dains, F. B. *J. Am. Chem. Soc.* **1933**, *55*, 1289.
- (98) Raymond, E. A.; Richmond, G. L. *J. Phys. Chem. B* **2004**, *108*, 5051.

- (99) Reichardt, C. *Solvents and Solvent Effects in Organic Chemistry*, 2nd ed., 1988.
- (100) Richmond, G. L. *Annu. Rev. Phys. Chem.* **2001**, 52, 357.
- (101) Rosen, M. J. *Surfactants and Interfacial Phenomena*, 1978.
- (102) Rosen, M. J. *Surfactants and Interfacial Phenomena*, 3rd ed.; John Wiley & Sons, Inc.: Hoboken, NJ, 2004.
- (103) Safran, S. A. *Statistical Thermodynamics of Surfaces, Interfaces, and Membranes*; Addison-Wesley Publishing Co.: Reading, MA, 1994; Vol. 90.
- (104) Saldana, M. D. A.; Mazzafera, P.; Mohamed, R. S. *Ciencia e Tecnologia de Alimentos* **1997**, 17, 371.
- (105) Sassaman, J. L.; Wirth, M. J. *Colloids Surf., A* **1994**, 93, 49.
- (106) Scatena, L. F.; Brown, M. G.; Richmond, G. L. *Science* **2001**, 292, 908.
- (107) Schalke, M.; Losche, M. *Adv. Colloid Interface Sci.* **2000**, 88, 243.
- (108) Schefflan, L.; Jacobs, M. B. *The Handbook of Solvents*, 1953.
- (109) Schlossman, M. L.; Li, M.; Mitrinovic, D. M.; Tikhonov, A. M. *High Perform. Polym.* **2000**, 12, 551.
- (110) Schlossman, M. L.; Schwartz, D. K.; Kawamoto, E. H.; Kellogg, G. J.; Pershan, P. S.; Kim, M. W.; Chung, T. C. *J. Phys. Chem.* **1991**, 95, 6628.
- (111) Senapati, S.; Berkowitz, M. L. *Phys. Rev. Lett.* **2001**, 87, 176101.
- (112) Shen, Y. R. *Nature* **1989**, 337, 519.
- (113) Simpson, G. J.; Rowlen, K. L. *Chem. Phys. Lett.* **2000**, 317, 276.

- (114) Siuzdak, G.; Bothner, B. *Angew. Chem., Int. Ed. Engl.* **1995**, *34*, 2053.
- (115) Starks, C. M. *J. Am. Chem. Soc.* **1971**, *93*, 195.
- (116) Starks, C. M.; Owens, R. M. *J. Am. Chem. Soc.* **1973**, *95*, 3613.
- (117) Steel, W. H.; Beildeck, C. L.; Walker, R. A. *J. Phys. Chem. B* **2004**, *108*, 16107.
- (118) Steel, W. H.; Damkaci, F.; Nolan, R.; Walker, R. A. *J. Am. Chem. Soc.* **2002**, *124*, 4824.
- (119) Steel, W. H.; Lau, Y. Y.; Beildeck, C. L.; Walker, R. A. *J. Phys. Chem. B* **2004**, *108*, 13370.
- (120) Steel, W. H.; Walker, R. A. *J. Am. Chem. Soc.* **2003**, *125*, 1132.
- (121) Steel, W. H.; Walker, R. A. *Nature* **2003**, *424*, 296.
- (122) Stern, O. *Z. Elektrochem.* **1924**, *30*, 508.
- (123) Stolle, R.; Marowsky, G.; Schwarzberg, E.; Berkovic, G. *Applied Physics B: Lasers and Optics* **1996**, *B63*, 491.
- (124) Stonehouse, J.; Adell, P.; Keeler, J.; Shaka, A. J. *J. Am. Chem. Soc.* **1994**, *116*, 6037.
- (125) Stott, K.; Stonehouse, J.; Keeler, J.; Hwang, T.-L.; Shaka, A. J. *J. Am. Chem. Soc.* **1995**, *117*, 4199.
- (126) Strutwolf, J.; Barker, A. L.; Gonsalves, M.; Caruana, D. J.; Unwin, P. R.; Williams, D. E.; Webster, J. R. P. *J. Electroanal. Chem.* **2000**, *483*, 163.
- (127) Suppan, P.; Ghoneim, N. *Solvatochromism*; The Royal Society of Chemistry: Cambridge, UK, 1997.

- (128) Tsuyumoto, I.; Noguchi, N.; Kitamori, T.; Sawada, T. *J. Phys. Chem. B* **1998**, *102*, 2684.
- (129) Velegol, S. B.; Fleming, B. D.; Biggs, S.; Wanless, E. J.; Tilton, R. D. *Langmuir* **2000**, *16*, 2548.
- (130) Volkov, A. G. *Interfacial Catalysis*, 2003.
- (131) Volkov, A. G.; Deamer, D. W.; Tanelian, D. L.; Markin, V. S. *Liquid Interfaces in Chemistry and Biology*; John Wiley & Sons, Inc.: New York, 1998.
- (132) Wang, H.; Borguet, E.; Eiseenthal, K. B. *J. Phys. Chem. A* **1997**, *101*, 713.
- (133) Wang, H.; Borguet, E.; Eiseenthal, K. B. *J. Phys. Chem. B* **1998**, *102*, 4927.
- (134) Weber, R.; Winter, B.; Schmidt, P. M.; Widdra, W.; Hertel, I. V.; Dittmar, M.; Faubel, M. *J. Phys. Chem. B* **2004**, *108*, 4729.
- (135) Weissenborn, P. K.; Pugh, R. J. *J. Colloid Interface Sci.* **1996**, *184*, 550.
- (136) Wilson, M. A.; Pohorille, A.; Pratt, L. R. *J. Phys. Chem.* **1987**, *91*, 4873.
- (137) Winde, H. *Z. Phys. Chem. (Munich)* **1996**, *193*, 217.
- (138) Wong, M. W.; Frisch, M. J.; Wiberg, K. B. *J. Am. Chem. Soc.* **1991**, *113*, 4776.
- (139) Zorbakhsh, A.; Bowers, J.; Webster, J. R. P. *Meas. Sci. Technol.* **1999**, *10*, 738.
- (140) Zekovic, Z. P.; Lepojevic, Z. D.; Milosevic, S. G.; Tolic, A. S. *Acta Periodica Technologica* **2001**, *32*, 163.
- (141) Zhang, X. *Investigations of Surface Mediated Solvation at Solid/Liquid Interfaces by SHG Spectroscopy*, University of Maryland, 2003.

- (142) Zhang, X.; Esenturk, O.; Walker, R. A. *J. Am. Chem. Soc.* **2001**, *123*, 10768.
- (143) Zhang, X.; Steel, W. H.; Walker, R. A. *J. Phys. Chem. B* **2003**, *107*, 3829.
- (144) Zhang, X.; Walker, R. A. *Langmuir* **2001**, *17*, 4486.
- (145) Zhuang, X.; Miranda, P. B.; Kim, D.; Shen, Y. R. *Phys. Rev. B: Condens. Matter* **1999**, *59*, 12632.